St. John's University

St. John's Scholar

Theses and Dissertations

2022

PBK/TOPK INHIBITOR OTS964 RESISTANCE IS MEDIATED BY ABCG2- AND ABCB1-DEPENDENT TRANSPORT FUNCTION IN CANCER

Yuqi Yang

PBK/TOPK INHIBITOR OTS964 RESISTANCE IS MEDIATED BY ABCG2- AND
ABCB1-DEPENDENT TRANSPORT FUNCTION IN CANCER

A dissertation submitted in partial fulfillment
of the requirements for the degree of

DOCTOR OF PHILOSOPHY

to the faculty of the

DEPARTMENT OF PHARMACERTICAL SCIENCES

of

COLLEGE OF PHARMACY AND HEALTH SCIENCES
at
ST. JOHN'S UNIVERSITY
New York
by
Yuqi Yang

Date Submitted _____   Date Approved _____

_____   _____
Yuqi Yang   Dr. Zhe-Sheng Chen

ABSTRACT

PBK/TOPK INHIBITOR OTS964 RESISTANCE IS MEDIATED BY ABCG2- AND

ABCB1-DEPENDENT TRANSPORT FUNCTION IN CANCER

Yuqi Yang

Accumulating evidence has suggested that multi-drug resistance (MDR) in cancer cells is a phenotype whereby cancer cells have attenuated sensitivity to drugs. ATP-binding cassette super-family G member 2 (ABCG2/BCRP) and ATP-binding cassette sub-family B member 1 (ABCB1/P-gp) are members of the ATP-binding cassette (ABC) transporter family and involved in MDR. OTS964 is a potent inhibitor targeting to PDZ-binding kinase (PBK)/T-lymphokine-activated killer cell-originated protein kinase (TOPK). Herein, we aimed to explore the relationship between MDR-associated ABC transporters, including ABCG2 and ABCB1, and the regulation of OTS964 efficacy.

PBK/TOPK inhibitor OTS964 resistance is mediated by ABCG2-dependent transport function in cancer: *in vitro* study

The efficacy of OTS964 is limited in drug-selected and drug resistant gene-transfected cells, which overexpress ABCG2, compared to those of corresponding drug-sensitive cells. Also, a verified ABCG2 inhibitor Ko143 can re-sensitize the acquired resistance to OTS964. In mechanism-based studies, OTS964 shows inhibitory effect on the efflux function mediated by ABCG2. Furthermore, OTS964 stimulates ATPase activity of ABCG2 and upregulates ABCG2 expression, resulting in enhanced resistance

to substrate-drugs transported by ABCG2. The *in silico* molecular docking analysis suggested that OTS964 interacts with drug-binding pocket of ABCG2.

PBK/TOPK inhibitor OTS964 resistance is mediated by ABCB1-dependent transport function in cancer: *in vitro* and *in vivo* study

The overexpression of ABCB1 significantly desensitizes both drug-selected and gene-transfected cell lines, which overexpress ABCB1, to OTS964 and that this drug resistance can be antagonized by a verified ABCB1 inhibitor verapamil. Also, a similar trend was observed in tumor-bearing mouse model. In mechanistic studies, OTS964 inhibits the efflux function mediated by ABCB1. Moreover, OTS964 stimulates ATPase activity and expression levels of ABCB1, leading to induced resistance to substrate-drugs transported by ABCB1. OTS964 receives a comparable affinity score and can dock into the substrate-binding site of human ABCB1 protein.

Altogether, OTS964 is susceptible to ABCG2- and ABCB1-mediated drug resistance, and that this effect can be antagonized by known inhibitors. Our findings strongly support the importance of monitoring the level of ABCG2 and ABCB1 in cancer patients under OTS964 treatment. These findings may also serve as a valuable indication for follow-up clinical investigation on potential use of OTS964.

ACKNOWLEDGEMENT

I would like to express my gratitude to many individuals who have made my Ph.D. journey so wonderful and pleasurable.

First and foremost, I would express my appreciation to my mentor, Dr. Zhe-Sheng Chen, who always supported and encouraged me throughout my Ph.D. years. Without his insightful minds, patient guidance, and dedicated involvement in every step throughout the research, I would have never been able to make such progress. I am also sincerely thankful to Dr. John N.D. Wurpel, Dr. Sandra E. Reznik, Dr. Xingguo Cheng, and Dr. Aaron Muth for serving members of my Ph.D. committee, and Dr. Sabesan Yoganathan for chairing my defense committee. Their critical comments and valuable suggestions helped me improve the research design and scientific writing in every step throughout my dissertation project.

I am grateful to the Department of Pharmaceutical Sciences for providing tuition coverage and graduate assistantship/teaching fellowship stipend. I would like to extend my gratitude to the College of Pharmacy and Health Sciences and the Science Supply Office at St. John's University for offering lots of supports throughout my graduate education. Heartfully thanks are also given to all colleagues and laboratory members, past and present, who kindly helped, encouraged, and supported me during my Ph.D. period, and maintained a wonderful research environment.

Last but not the least, my appreciation also goes out to my family and friends. This tough journey would not have been accomplished smoothly without their unconditional love, understanding and encouragement.

TABLE OF CONTENTS

LIST OF TABLES

LIST OF FIGURES

LIST OF ABBREVIATIONS

ABC transporter: ATP-binding cassette transporter

ABCB1: ATP-binding cassette sub-family B member 1

ABCG2: ATP-binding cassette super-family G member 2

ATP: Adenosine triphosphate

CDDP: Cisplatin

COL: Colchicine

DMEM: Dulbecco's modified Eagle medium

DMSO: Dimethyl sulfoxide

DOX: Doxorubicin

EMEM: Eagle's minimum essential medium

FBS: Fetal bovine serum

GAPDH: Glyceraldehyde 3-phosphate dehydrogenase

MDR: Multidrug resistance

MTT: Methylthiazolyldiphenyl-tetrazolium bromide

MX: Mitoxantrone

NBDs: Nucleotide-binding domains

P/S: Penicillin/Streptomycin

PBK: PDZ-binding kinase

PTX: Paclitaxel

PVDF: Polyvinylidene fluoride

qRT-PCR: Quantitative real-time PCR

SDS: Sodium dodecyl sulfate

SDS-PAGE: Sodium dodecyl sulfate-polyacrylamide gel electrophoresis

TMDs: Transmembrane domains

TOPK: T-lymphokine-activated killer cell-originated protein kinase

TPT: Topotecan

VCR: Vincristine

VPL: Verapamil

WBCs: White blood cells

CHAPTER 1

INTRODUCTION

1.1 Multidrug resistance (MDR)-associated ATP-bind cassette (ABC) transporters

Cancer is a major public health problem in many countries and has a trend to become the most serious life-threatening disease [1]. Many anti-cancer drugs have been developed over the past decades to attack cancer cells in regulating cancer cell growth and survival. However, accumulating evidence has suggested that the clinical effect is limited and cannot last for a long time period due to the acquired drug resistance of tumor cells [2]. Overexpression of multidrug resistance (MDR)-associated ATP-binding cassette (ABC) transporters remains one of the major obstacles for cancer chemotherapy and induces acquired drug resistance [3].

Hitherto, 49 human ABC transporters (there appear to be 48 functional proteins) have been identified and can be further classified into 7 subfamilies of proteins, designated with ABCA to ABCG and followed by a number that refers to the specific transporter [4]. Typically, all subfamilies of ABC transporter share common structural features, including transmembrane domains (TMDs) and nucleotide-binding domains (NBDs). TMDs are embedded in the membrane bilayer and serve as ligand recognition and transportation sites, and NBDs are located in the cytoplasmic side of the membranes and serve as ATP-binding sites for hydrolyzing ATP [5-7]. As ABC transporters are ATP-dependent, the energy requirement for substrate transportation is derived from ATP hydrolysis, which drives ABC transporters transport substrates across the cell membrane against their concentration gradient (active transport) [8]. Interestingly, it was found that NBDs can convert the chemical energy stored in the phosphate bonds of ATP into

potential energy that leads to conformational changes and subsequent substrate translocation across the membrane [9, 10]. In detail [11, 12], the substrate transported by ABC transporter binds to the substrate-binding site in the TMD, and ATP binds to the ATP-binding site in the NBD. After binding the substance, ATP is hydrolyzed, and the resulting phosphate group is released. The energy from ATP hydrolysis generates a conformational change in the ATP-binding domain. The close interaction between the ATP-binding domains and the TMDs creates the transmission of force to the TMDs, resulting in a conformational change in the TMDs driving substrate translocation [8]. As a result, the transported substrate is released into the extracellular space, reducing the intracellular amount of substrate-drugs accumulating in certain cancer cells.

1.1.1 ATP-binding cassette super-family G member 2 (ABCG2, breast cancer resistance protein/BCRP, mitoxantrone resistance protein/MXR)

ATP-binding cassette super-family G member 2 (ABCG2, breast cancer resistance protein/BCRP, mitoxantrone resistance protein/MXR), encoded by *ABCG2* gene maps on chromosomal locus 4q22, mediates efflux of endogenous ligands and exogenous drugs [13, 14]. Based on the structure and arrangement of TMDs and NBDs, ABCG2 is grouped as a half transporter that has one hydrophobic TMD and one hydrophilic NBD located in cytoplasm with a reversed NBD-TMD configuration [15, 16]. Thus, ABCG2 functions as a homodimer [17]. As a protector, ABCG2 is ubiquitously distributed on the apical membrane in certain tissues, such as breast, ovary, testis, placenta, intestine, liver, blood-brain barrier, etc. [16, 18]. It is believed that ABCG2 acts as a central contributor to MDR and transports a wide range of anticancer compounds, anthracyclines (e.g., doxorubicin and mitoxantrone), plant alkaloids (e.g., topotecan and SN-38), etc. [16].

1.1.2 ATP-binding cassette sub-family B member 1 (ABCB1, P-glycoprotein/P-gp, multidrug resistance 1/MDR1)

ATP-binding cassette sub-family B member 1 (ABCB1, P-glycoprotein/P-gp, multidrug resistance 1/MDR1), encoded by *ABCB1* gene maps on chromosomal locus 7p21, has a crucial role in protecting cells from endogenous and exogenous toxicants [19-21]. Based on the structure and arrangement of TMDs and NBDs, ABCB1 is grouped into full transporter that has two hydrophobic TMDs and two hydrophilic NBDs located in cytoplasm with an arrangement of TMD_1-NBD_1-TMD_2-NBD_2, comprising two homologous halves [15, 16]. As a gatekeeper, ABCB1 is widely expressed on the apical membrane in multiple tissues, liver, kidney, intestine, placenta, and blood-brain barrier, etc. [16]. The ABCB1 transporter has identified as a mediator of MDR and catalyzes the transportation of various classes of chemotherapeutic agents, anthracyclines (e.g., daunorubicin and doxorubicin), plant alkaloids (e.g., vincristine and vinblastine), taxanes (e.g., docetaxel and paclitaxel), etc. [16, 22].

1.2 PDZ-binding kinase (PBK)/ T-lymphokine-activated killer cell-originated protein kinase (TOPK)

T-lymphokine-activated killer cell-originated protein kinase (TOPK), also known as PDZ-binding kinase (PBK), is a Ser/Thr protein kinase of the mitogen-activated protein kinase kinase (MAPKK) family. Functionally, PBK/TOPK performs central roles in regulating cell proliferation, DNA damage repair, cell cycle, apoptosis, immune responses, and inflammation [23]. Based on evidence from The Cancer Genome Atlas database (*gepia.cancer-pku.cn*), the PBK/TOPK expression is remarkably higher in samples from patients with 24 of 31 cancer types compared with in normal tissues.

3

Moreover, according to UALCAN database (*ualcan.path.uab.edu*), 11 of 33 tumor

samples show that a high level of PBK/TOPK is linked with survival. Indeed, many

studies have been validated that PBK/TOPK overexpression promotes cancer

development, malignancy, and poor prognosis in various cancer types, including

epithelial ovarian cancer [24], non-small cell lung cancer [25], chordoma [26], gastric

carcinoma [27], etc. The findings from Joel et al. [28] have supported the use of

PBK/TOPK as a therapeutic target in cancer stem cells-enriched tumors. Importantly,

PBK/TOPK is rarely detected in normal tissues with exception for tissues from testis,

placenta, and thymus [29, 30]. This highlights the use of PBK/TOPK as a target for

cancer therapy and an indicator for cancer prognosis. Interestingly, PBK/TOPK inhibitor

labeled with fluorescent or radioactivity can be used for *in vivo* cancer-specific imaging

and tumor delineation [31, 32], which further highlights the importance of studies on

potential PBK/TOPK inhibitor.

1.3 PBK/TOPK inhibitors

Advances in PBK/TOPK-target therapy have been widely studied as potent

PBK/TOPK inhibitors, HI-TOPK-032, OTS514, OTS964, ADA-07, and SKLB-C05.

Chemical structures of several PBK/TOPK inhibitors reported in pre-clinical research are

presented in Fig. 1A-1F. The first of these, in 2012, Kim et al. [33] have identified a

novel PBK/TOPK inhibitor HI-TOPK-032. Subsequent studies showed that HI-TOPK-

032 reduces ERK-RSK phosphorylation and regulates p53 protein abundance, but has no

effects on ERK1, p38, or JNK1 activity. Meanwhile, Matsuo et al. [34] have found that

some thieno[2,3-c]quinolone compounds have the ability to inhibit PBK/TOPK through

high-throughput compound library screening and extensive structure-activity relationship

studies, and subsequently OTS514 and its demethylated analog OTS964 were developed

and identified as extremely potent PBK/TOPK inhibitors. Furthermore, the

pharmacophore of OTS964 can be used as a template to explore new PBK/TOPK

inhibitors. Hu et al. [30] have synthesized a series of candidate drugs as possible

PBK/TOPK inhibitors and described 9g compound as a novel potent PBK/TOPK

inhibitor. In addition, ADA-07 can bind with PBK/TOPK protein at ATP-binding pocket

and subsequent inhibit its kinase activity in SUV-induced skin carcinogenesis. This

inhibition is attributed to suppressing phosphorylation of PBK/TOPK downstream

signaling, such as ERK1/2, p38, and JNKs, and subsequently inhibiting AP-1 activity

[35]. Moreover, the compound SKLB-C05 was described as a novel selective

PBK/TOPK inhibitor with sub-nanomolar potency toward colorectal cancer. Mechanistic

studies indicated that the inhibitory effect of SKLB-C05 results from regulating MAPK

family members, including ERK1/2, p38, and JNK1/2/3 signaling [36]. Apart from the

aforementioned potential PBK/TOPK inhibitors, several compounds have shown

inhibitory effect on PBK/TOPK. Chemical structures of several reported small molecular

PBK/TOPK inhibitors are presented in Fig. 1G-1J. Glycyrol shows a strong interaction

with PBK/TOPK protein and inhibitory effect of its kinase activity in lung cancer models

[37]. In addition, an FDA-approved drug sulfasalazine has binding and inhibition toward

PBK/TOPK in thyroid cancer models [38]. Also, FDA-approved proton pump inhibitors,

such as ilaprazole and pantoprazole, have been shown to target PBK/TOPK in multiple

cancer types [23].
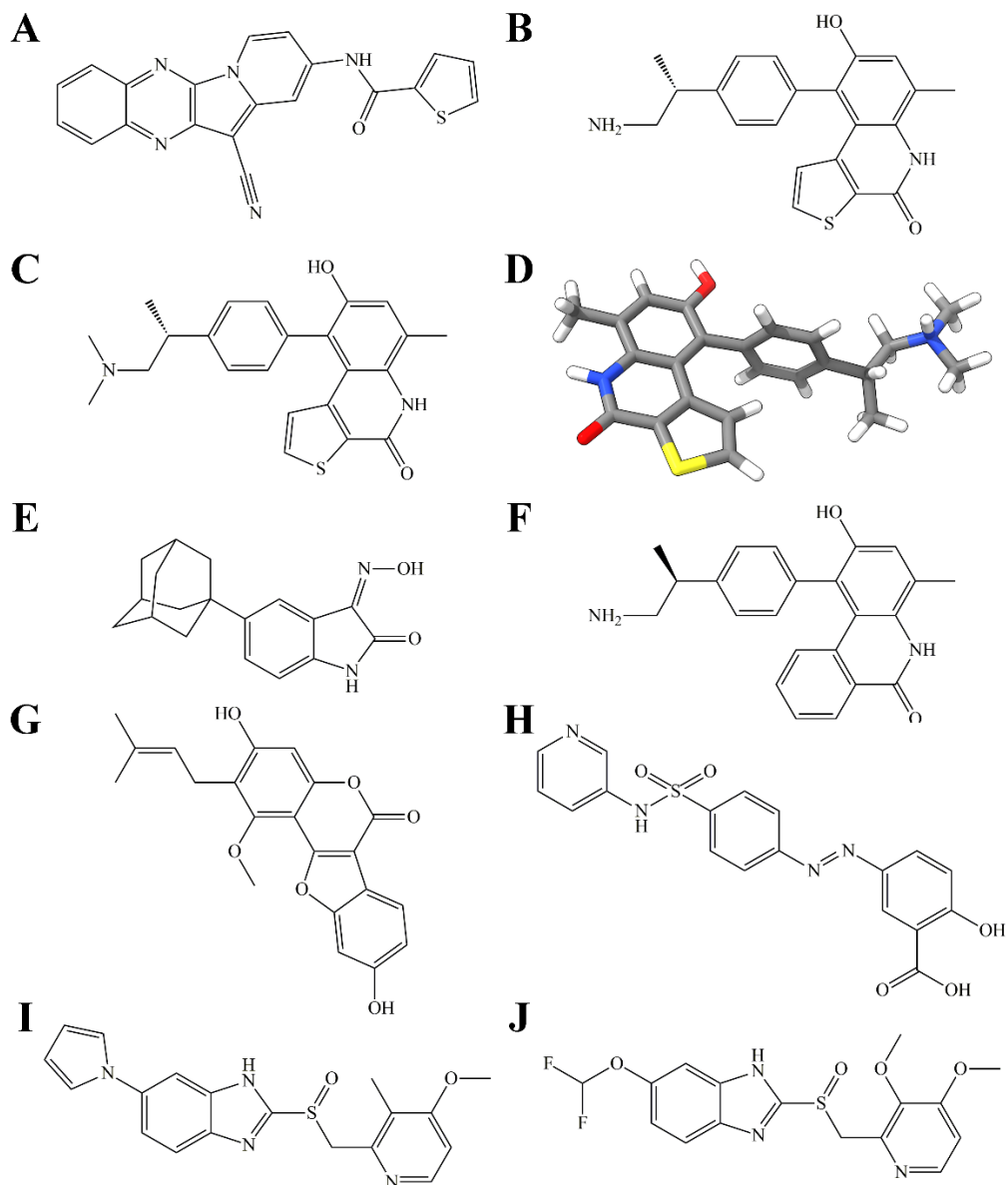
Figure 1. Chemical structures of reported PBK/TOPK inhibitors.

A) HI-TOPK-032. **B)** OTS514. **C)** 2D view of OTS964 structure. **D)** 3D view of OTS964

structure. OTS964 molecule is exhibited as colored sticks. Grey: carbon; white:

hydrogen; red: oxygen; blue: nitrogen; yellow: sulfur. **E)** ADA-07. **F)** SKLB-C05. **G)**

Glycyrol. **H)** Sulfasalazine. **I)** Ilaprazole. **J)** Pantoprazole.

1.4 OTS964

Despite identifying PBK/TOPK as a promising novel therapeutic target, the 3D structure of PBK/TOPK has not been reported. To date, Kim et al. [33] have reported the crystal structure of an inactive dimer and indicated that it exists in a conformational transition between dimers and monomers at different pH conditions. However, the active state of PBK/TOPK is a monomer and does not form a dimer. The unavailability of crystalline structure of PBK/TOPK makes the discovery of its inhibitors a little bit slow.

OTS964, as a PBK/TOPK inhibitor, suppresses cell proliferation with nanomolar inhibitory potency [39], which is consistent with our results. Several comprehensive studies have demonstrated that OTS964 strongly suppresses the growth of PBK/TOPK-positive cancer cells in cell-based assays [24, 34], and more importantly, OTS964 promotes complete regression in lung cancer xenograft models [34] and inhibits the growth of patient-derived ovarian cancer cells [24]. In terms of unfavorable hematological toxicity, anemia and leukocytopenia with increased platelets, this effect recovered within 2 weeks and could be circumvented via a liposome-based delivery system [34]. Using [^{18}F]FE-OTS964 as a tracer in glioblastoma has proved that OTS964 has a favorable biodistribution and pharmacokinetics, and also, due to the tumor specificity of PBK/TOPK expression, has presented a starting point for developing a noninvasive PBK/TOPK imaging platform, *in vivo* PET imaging, optical imaging, etc. [32]. These findings strongly support the clinical use of OTS964.

Taking inhibitor OTS964 as a lead structure, Hu et al. [30] have synthesized a series of anti-PBK/TOPK compounds and explored suitable candidates via preliminary kinase study and biological evaluation. Through a systematic structure-activity

relationship study, Hu et al. [30] have summarized that 1) replacing thiophene core in the left side with phenyl core is proved to be an effective pharmacophore for inhibitory activity, presumably by the formation of hydrogen bonds; 2) the best substituent of crucial aminoalkyl group is (R)-1-aminopropan-2-yl; 3) the alkyl substitution of phenyl core is not necessary; 4) the substitutions on hydroxyl group completely abolish the potency. These findings provide significant advances in discovery and development of PBK/TOPK inhibitors.

1.5 Rationale and hypothesis

In decade, PBK/TOPK emerges as an attractive cancer-specific therapeutic target and is considered as an oncogenic target or a prognostic marker [23, 29]. As PBK/TOPK is considered as a MAPKK-like protein, it plays a role in MAPK signaling including ERK pathway, p38 MAPK pathway, and JUN pathway, and thus regulates cell proliferation [23, 40]. It was found that PBK/TOPK is also involved in PI3K-PTEN-Akt pathway, and thereby promotes tumor development [23, 40] and increases cell migration [25, 30]. Interestingly, it has reported that the expression levels of ABCG2 protein and gene can be regulated through MAPK pathway and/or PI3K-Akt pathway [41-44], and more interestingly, To et al. [45] have revealed that inhibiting PI3K-Akt pathway alters ABCG2 subcellular localization from plasma membrane to the cytoplasm. Similarly, MAPK signaling and PI3K-Akt signaling are either directly or indirectly linked with regulation of ABCB1 protein expression and/or transcription of *ABCB1* gene [46]. This may support our hypothesis that PBK/TOPK has potential to interact with ABC transporters, especially ABCB1 and ABCG2. It has reported that OTS514-resistant can be conferred by ABCB1-overexpressing and antagonized by an ABCB1 inhibitor [47]. In

addition, OTS964 shows an inhibition toward cyclin-dependent kinase CDK11 activity [39]. Taken together, PBK/TOPK inhibitors often cause on-target and/or off-target toxicity. Hence, we considered that OTS964 has high possibility to interact with MDR-associated ABC transporters. In the present study, we focused on the ABCG2- and ABCB1-induced acquired resistance to OTS964 and investigated its potential factors.

In this study, we aimed to comprehensively investigate the relationship between ABCG2 and ABCB1 transporters and the regulation of OTS964 efficacy by exploring the transport function, ATPase activity, ligand-receptor interaction, and expression level.

CHAPTER 2

MATERIALS AND METHODS

2.1 Reagents, kits, apparatus, and software

OTS964 was purchased from ChemieTek (Indianapolis, IN). Fetal bovine serum (FBS) was obtained from Atlanta Biologicals (Minneapolis, MN). Dulbecco's modified Eagle medium (DMEM), antibiotics (penicillin/streptomycin, P/S), and trypsin-EDTA were purchased from Corning (Corning, NY). Eagle's minimum essential medium (EMEM) was purchased from Quality Biological (Gaithersburg, MD). Doxorubicin (DOX), mitoxantrone (MX), and SN-38 was obtained from Medkoo Biosciences (Morrisville, NC). Topotecan (TPT) was obtained from Selleckchem (Houston, TX). Cisplatin (CDDP), G418 (geneticin), and Ko143 were purchased from Enzo Life Sciences (Farmingdale, NY). Dimethyl sulfoxide (DMSO), methylthiazolyldiphenyl-tetrazolium bromide (MTT), paclitaxel (PTX), verapamil (VPL), vincristine (VCR), anti-P-gp antibody (F4), and anti-BCRP antibody (BXP-21) were purchased from Millipore-Sigma (Burlington, MA). HRP-conjugated secondary antibody was obtained from Cell Signaling Technology (Dancers, MA). Anti-GAPDH antibody (GA1R), Pierce™ BCA protein assay kit, and zeocin (100 mg/ml in HEPES) were obtained from Thermo Fisher Scientific (Waltham, MA). [^{3}H]-PTX (26.1 Ci/mmol) and [^{3}H]-MX (11 μCi/mmol) was purchased from Moravek Biochemicals (Brea, CA).

Other reagents were purchased from Thermo Fisher Scientific (Waltham, MA) unless mentioned otherwise.

2.2 Cell lines and cell culture conditions

MX-selected MDR cell lines expressing ABCG2, NCI-H460/MX20 and S1-M1-

80, were developed in medium with MX at 20 nM and 80 μM concentrations, respectively [48]. Their respective parental cell lines are non-small cell lung cancer cell line NCI-H460 and human colon carcinoma cell line S1. NCI-H460/MX20 cells were shown to overexpress wild-type ABCG2 protein [49, 50], while S1-M1-80 cells were shown to overexpress a mutant allele (R482G) in *ABCG2* gene [51, 52]. The *ABCG2* gene knockout subline of NCI-H460/MX20 and NCI-H460 were constructed using clustered regularly interspaced short palindromic repeats (CRISPR)/CRISPR-associated (Cas) 9 system [53]. HEK293/pcDNA3.1, HEK293/ABCG2-482-R2, HEK293/ABCG2-482-G2, and HEK293/ABCG2-482-T7 were transfected with either an empty vector pcDNA3.1 or a pcDNA3.1 vector containing a full length ABCG2 encoding arginine (R), glycine (G), or threonine (T) at position 482 [54]. ABCG2-knockout and -transfected cell lines were maintained in complete medium in the presence of 1.5 mg/ml and 2 mg/ml G418 (geneticin), respectively.

The ABCB1-overexpressing MDR cell line KB-C2 was developed and maintained in complete medium supplemented with 2 μg/ml colchicine (COL) [55]. SW620/Ad300 cells expressing ABCB1 were established and cultured in complete medium containing 300 ng/ml doxorubicin (DOX) [56]. Their respective drug-sensitive cell lines are human epidermoid carcinoma cell line KB-3-1 and human colon cancer cell line SW620. The *ABCB1* gene knockout subline of SW620/Ad300 and SW620 were constructed using clustered regularly interspaced short palindromic repeats (CRISPR)/CRISPR-associated (Cas) 9 system [57]. HEK293/ABCB1 and HEK293/pcDNA3.1 were transfected with either a pcDNA3.1 vector encoding a full length ABCB1 or an empty vector pcDNA3.1 [58]. ABCB1-knockout and -transfected

11

cell lines were maintained in complete medium in the presence of 1.5 mg/ml and 2 mg/ml G418 (geneticin), respectively.

PEL and B1/G2 cells were transfected with a bicistronic vector containing full-length ABCB1 and ABCG2 or an empty vector pcDNA3.1 [59]. Cells co-expressed with ABCB1 and ABCG2 were selected with complete medium with 250 μg/ml zeocin.

PEL and B1/G2 cells were cultured in EMEM supplemented with 10% FBS and 1% P/S. Other cell lines were cultured in DMEM supplemented with 10% FBS and 1% P/S unless mentioned otherwise. All cells were cultured in complete medium at 37°C in a humidified incubator supplied with 5% CO_2. All MDR cells were cultured in drug-free complete medium for at least 3 weeks and passaged for at least 3 generations before further experimental use.

2.3 Cell viability assay

The cell viability of chemotherapeutic agents in MDR cell lines and their respective parental cell lines was assessed using an MTT assay. As described previously [7], cells (5,000-7,000 cells/well) were seeded into a 96-well plate and allowed to attach. On the following day, serial concentrations of therapeutic drug were added to the designated wells with or without 2 h pretreatment of modulator at non-toxic concentrations. After a 3-day incubation period, an MTT solution (4 mg/ml in PBS) was added and incubated for an additional 3 h. Followed by removing the supernatant, DMSO was added to dissolve the resulting formazan crystals. The OD570 value was measured using Fisherbrand™ accuSkan™ GO UV/Vis microplate spectrophotometer (Fisher Scientific, Fair Lawn, NJ).

2.4 Accumulation assay

The ABCG2- and ABCB1-mediated transport function was evaluated using a tritium-labeled MX or PTX accumulation assay, respectively. Based on an established protocol [60], cells (1×10^6 cells/well) were seeded into a 24-well plate and allowed to attach. On the following day, modulator at indicated concentrations was added to the designated wells. Following 2 h pretreatment, [^{3}H]-MX or [^{3}H]-PTX was added to designated wells and incubated for an additional 2 h or 72 h, separately. Cells were washed twice with ice-cold PSB, and this was followed by transferring into scintillation fluid (Thermo Fisher Scientific, Waltham, MA). The radioactivity was measured using Packard TRI-CARB® 1900CA liquid scintillation analyzer (Packard Instrument, Downers Grove, IL).

2.5 ATPase assay

As previously described [61], the vanadate-sensitive ATPase activity of ABCG2 and ABCB1 was determined by quantifying the amount of inorganic phosphate (P_i) produced from hydrolyzed ATP. Briefly, membrane vesicles (10 μg total protein) extracted from High Five insect cells expressing ABCG2 or ABCB1 was incubated in assay buffer containing 5 mM sodium azide (NaN_3), 1 mM ouabain (g-strophanthin), 2 mM dithiothreitol (DTT), 10 mM magnesium chloride ($MgCl_2$), 50 mM potassium chloride (KCl), 2 mM ethylene glycol-bis(β-aminoethyl ether)-N,N,N′,N′-tetra acetic acid (EGTA), and 50 mM pH 6.8 2-(N-morpholino) ethanesulfonic acid (MES), with or without 0.3 mM sodium orthovanadate (Na_3VO_4), at 37 °C for 5 min. Then the mixture was incubated with OTS964 (0-40 μM final concentration) or OTS964 (0-40 μM final concentration) with 1 μM CYB-2 or tepotinib at the same temperature for 3 min. Mg-ATP

(5 mM) solution was then added to initiate a 20-min reaction at 37°C, followed by adding

5% SDS to terminate the reaction. The P_i was quantified by measuring the absorbance at

880 nm using a spectrophotometer (Bio-Rad, Hercules, CA).

2.6 Molecular docking analysis

The 3D structure of OTS964, MX, or PTX was constructed for docking

simulation as previously described [62]. Human ABCG2 6VXI (MX-bound) [63] and

human ABCB1 6QEX (PTX-bound) [64] were obtained from RCSB Protein Data Bank

(PDB). The protein models are inward-facing. Docking calculations were performed in

AutoDock Vina (version 1.1.2) [65]. Hydrogen atoms and partial charges were added

using AutoDockTools (ADT, version 1.5.4). Docking grid center coordinates were

determined from the bound ligands provided in PDB files. Receptor/ligand preparation

and docking simulation were performed using default settings. The top-scoring pose

(sorted by affinity score: kcal/mol) was selected for further analysis and visualization.

2.7 Western blot analysis

The ABCG2 and ABCB1 protein expression level was investigated using a

Western blot analysis as previously described [48]. Briefly, cells were incubated with

OTS964 at indicated concentrations for a serial time-course. Following lysate collection,

equal amounts of total proteins were subjected to SDS-PAGE, and then transferred on to

a Immobilon-P PVDF membrane (Millipore-Sigma, Burlington, MA). The membrane

was blocked with 4% non-fat milk, and this was followed by incubation with primary and

secondary antibody (1:1000 dilution). The chemiluminescence signal of protein-antibody

complex was visualized using ECL substrate and captured using C-DiGit® blot scanner

(LI-COR Biotechnology, Lincoln, NE) as per manufacturer's instruction. The relative

density of each protein band was analyzed by Fiji software for Windows (NIH, Bethesda, MD).

2.8 Quantitative real-time PCR (qRT-PCR)

The ABCG2 and ABCB1 mRNA expression level was detected using qRT-PCR based on an established protocol [66]. Total RNA was extracted from cultured cells following designated treatment with RNeasy plus mini kit (QIAGEN, Germantown, MD) as per manufacturer's instructions. Total RNA concentrations were quantified at 260 nm with Eppendorf BioSpectrometer (Eppendorf North America, Hauppauge, NY). RNA samples with an A260/A280 ratio between 1.8 and 2.0 were used for further analysis. The cDNA was prepared from the extracted RNA in the reverse transcriptase reaction with SuperScript™ II reverse transcriptase (Thermo Fisher Scientific, Waltham, MA) as per manufacturer's protocol. The transcriptome level of ABCG2 or ABCB1 transporter was determined by quantitative PCR in an AriaMx real-time PCR system (Agilent Technologies, Santa Clara, CA) with SYBR™ select master mix (Thermo Fisher Scientific, Waltham, MA) and following specific primer set (Eurofins Genomics, Louisville, KY): ABCG2-Forward: 5'-GCCACAGAGATCATAGAGCCT-3', ABCG2-Reverse: 5'-TCACCCCCGGAAAGTTGATG-3'; ABCB1-Forward: 5'-CTCTTTGCCACAGGAAGCCT-3', ABCB1-Reverse: 5'-CATTGCGGTCCCCTTCAAGA-3'; GAPDH-Forward: 5'-CTGGGCTACACTGAGCACC-3', GAPDH-Reverse: 5'-AGTGGTCGTTGAGGGCAATG-3'. The PCR reaction has 40 cycles of 95℃ for 30 s, 55℃ for 1 min, and 72℃ for 1 min. Data were calculated based on the comparative $\Delta\Delta C_T$ method and expressed as the relative fold changes.

2.9 Experimental animals and xenograft model

Athymic NCR (nu/nu) nude mice (male, 4-5 weeks age) (Taconic Farms, Albany, NY) were used for tumor xenograft models. The animals were housed and cared under the St. John's University animal facility and were monitored closely for tumor growth by palpation and visual examination daily. The protocol for animal experiments was approved by the St. John's University Institutional Animal Care & Use Committee (IACUC) (Protocol #1984). The research was conducted in compliance with the Animal Welfare Act and other federal statutes.

As previously established by Chen's laboratory [67], SW620 (5×10^6 cells/0.2 ml PBS) and SW620/Ad300 (5×10^6 cells/0.2 ml PBS) cells were injected subcutaneously under armpits of the nude mice. Once the tumor reached approximately 5×5 mm in size, the mice (n = 6 per group) were randomized into the following treatment groups. Group 1 mice were administrated with normal saline intraperitoneally. Group 2 mice were administered with 15 mg/kg OTS964 orally. Group 3 mice were administrated with 10 mg/kg VPL intraperitoneally 1 h before receiving oral gavage of 15 mg/kg OTS964. All treatments were given once daily for a period of 18 days. The OTS964 was prepared in autoclaved water and the VPL was prepared in normal saline. The dosage and administration interval of OTS964 and VPL were selected based on previous studies from Hu et al. [30] and Shen et al. [68], respectively, without any remarkable toxicity in mice. The body weight of mice was measured every 3rd day for monitoring drug dosage. The two perpendicular diameters were recorded every 3rd day and tumor volume was estimated based on the formula: V = (length $\times$ width^2) $\times$ 0.5 [7]. Blood was collected in Microvette® 500 capillary blood collection tubes (VWR Chemicals, Radnor, PA) with

heparin to prevent coagulation and to perform blood cell counting. The white blood cells (WBCs) and platelets were counted with Eng Scientific WBC diluting fluid and Eng Scientific platelet diluent (Fisher Scientific, Fair Lawn, NJ), respectively, as described previously [67]. At the end of the experiment, all mice from each group were euthanized using carbon dioxide, and the tumor tissues were excised, measured, weighed, collected, and stored at -80°C.

2.10 Statistics

All data are shown as mean ± SD. Comparisons were made between control group and respective treatment group. Data analysis and follow-up statistical evaluation were performed by GraphPad Prism software version 8.3.0 for Windows (GraphPad Software, La Jolla, CA). The p values were computed by one-way or two-way ANOVA followed by Tukey *post hoc* analysis, if appropriate. The *a priori* significance level was $p < 0.05$.

CHAPTER 3

RESULTS

3.1 PBK/TOPK inhibitor OTS964 resistance is mediated by ABCG2-dependent transport function in cancer: *in vitro* study

3.1.1 The cytotoxic effect of OTS964 is limited in ABCG2 overexpression cells, and ABCG2 inhibitor sensitizes ABCG2 overexpression cells to OTS964.

An MTT assay was performed to examine the susceptibility of OTS964 to MDR mediated by ABCG2. Herein, RF value was used to evaluate the degree of increased resistance to OTS964 resulting from the presence of ABCG2 transporter. Fig. 2 and Fig. 3 present the concentration-response curves and IC_{50} values for OTS964 and MX with or without a verified ABCG2 inhibitor Ko143 in various cell lines. Our results showed that drug sensitivity to OTS964 was attenuated in S1-M1-80 (Fig. 2A and Table 1) and NCI-H460/MX20 (Fig. 2B and Table 2) cell lines by 6.30- and 5.13-fold, respectively, relative to their respective drug-sensitive cell lines. Subsequently, gene-knockout and gene-transfected sublines were used to validation. Upon *ABCG2* gene-knockout, NCI-H460/MX20 ABCG2 KO cells that do not overexpress ABCG2 transporter restored the sensitivity to OTS964, as evidenced by the reduced gap and decreased IC_{50} value for OTS964 (Fig. 4A and Table 2). Given that Robey et al. [54] have demonstrated that variations at amino acid 482 in the *ABCG2* gene affect the substrate specificity of the ABCG2 protein, cells transfected with wild-type (R482) or mutant (R482T or R482G) ABCG2 were used. As shown in Fig. 2D and Table 1, the effectiveness of OTS964 was limited by 6.69-, 33.52-, and 36.93-fold, in HEK293/ABCG2-482-R2, HEK293/ABCG2-482-G2, and HEK293/ABCG2-482-T7 cells, respectively, compared with counterpart in

HEK293/pcDNA3.1 cells. Notably, upon combined with a verified ABCG2 inhibitor Ko143 at 3 μM, the IC_{50} value of OTS964 was significantly decreased in ABCG2-overexpressing cells, and thereby restored the efficacy of OTS964 to the similar level as their respective drug-sensitive cells do (Fig. 2, Table 1, and Table 2). By contrast, 3 μM of Ko143 did not significantly affect the cytotoxic activity of OTS964 in drug-sensitive or ABCG2-knockout cells, as indicated by the overlapping curves with that of the respective cell lines without Ko143 treatment.

Meanwhile, MX served as a reference ABCG2 substrate. The RF values for S1-M1-80, NCI-H460/MX20, HEK293/ABCG2-482-R2, HEK293/ABCG2-482-G2, and HEK293/ABCG2-482-T7 cell lines were 22.20, 97.78, 11.08, 24.49 and 38.90, respectively (Fig. 3, Table 1, and Table 2). Similarly, the drug resistance to MX was sensitized by Ko143 at 3 μM in MDR cell lines mediated by ABCG2 overexpression, as indicated by Fig. 3.

Considering different responses in wild-type (R482) and mutant (R482G and R482T) ABCG2, gene-transfected HEK293 cell lines were used for further studies. Together, above results indicated that ABCG2 transporter could confer resistance to OTS964 and known ABCG2 inhibitor can re-sensitize the acquired resistance to OTS964.
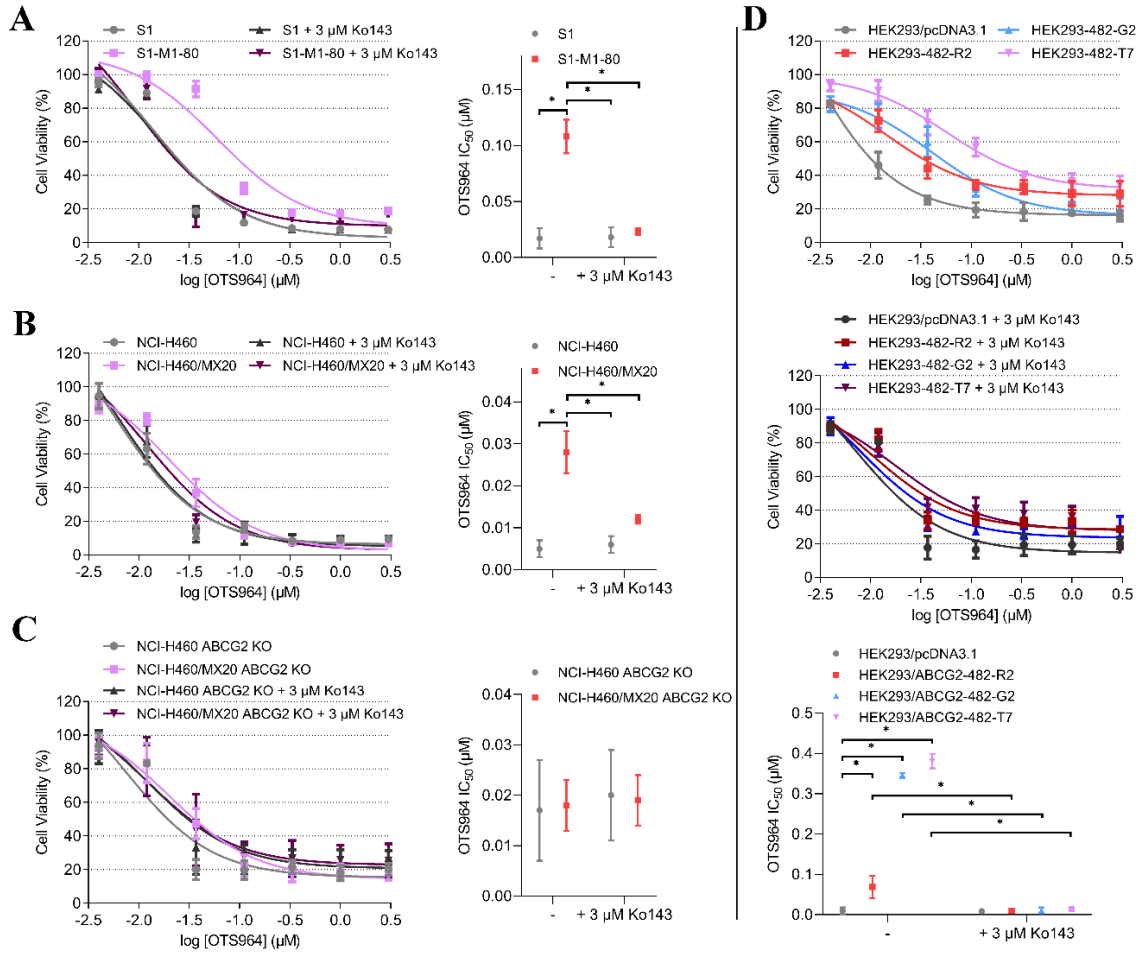
Figure 2. Cytotoxic activity of OTS964 in drug-selected, gene-knockout, or gene-transfected cells and their respective parental cells.

The concentration-response curves and IC_{50} values for OTS964 with or without a verified ABCG2 inhibitor in **A)** S1-M1-80 and S1, **B)** NCI-H460/MX20 and NCI-H460, **C)** NCI-H460/MX20 ABCG2 KO and NCI-H460 ABCG2 KO, and **D)** ABCG2-transfected HEK293 cells (HEK293/ABCG2-482-R2, HEK293/ABCG2-482-G2, and HEK293/ABCG2-482-T7) and HEK293/pcDNA3.1. The GraphPad software [log(inhibitor) vs. response] was used to fit nonlinear regression and to calculate IC_{50} values. Each dot is expressed as mean ± SD from a representative of three independent experiments. *$p < 0.05$ versus the respective control group.

20

Figure 3. Cytotoxic activity of MX in in drug-selected, gene-knockout, or gene-transfected cells and their respective parental cells.

The concentration-response curves and IC_{50} values for MX with or without a verified

ABCG2 inhibitor in **A)** S1-M1-80 and S1, **B)** NCI-H460/MX20 and NCI-H460, **C)** NCI-H460/MX20 ABCG2 KO and NCI-H460 ABCG2 KO, and **D)** ABCG2-transfected HEK293 cells (HEK293/ABCG2-482-R2, HEK293/ABCG2-482-G2, and HEK293/ABCG2-482-T7) and HEK293/pcDNA3.1. The GraphPad software [log(inhibitor) vs. response] was used to fit nonlinear regression and to calculate IC_{50} values. Each dot is expressed as mean ± SD from a representative of three independent experiments. *$p < 0.05$ versus the respective control group.
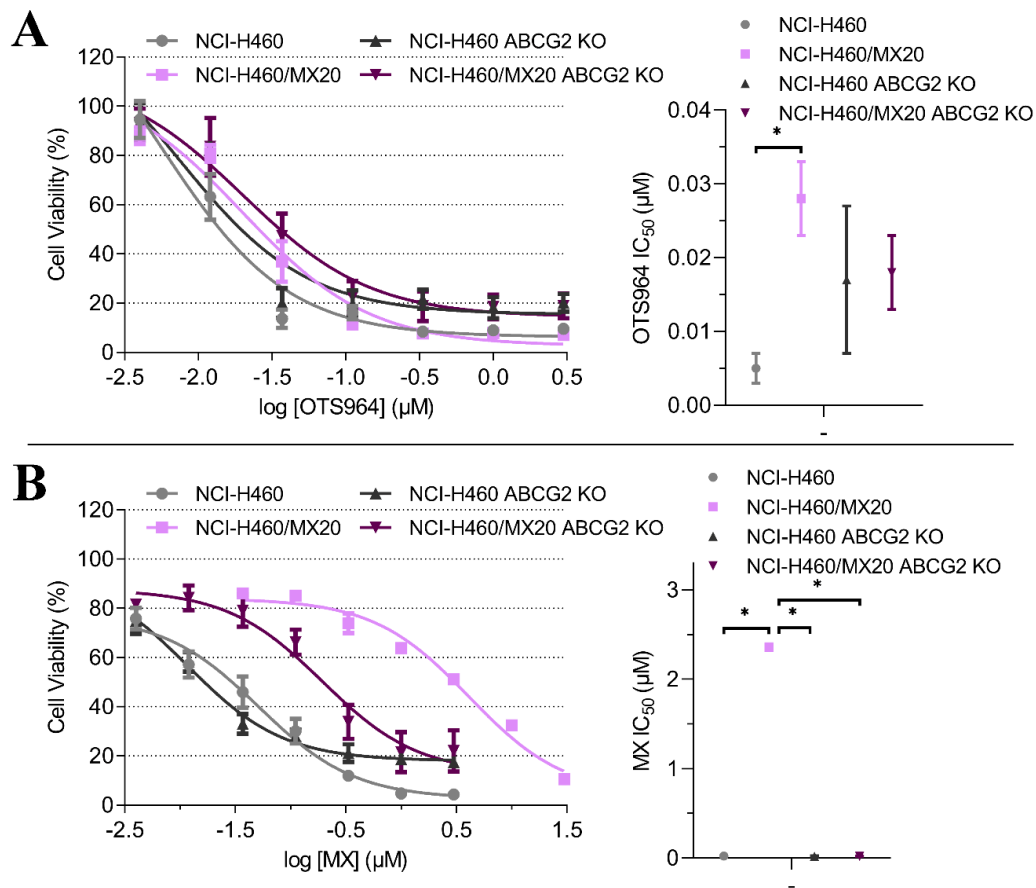
Figure 4. Cytotoxic activity of OTS964 or MX in gene-knockout cells and their respective parental cells.

The concentration-response curves and IC_{50} values for **A)** OTS964 and **B)** MX in NCI-

H460/MX20 and NCI-H460, and NCI-H460/MX20 ABCG2 KO and NCI-H460 ABCG2 KO cells. The GraphPad software [log(inhibitor) vs. response] was used to fit nonlinear regression and to calculate IC_{50} values. Each dot is expressed as mean $\pm$ SD from a representative of three independent experiments. $*p < 0.05$ versus the respective control group.

Table 1. The anticancer effectiveness of OTS964 or MX in drug-sensitive and ABCG2-overexpressing cell lines.

Treatment	$IC_{50}{}^a \pm$ SD (μM) (RF[b])	
	S1	S1-M1-80
OTS964	0.017 ± 0.009 (1.000)	0.108 ± 0.015 (6.304) *
+ Ko143 3 μM	0.018 ± 0.009 (1.077)	0.023 ± 0.003 (1.368)
MX	0.169 ± 0.020 (1.000)	3.752 ± 0.437 (22.204) *
+ Ko143 3 μM	0.183 ± 0.017 (1.083)	0.120 ± 0.004 (0.708)
	HEK293/pcDNA3.1	HEK293/ABCG2-482-R2
OTS964	0.010 ± 0.008 (1.000)	0.069 ± 0.028 (6.689) *
+ Ko143 3 μM	0.009 ± 0.001 (0.845)	0.010 ± 0.005 (0.973)
MX	0.015 ± 0.002 (1.000)	0.167 ± 0.053 (11.079) *
+ Ko143 3 μM	0.018 ± 0.001 (1.196)	0.053 ± 0.011 (3.511)
	HEK293/ABCG2-482-G2	HEK293/ABCG2-482-T7
OTS964	0.346 ± 0.006 (33.518) *	0.381 ± 0.018 (36.927) *
+ Ko143 3 μM	0.011 ± 0.007 (1.079)	0.013 ± 0.003 (1.222)
MX	0.369 ± 0.030 (24.490) *	0.586 ± 0.039 (38.896) *

+ Ko143 3 μM	0.056 ± 0.026 (3.723)	0.067 ± 0.005 (1.622)

[a] IC_{50} values are expressed as mean ± SD from a representative of three independent experiments.

[b] Resistance fold (RF) was calculated by dividing the IC_{50} values of verified substrate-drugs with or without modulator in drug-sensitive or drug-resistant cells by the IC_{50} values of verified substrate-drugs without modulator in drug-sensitive cells.

*$p < 0.05$ versus the respective control group without modulator.

Table 2. The anticancer effectiveness of OTS964 or MX in ABCG2-overexpressing and ABCG2-knockout cell lines.

Treatment	$IC_{50}{}^{a}$ ± SD (μM) (RF[b])	
	NCI-H460	NCI-H460/MX20
OTS964	0.005 ± 0.002 (1.000)	0.028 ± 0.005 (5.127) *
+ Ko143 3 μM	0.006 ± 0.002 (1.101)	0.012 ± 0.001 (2.267)
MX	0.024 ± 0.009 (1.000)	2.359 ± 0.037 (97.782) *
+ Ko143 3 μM	0.035 ± 0.005 (1.456)	0.212 ± 0.013 (8.769) *
	NCI-H460-ABCG2 ko	NCI-H460/MX20-ABCG2 ko
OTS964	0.017 ± 0.010 (1.000)	0.018 ± 0.005 (1.112)
+ Ko143 3 μM	0.020 ± 0.009 (1.224)	0.019 ± 0.005 (1.171)
MX	0.021 ± 0.006 (1.000)	0.020 ± 0.003 (0.944)
+ Ko143 3 μM	0.033 ± 0.016 (1.557)	0.029 ± 0.015 (1.392)

[a] IC_{50} values are expressed as mean ± SD from a representative of three independent experiments.

[b] Resistance fold (RF) was calculated by dividing the IC_{50} values of verified substrate-

drugs with or without modulator in drug-sensitive or drug-resistant cells by the IC_{50}

values of verified substrate-drugs without modulator in drug-sensitive cells.

$^*p < 0.05$ versus the respective control group without modulator.

3.1.2 OTS964, at a high-concentration and with short-exposure times,

increases the intracellular accumulation of [^{3}H]-MX in cells overexpressed ABCG2.

To further elucidate the possible interaction between ABCG2 transporter and

OTS964, transport function mediated by ABCG2 was analyzed by an accumulation assay.

As presented in Fig. 5, in the control group of ACBG2-transfected HEK293 cell lines, the

intercellular accumulation of MX was significantly decreased relative to that of HEK293

cells transfected with an empty vector. More importantly, OTS964 at 3 μM significantly

increased intracellular accumulation level of [^{3}H]-MX from 29.6% to 72.6% in

HEK293/ABCG2-482-T7 cells relative to that in the control group of

HEK293/pcDNA3.1 cells; however, there was no significant difference in [^{3}H]-MX

accumulation in HEK293/ABCG2-482-R2 and HEK293/ABCG2-482-G2 cell lines

compared with counterparts in their control groups. Meanwhile, 3 μM of Ko143

effectively inhibited the efflux activity of ABCG2, resulting in an increased amount of

MX accumulating in cells overexpressed ABCG2. By contrast, treatment with either

OTS964 or Ko143 did not significantly affect the intracellular accumulation level of MX

in drug-sensitive cells. Together, these results demonstrated that OTS964 at 3 μM could

inhibit ABCG2-mediated efflux of MX, which is an established substrate of ABCG2, in

R482T-mutant-ABCG2-overexpressing cell line.
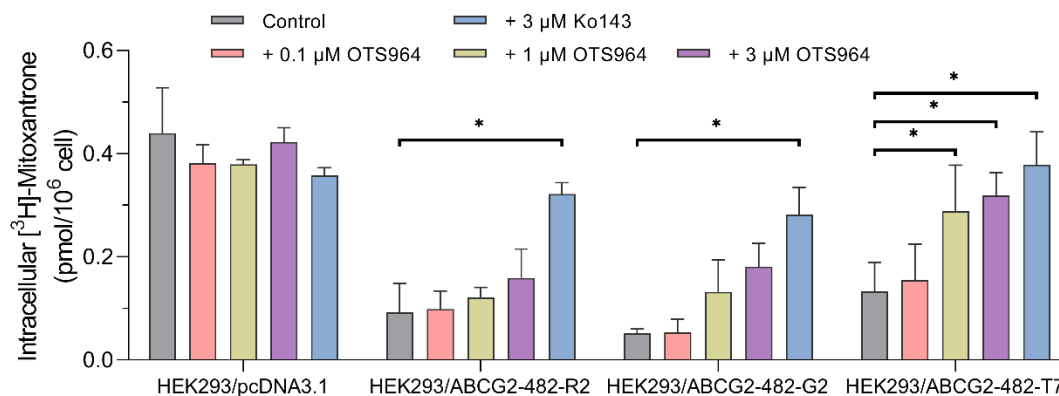
Figure 5. Effects of OTS964 on transport function mediated by ABCG2.

The intracellular accumulation of [^{3}H]-MX in ABCG2-transfected HEK293 cells (HEK293/ABCG2-482-R2, HEK293/ABCG2-482-G2, and HEK293/ABCG2-482-T7) and their corresponding drug-sensitive cells HEK293/pcDNA3.1 after 2 h of pretreatment with vehicle, OTS964, or Ko143. Data are expressed as mean ± SD from a representative of three independent experiments. *$p < 0.05$ versus the respective control group.
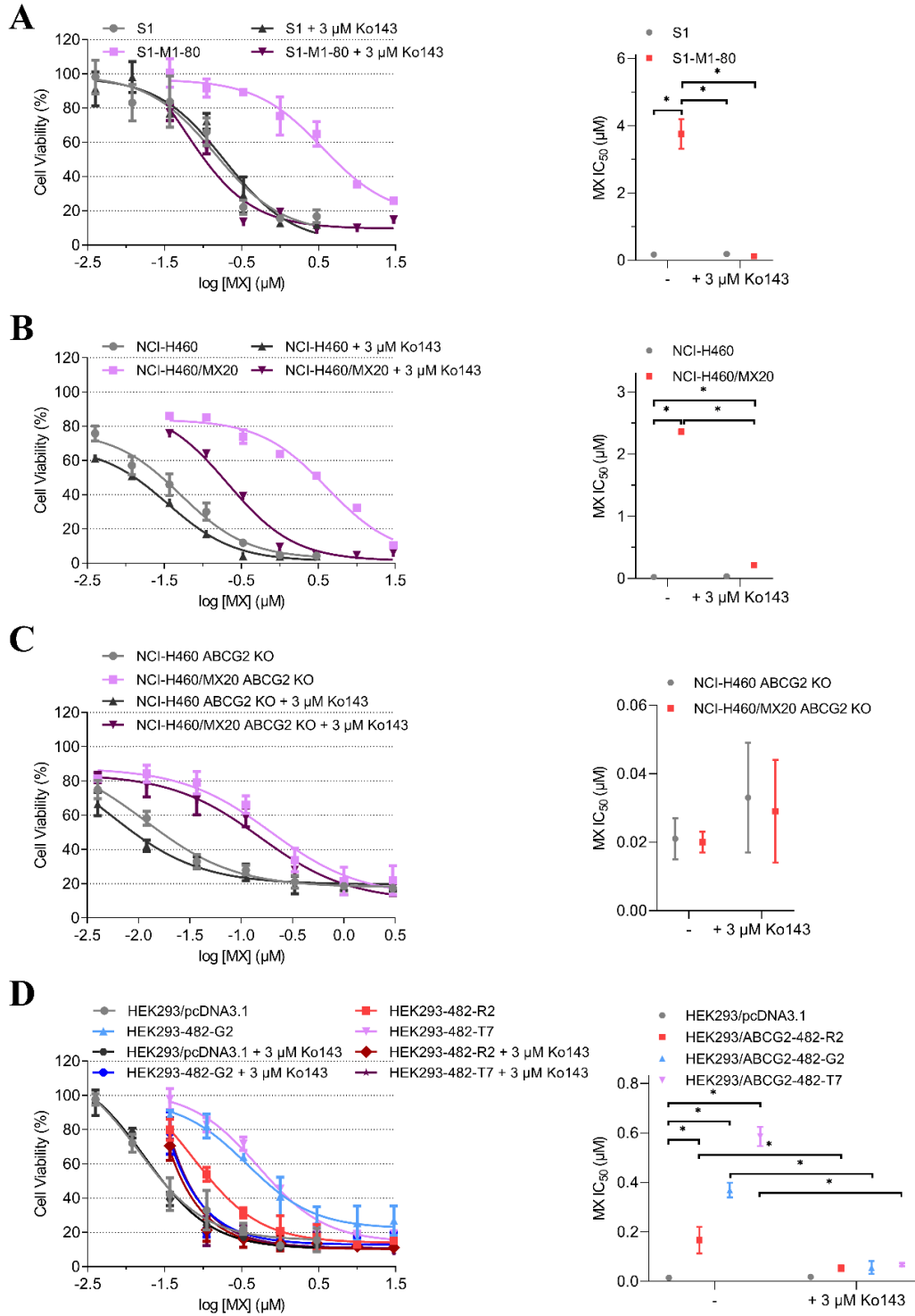
3.1.3 OTS964 stimulated ATPase activity of ABCG2.

ATP hydrolysis is an energy requirement for substrate-drugs transported by ABCG2 across the cell membrane against concentration gradient, thus an ATPase assay was performed. ABCG2-mediated ATP hydrolysis was assessed in membrane vesicles after incubation with serial concentrations of OTS964 with or without an inhibitor to ABCG2 ATPase activity. As indicated by Fig. 6, OTS964 within 40 μM stimulated ABCG2 ATPase activity to a maximum of 171.7% of basal activity and achieved 50% of maximum stimulatory activity at 32.5 μM. Herein, CYB-2 served as an inhibitor to ABCG2 ATPase activity [69]. When incubating with 1 μM of CYB-2, the stimulatory effect of OTS964 on ABCG2 ATPase was antagonized to the basal level. These results suggested that OTS964 can bind to the drug-binding pocket of ABCG2, and thereby may

be a potential substrate of ABCG2.
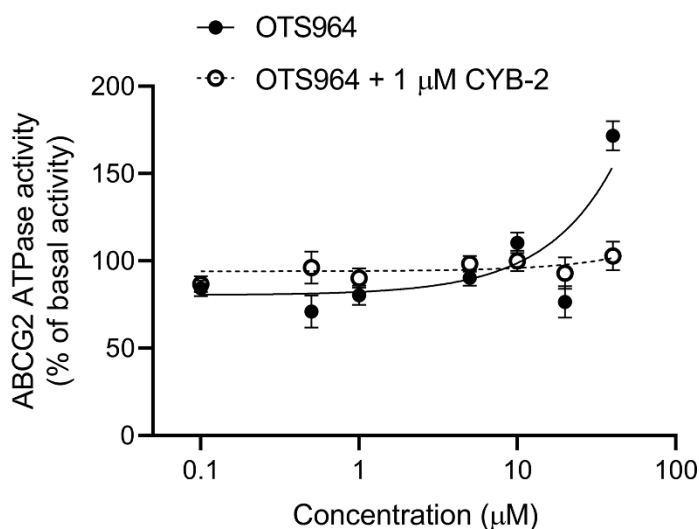
Figure 6. Effects of OTS964 on ATPase activity mediated by ABCG2.

Effects of 0-40 μM OTS964 with or without 1 μM CYB-2 on ATPase activity of ABCG2.

Concentration of OTS964 was plotted against basal level (without OTS964) of ABCG2

ATPase activity. Data are expressed as mean ± SD from a representative of three

independent experiments.

3.1.4 OTS964 docks into the substrate-binding site of human ABCG2 protein.

According to above ATPase results, OTS964 had a stimulatory effect due to its

interaction at the drug-binding pocket. To assess this, we applied a docking simulation in

the MX-binding site of ABCG2 protein (6VXI). The results showed that OTS964 docked

into ABCG2 substrate-binding site with an affinity score of -8.4 kcal/mol. Details of the

ligand-receptor interaction are displayed in Fig. 7. OTS964 is positioned and stabilized in

a hydrophobic cavity formed by Phe431, Phe432, Phe439 (chain A), and Val442, Phe439,

Phe432, Phe405 (chain B). Additionally, OTS964 was stabilized by *pi-pi* stacking

interactions formed with Phe439 in both chains. The ionized amine group of OTS964 was

stabilized by a hydrogen bond formed with Asn436. To further evaluate the possibility

that OTS964 may be a human ABCG2 substrate, a verified ABCG2 substrate MX was

analyzed under the same parameters. As indicated by Fig. 7 and Fig. 8, the poses of

docked OTS964 and MX (docking score: -9.2 kcal/mol) overlapped and shared similar

binding sites. Combined with ATPase data, the results from molecular docking analysis

corroborated that OTS964 interacts with drug-binding pocket of ABCG2 and behaves as

a substrate for ABCG2 transporter.
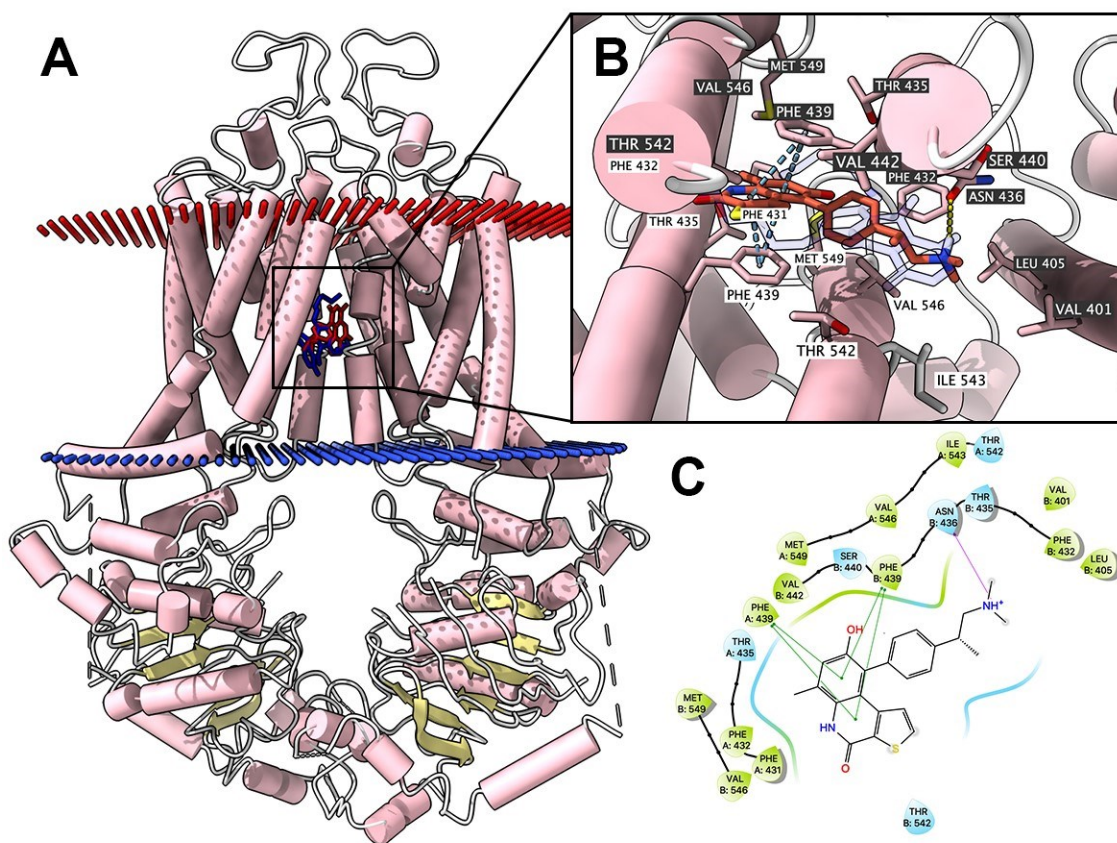
Figure 7. Highest-scoring docked pose of OTS964 within human ABCG2 at

substrate-binding site.

A) Overview of MX and best-scoring pose of OTS964 in drug-binding pocket of ABCG2

protein. MX and OTS964 are displayed as colored sticks, blue: MX; red: OTS964. **B)**

Details of interactions between OTS964 and ABCG2 binding pocket. Predicted bonds are

displayed as colored dash lines: hydrogen bond: yellow; *pi-pi* stacking: blue. Labels with

white or black background indicate chain A or B, respectively. **C)** 2D OTS964-ABCG2

interaction. Important amino acids are displayed as colored bubbles (green: hydrophobic;

blue: polar). Predicted bonds are displayed as colored lines: green line: *pi-pi* stacking;

purple line with arrow: hydrogen bond.
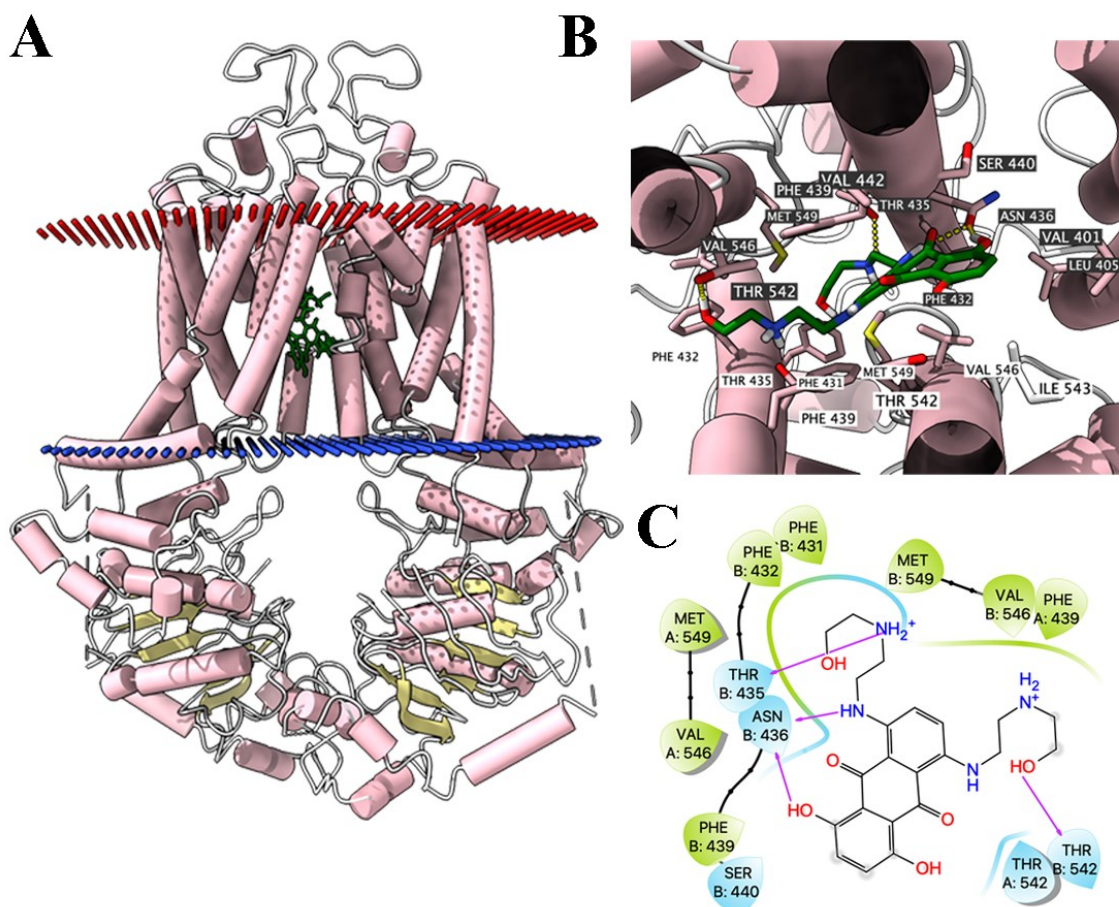
Figure 8. Highest-scoring docked pose of MX within human ABCG2 at substrate-binding site.

A) Overview of the best-scoring pose of MX in drug-binding pocket of ABCG2 protein.

B) Details of interactions between MX and ABCG2 binding pocket. Predicted bonds are

displayed as colored dash lines: hydrogen bond: yellow. Labels with white or black background indicate chain A or B, respectively. **C)** 2D MX-ABCG2 interaction. Important amino acids are displayed as colored bubbles (green: hydrophobic; blue: polar). Predicted bonds are displayed as colored lines: purple line with arrow: hydrogen bond.

3.1.5 OTS964, at a low-concentration and with long-exposure times, decreases the anticancer efficacy of substrate-drugs in cells overexpressed ABCG2.

Some repurposed compounds behave as chemosensitizers or substrates based on different cellular settings caused by ABC transporters [70, 71]. Hence, an MTT assay was performed to examine the ability of OTS964 to restore drug sensitivity in MDR cells mediated by ABCG2. Due to the high cytotoxic nature of OTS964, 10 nM was selected as the maximum non-toxic concentration (the concentration at which cell viability rate was more than 80%) to prevent overlapping effect. In this section, the value of RF was used to assess the ability of OTS964 or known ABCG2 inhibitor to antagonize ABCG2-mediated MDR. Table 3 summarized the IC_{50} and RF values for anticancer drugs, which are substrate-drugs to ABCG2 transporter, with or without OTS964 or Ko143 at non-toxic concentrations. As shown in Fig. 9A, 5 nM and 10 nM of OTS964 promoted MX-resistant in S1-M1-80 cells, as evidenced by the increased IC_{50} value of MX and the increased RF value for MX from 19.6-fold to 61.5- and 57.6-fold, respectively, in resistant S1-M1-80 cells relative to those cells without a modulator (Table 3), and more importantly, without affecting the MX sensitivity in parental S1 cells. By contrast, OTS964 at 5 or 10 nM did not significantly affect IC_{50} values for TPT or SN-38 in S1-M1-80 cells relative to their counterparts in S1-M1-80 cells without a modulator (Fig. 9B

and 9C). Additionally, OTS964 showed a similar effect to MX and SN-38 in HEK293/ABCG2-482-G2 cells, but not to TPT, as indicated by Fig. 10A-C and Table 3. Moreover, 3 µM of Ko143 as a positive ABCG2 modulator reversed drug resistance to ABCG2 substrate-drugs (Fig. 9-10 and Table 3). Of note, either OTS964 or Ko143 did not significantly affect cell viability of non-substrate drug CDDP in ABCG2-overexpressing cells. Together, these results demonstrated that OTS964 cannot restore drug efficacy in ABCG2-overexpressing MDR cell lines, but may induce MDR mediated by ABCG2.
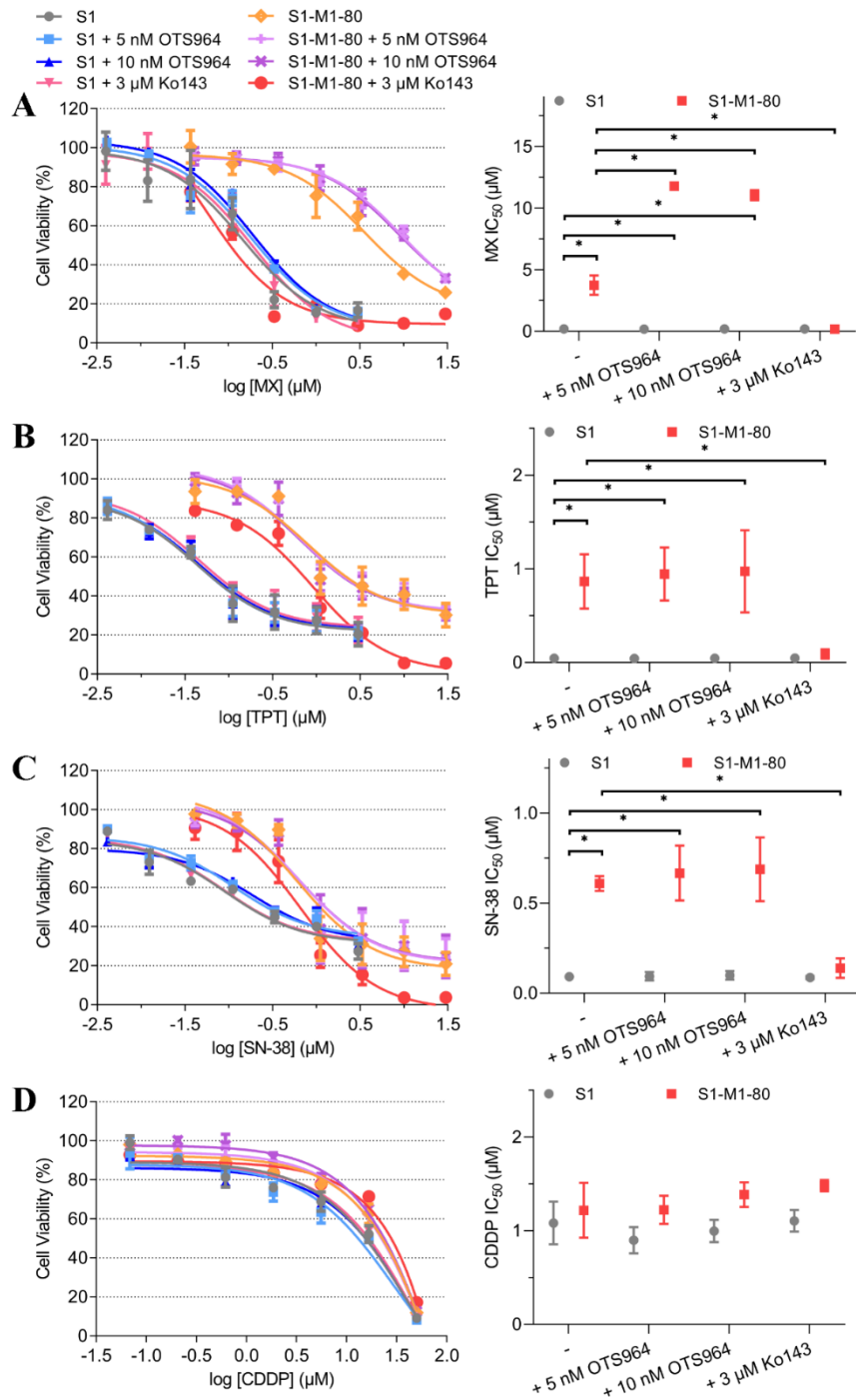
Figure 9. Effects of OTS964 on the cytotoxicity of chemotherapeutic drugs in drug-selected cells overexpressed ABCG2.

The effect of OTS964 on the cytotoxicity of **A)** MX, **B)** TPT, **C)** SN-38, and **D)** CDDP in S1-M1-80 and S1 cells. The GraphPad software [log(inhibitor) vs. response] was used to

fit nonlinear regression and to calculate IC_{50} values. Each dot is expressed as mean ± SD from a representative of three independent experiments. *$p < 0.05$ versus the respective control group.
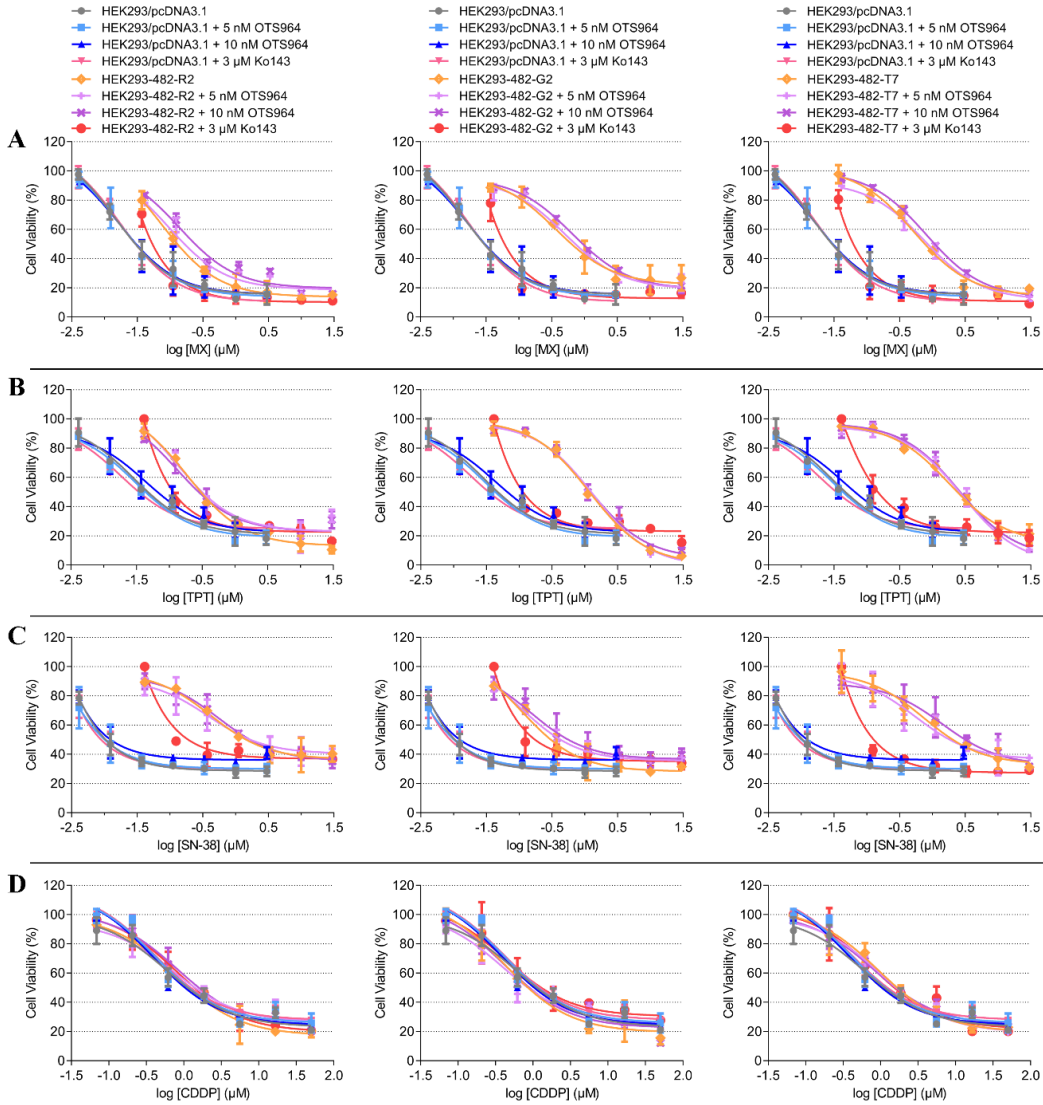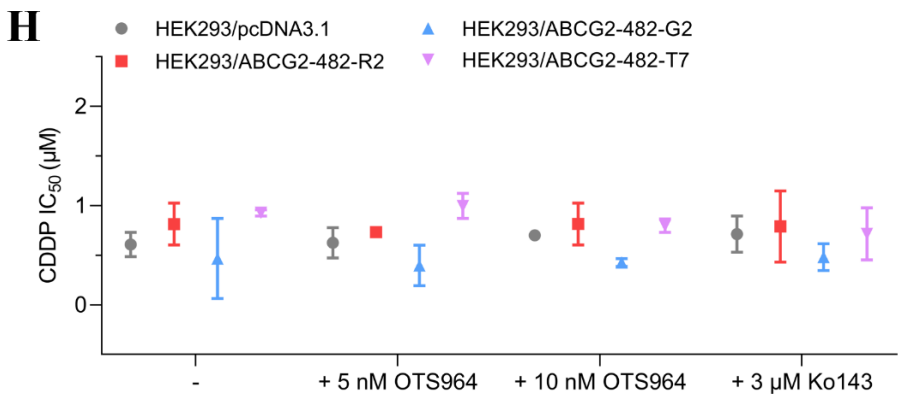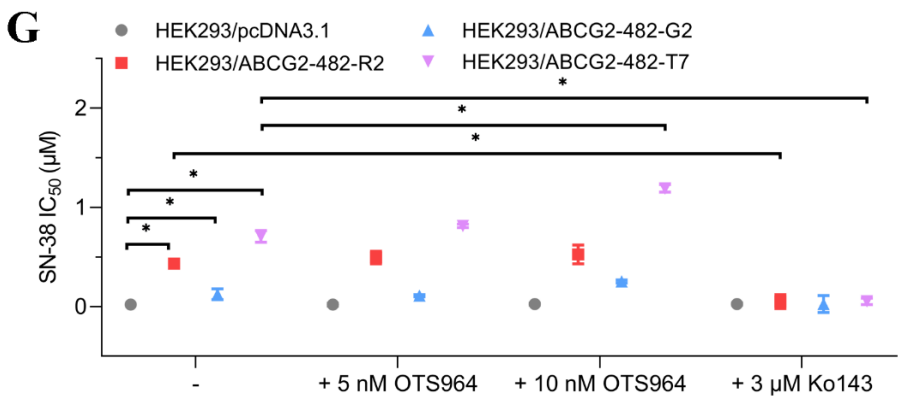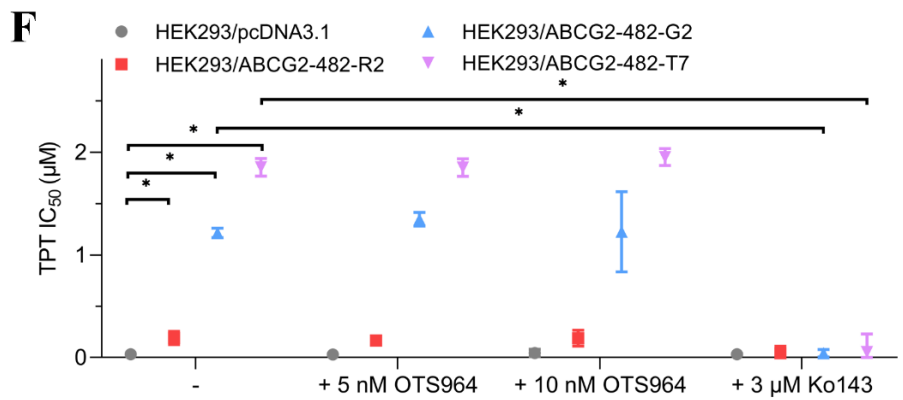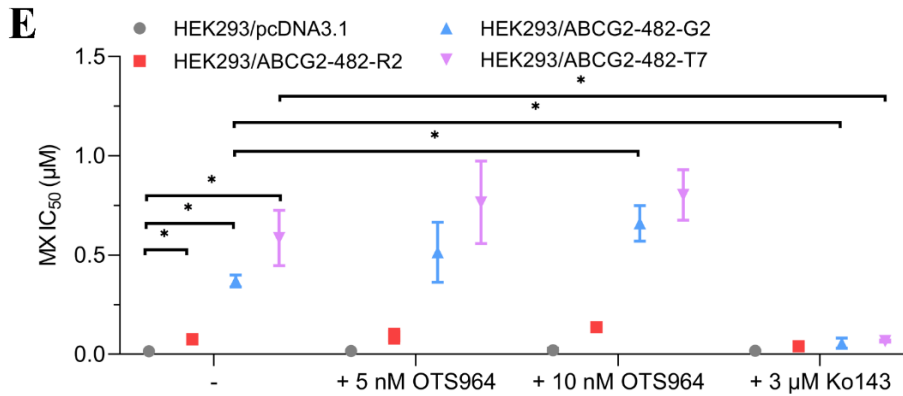
Figure 10. Effects of OTS964 on the cytotoxicity of chemotherapeutic drugs in gene-transfected cells overexpressed ABCG2.

The concentration-response curves for **A)** MX, **B)** TPT, **C)** SN-38, and **D)** CDDP with or without OTS964 or modulator in ABCG2-transfected HEK293 cells (HEK293/ABCG2-482-R2, HEK293/ABCG2-482-G2, and HEK293/ABCG2-482-T7) and HEK293/pcDNA3.1 cells. The IC_{50} values for **E)** MX, **F)** TPT, **G)** SN-38, and **H)** CDDP with or without OTS964 or modulator in ABCG2-transfected HEK293 cells (HEK293/ABCG2-482-R2, HEK293/ABCG2-482-G2, and HEK293/ABCG2-482-T7) and HEK293/pcDNA3.1 cells. The GraphPad software [log(inhibitor) vs. response] was used to fit nonlinear regression and to calculate IC_{50} values. Each dot is expressed as mean $\pm$ SD from a representative of three independent experiments. *$p < 0.05$ versus the respective control group.

Table 3. The anticancer effectiveness of chemotherapeutic drugs with or without modulator in ABCG2-overexpressing cell lines.

Treatment	$IC_{50}{}^{a} \pm$ SD (µM) (RF[b])	
	S1	S1-M1-80
MX	0.192 ± 0.134 (1.000)	3.752 ± 0.781 (19.567) *
+ OTS964 5 nM	0.179 ± 0.011 (0.933)	11.785 ± 0.078 (61.466) *
+ OTS964 10 nM	0.190 ± 0.010 (0.989)	11.050 ± 0.410 (57.632) *
+ Ko143 3 µM	0.201 ± 0.066 (1.050)	0.175 ± 0.102 (0.912)
TPT	0.044 ± 0.001 (1.000)	0.866 ± 0.289 (19.720) *
+ OTS964 5 nM	0.042 ± 0.007 (0.962)	0.945 ± 0.284 (21.512) *
+ OTS964 10 nM	0.045 ± 0.003 (1.023)	0.974 ± 0.439 (22.181) *

+ Ko143 3 μM	0.046 ± 0.004 (1.056)	0.091 ± 0.050 (2.082)
SN-38	0.091 ± 0.006 (1.000)	0.609 ± 0.041 (6.717) [*]
+ OTS964 5 nM	0.094 ± 0.023 (1.038)	0.667 ± 0.152 (7.364) [*]
+ OTS964 10 nM	0.099 ± 0.024 (1.097)	0.688 ± 0.177 (7.593) [*]
+ Ko143 3 μM	0.087 ± 0.008 (0.965)	0.139 ± 0.054 (1.529)
CDDP	1.083 ± 0.228 (1.000)	1.218 ± 0.293 (1.125)
+ OTS964 5 nM	0.899 ± 0.140 (0.831)	1.223 ± 0.150 (1.130)
+ OTS964 10 nM	0.997 ± 0.119 (0.921)	1.387 ± 0.131 (1.281)
+ Ko143 3 μM	1.106 ± 0.116 (1.022)	1.482 ± 0.060 (1.369)
	HEK293/pcDNA3.1	HEK293/ABCG2-482-R2
MX	0.015 ± 0.002 (1.000)	0.076 ± 0.023 (5.035) [*]
+ OTS964 5 nM	0.017 ± 0.001 (1.100)	0.092 ± 0.035 (6.098) [*]
+ OTS964 10 nM	0.020 ± 0.010 (1.331)	0.137 ± 0.001 (9.071) [*]
+ Ko143 3 μM	0.018 ± 0.001 (1.196)	0.040 ± 0.011 (2.682)
TPT	0.032 ± 0.023 (1.000)	0.191 ± 0.064 (6.046) [*]
+ OTS964 5 nM	0.030 ± 0.003 (0.943)	0.166 ± 0.045 (5.249) [*]
+ OTS964 10 nM	0.044 ± 0.036 (1.391)	0.190 ± 0.077 (6.010) [*]
+ Ko143 3 μM	0.032 ± 0.009 (1.012)	0.042 ± 0.068 (1.318)
SN-38	0.022 ± 0.005 (1.000)	0.433 ± 0.009 (20.076) [*]
+ OTS964 5 nM	0.020 ± 0.013 (0.949)	0.495 ± 0.064 (22.939) [*]
+ OTS964 10 nM	0.027 ± 0.010 (1.269)	0.526 ± 0.094 (24.385) [*]
+ Ko143 3 μM	0.027 ± 0.012 (1.241)	0.051 ± 0.071 (2.363)
CDDP	0.608 ± 0.122 (1.000)	0.814 ± 0.211 (1.339)

	HEK293/ABCG2-482-G2	HEK293/ABCG2-482-T7
+ OTS964 5 nM	0.626 ± 0.152 (1.031)	0.734 ± 0.036 (1.207)
+ OTS964 10 nM	0.700 ± 0.019 (1.152)	0.815 ± 0.212 (1.341)
+ Ko143 3 μM	0.714 ± 0.183 (1.175)	0.790 ± 0.358 (1.300)
	HEK293/ABCG2-482-G2	HEK293/ABCG2-482-T7
MX	0.369 ± 0.030 (24.490) [*]	0.586 ± 0.139 (38.896) [*]
+ OTS964 5 nM	0.514 ± 0.151 (34.114) [*]	0.766 ± 0.208 (50.813) [*]
+ OTS964 10 nM	0.660 ± 0.089 (43.772) [*]	0.803 ± 0.128 (53.295) [*]
+ Ko143 3 μM	0.056 ± 0.026 (3.723)	0.067 ± 0.005 (4.478)
TPT	1.214 ± 0.046 (38.444) [*]	1.854 ± 0.086 (58.736) [*]
+ OTS964 5 nM	1.348 ± 0.066 (42.690) [*]	1.852 ± 0.086 (58.673) [*]
+ OTS964 10 nM	1.226 ± 0.390 (38.853) [*]	1.953 ± 0.082 (61.872) [*]
+ Ko143 3 μM	0.042 ± 0.036 (1.318)	0.054 ± 0.177 (1.722)
SN-38	0.124 ± 0.054 (5.742) [*]	0.708 ± 0.059 (32.804) [*]
+ OTS964 5 nM	0.111 ± 0.009 (5.136) [*]	0.814 ± 0.018 (37.733) [*]
+ OTS964 10 nM	0.254 ± 0.015 (11.764) [*]	1.192 ± 0.038 (55.248) [*]
+ Ko143 3 μM	0.026 ± 0.084 (1.215)	0.053 ± 0.033 (2.470)
CDDP	0.467 ± 0.404 (0.769)	0.928 ± 0.031 (1.527)
+ OTS964 5 nM	0.397 ± 0.204 (0.653)	0.997 ± 0.127 (1.641)
+ OTS964 10 nM	0.426 ± 0.040 (0.701)	0.798 ± 0.067 (1.313)
+ Ko143 3 μM	0.481 ± 0.135 (0.792)	0.716 ± 0.263 (1.179)

[a] IC_{50} values are expressed as mean ± SD from a representative of three independent experiments.

[b] Resistance fold (RF) was calculated by dividing the IC_{50} values of verified substrate-

drugs with or without modulator in drug-sensitive or drug-resistant cells by the IC_{50} values of verified substrate-drugs without modulator in drug-sensitive cells. $^*p < 0.05$ versus the respective control group without modulator.

3.1.6 OTS964 stimulates ABCG2 expression at protein and mRNA level.

It is possible that upregulated MDR-associated ABC transporters contributes to increased resistance and reduced efficacy to substrate-drugs. Thus, a Western blot analysis was conducted to determine the expression level of ABCG2 protein. As presented in Fig. 11A-C, followed by treatment with 5 nM of OTS964 for up to 72 h, no significant change in ABCG2 protein expression was observed in HEK293 cells transfected with wild-type or mutant (R482G and R482T) ABCG2. By contrast, upon 24 h treatment, OTS964 at 40 nM had the ability to increase ABCG2 protein expression level in cells expressing wide-type and R482G-mutant ABCG2 (Fig. 11A and 11B). In addition, OTS964 within 40 nM concentration-dependently upregulated R482T-mutant ABCG2 protein expression in cells expressing R482T-mutant ABCG2, after treated for 24 h (Fig. 11C). Given that ABCG2 protein upregulation could be the result from ABCG2 gene amplification, a qRT-PCR analysis was subsequently carried out. As indicated by Fig. 11D, followed by 24 h treatment with OTS964 at high-concentration, remarkably upregulated ABCG2 mRNA level was observed in HEK293 cells transfected with mutant (R482G and R482T) ABCG2. Together, above results suggested that OTS964 enables upregulation of ABCG2 expression at protein and mRNA levels, which may serve as a reason for increased drug resistance in ABCG2-overexpressing cells.
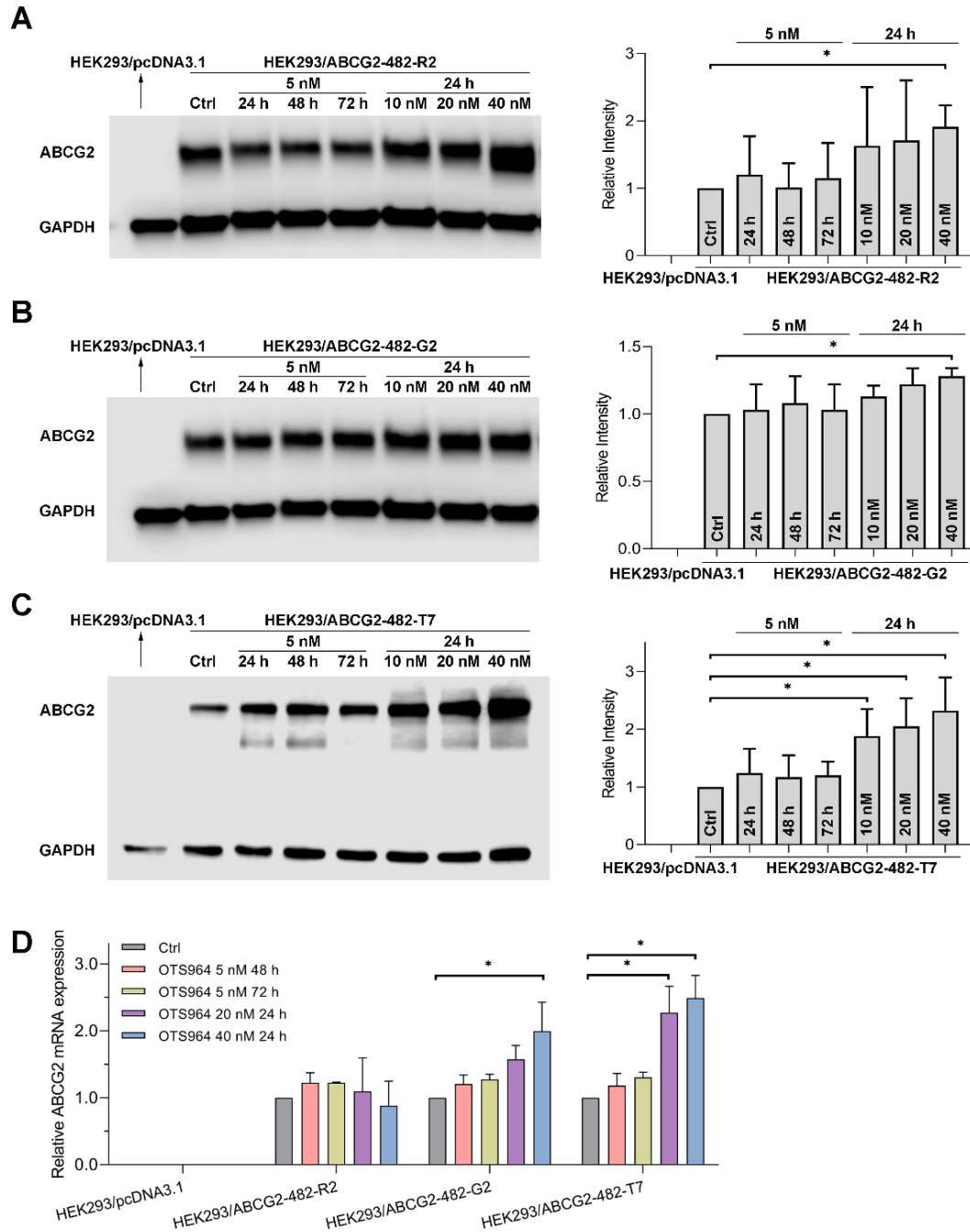
Figure 11. Effects of OTS964 on expression levels of ABCG2 protein and mRNA.

The effect of OTS964 on ABCG2 protein expression in **A)** HEK293/ABCG2-482-R2, **B)**

HEK293/ABCG2-482-G2, and **C)** HEK293/ABCG2-482-T7 cells. **D)** The effect of

OTS964 on ABCG2 mRNA expression in ABCG2-transfected HEK293 cells

(HEK293/ABCG2-482-R2, HEK293/ABCG2-482-G2, and HEK293/ABCG2-482-T7) cells. In the Western blot analysis, the relative density of each protein band was analyzed by Fiji software, and ABCB1 protein expression levels were normalized to GAPDH before comparison. In the qRT-PCR analysis, data were calculated based on the comparative $\Delta\Delta C_T$ method and expressed as the relative fold changes. Data are expressed as mean $\pm$ SD from a representative of three independent experiments. $*p < 0.05$ versus the respective control group.

3.2 PBK/TOPK inhibitor OTS964 resistance is mediated by ABCB1-dependent transport function in cancer: *in vitro* and *in vivo* study

3.2.1 The cytotoxic effect of OTS964 is limited in ABCB1 overexpression cells, and ABCB1 inhibitor sensitizes ABCB1 overexpression cells to OTS964.

The cytotoxic effect of OTS964 was analyzed by an MTT assay in various cell lines, which do or do not overexpress ABCB1. As shown in Fig.12, ABCB1-overexpressing cells were more resistant to OTS964 than their respective drug-sensitive cells, as indicated by the gap between curves of drug-sensitive and resistance cell lines. In detail, the IC_{50} values of OTS964 exhibited significant difference for KB-3-1 ($IC_{50} =$ 1.564 nM) and SW620 ($IC_{50} = 0.892$ nM) cells relative to their corresponding drug-selected sublines KB-C2 ($IC_{50} = 0.216$ μM) and SW620/Ad300 ($IC_{50} = 0.160$ μM) cells (Table 4 and Table 5). Furthermore, *ABCB1* gene-transfected subline (HEK293/ABCB1 and its parental HEK293/pcDNA3.1) and *ABCB1* gene-knockout subline (SW620/Ad300-ABCB1ko and SW620-ABCB1ko) were used to validation. Similarly, in ABCB1-transfected HEK293 cells, the IC_{50} value of OTS964 was significant higher in HEK293/ABCB1 cells ($IC_{50} = 0.102$ μM) than that in HEK293/pcDNA3.1 cells ($IC_{50} =$

8.976 nM) that are transfected with an empty DNA vector (Table 4). The *ABCB1* gene-knockout sublines showed that, upon *ABCB1* gene-knockout, SW620/Ad300-ABCB1ko cells that do not overexpress ABCB1 transporter restored the sensitivity to OTS964 (Fig. 14A and Table 5). In addition, to further investigate ABCB1 transporter and the regulation of OTS964 efficacy, cells were co-incubated with an established ABCB1 inhibitor VPL at 3 μM. As indicated by Table 4 and Table 5, after combined with 3 μM of VPL, the IC$_{50}$ values for OTS964 was significantly attenuated in KB-C2 (decreased from 0.216 μM to 38.937 nM), SW620/Ad300 (decreased from 0.160 μM to 6.180 nM), and HEK293/ABCB1 (decreased from 0.102 μM to 9.544 nM) cells. By contrast, VPL at 3 μM did not significantly affect the cytotoxic effect of OTS964 in drug-sensitive and *ABCB1* gene-knockout cells, as evidenced by the overlapping curves with that of corresponding cells without VPL treatment (Fig. 12).

Meanwhile, DOX, a verified ABCB1 substrate, was used as a reference to compare the degree of reduced efficacy caused by ABCB1-overexpressing. Fig. 13 shows the concentration-response curves and IC$_{50}$ values for DOX with or without VPL in various cell lines. The cytotoxicity of DOX was limited in KB-C2, SW620/Ad300, and HEK293/ABCB1 cells by 40.053-, 66.452-, and 61.620-fold, respectively, relative to their respective parental cells (Table 4 and Table 5). Similarly, DOX-resistant can be re-sensitized by 3 μM of VPL in various drug-selected and gene-transfected cell lines overexpressed ABCB1 transporter, as indicated by the reduced gap in drug-resistant cells with or without VPL, and more importantly, VPL at 3 μM did not significantly affect counterparts in their corresponding parental cell lines (Fig. 13).

Together, above results demonstrated that ABCB1-overexpressing may contribute

41

to OTS964-resistant in these MDR cell lines and be responsible for reduced efficacy in ABCB1-overexpressing cells.

As we previously demonstrated that OTS964 behaves as a substrate-drug for ABCG2, cells transfected with both transporters (B1/G2 cells) were used to corroborated. The cytotoxic activity of OTS964 was limited in B1/G2 cells relative to that in parental PEL cells, and that this effect can be partially re-sensitized by a known inhibitor of ABCB1 or ABCG2 (Fig. 15 and Table 6). These results verified that overexpression of ABCB1 and ABCG2 confers drug resistance to OTS964.
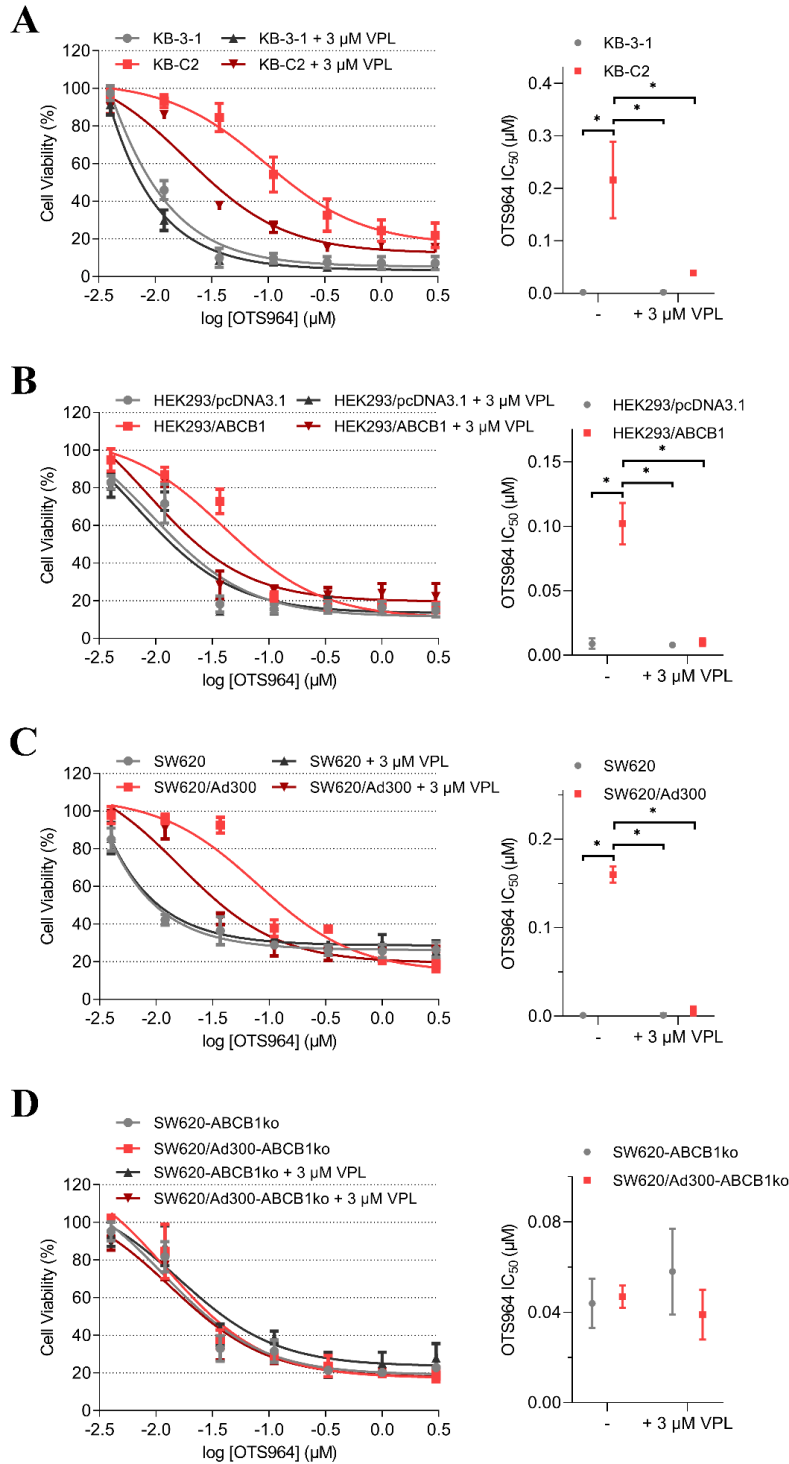
Figure 12. Cytotoxic activity of OTS964 in drug-selected, gene-transfected, or gene-knockout cells and their respective parental cells.

The concentration-response curves and IC_{50} values for OTS964 with or without a verified

ABCB1 inhibitor in **A)** KB-C2 and KB-3-1, **B)** HEK293/ABCB1 and

HEK293/pcDNA3.1, **C)** SW620/Ad300 and SW620, and **D)** SW620/Ad300-ABCB1ko

and SW620-ABCB1ko cells. The GraphPad software [log(inhibitor) vs. response] was

used to fit nonlinear regression and to calculate IC_{50} values. Each dot is expressed as

mean ± SD from a representative of three independent experiments. *$p < 0.05$ versus the

respective control group.
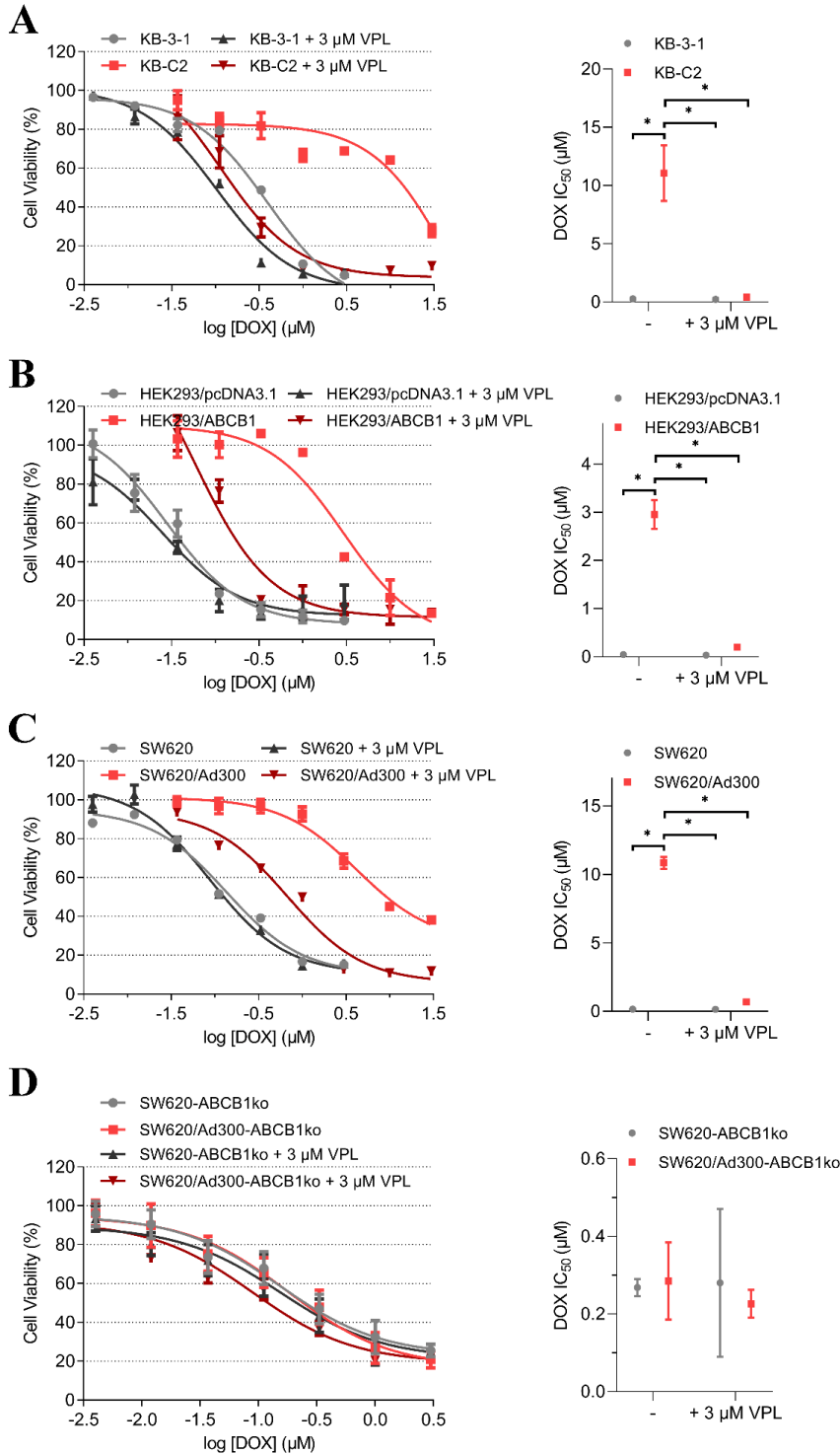
Figure 13. Cytotoxic activity of DOX in drug-selected, gene-transfected, or gene-knockout cells and their respective parental cells.

The concentration-response curves and IC_{50} values for DOX with or without a verified

45

ABCB1 inhibitor in **A)** KB-C2 and KB-3-1, **B)** HEK293/ABCB1 and
HEK293/pcDNA3.1, **C)** SW620/Ad300 and SW620, and **D)** SW620/Ad300-ABCB1ko
and SW620-ABCB1ko cells. The GraphPad software [log(inhibitor) vs. response] was
used to fit nonlinear regression and to calculate IC$_{50}$ values. Each dot is expressed as
mean ± SD from a representative of three independent experiments. *$p < 0.05$ versus the
respective control group.
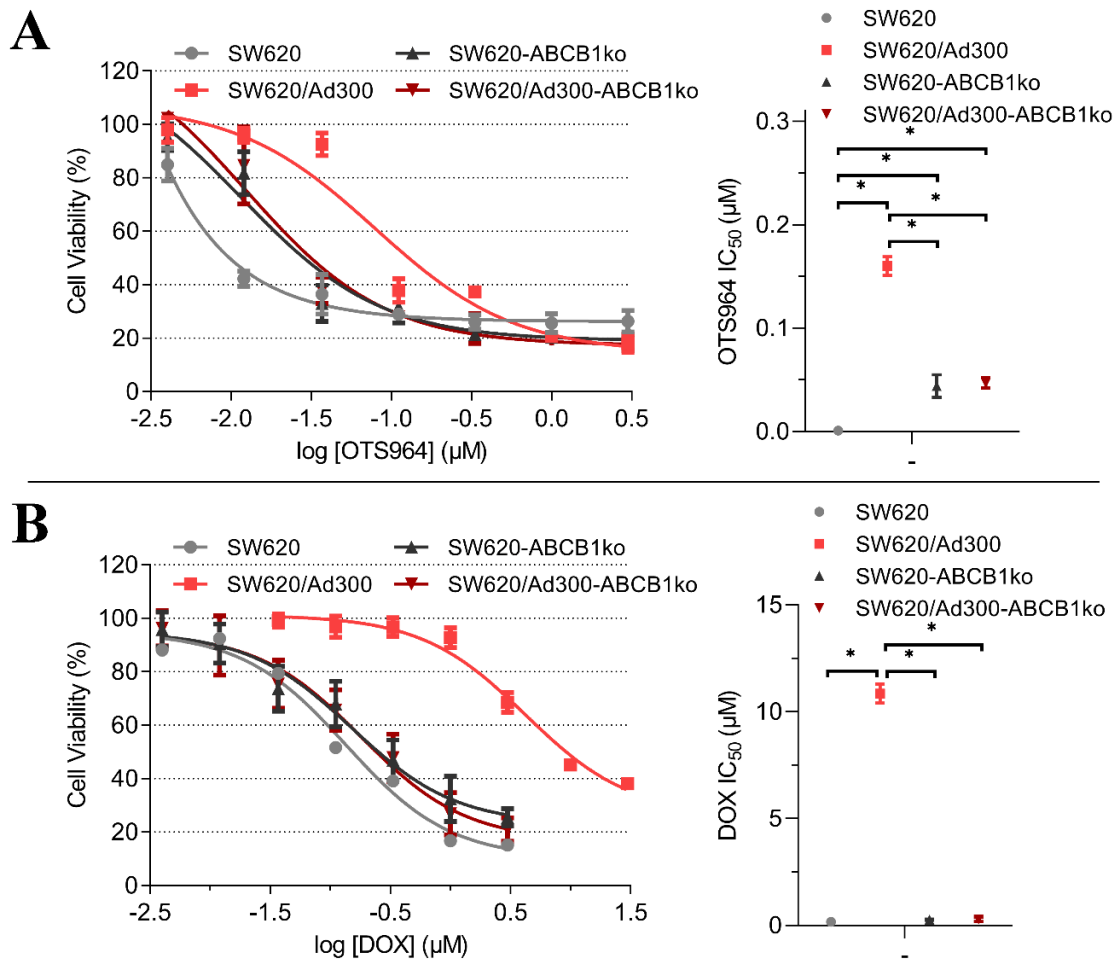
**Figure 14. Cytotoxic activity of OTS964 or DOX in gene-knockout cells and their
respective parental cells.**

The concentration-response curves and IC$_{50}$ values for **A)** OTS964 and **B)** DOX in
SW620/Ad300 and SW620, and SW620/Ad300-ABCB1ko and SW620-ABCB1ko cells.

The GraphPad software [log(inhibitor) vs. response] was used to fit nonlinear regression and to calculate IC_{50} values. Each dot is expressed as mean ± SD from a representative of three independent experiments. *$p < 0.05$ versus the respective control group.
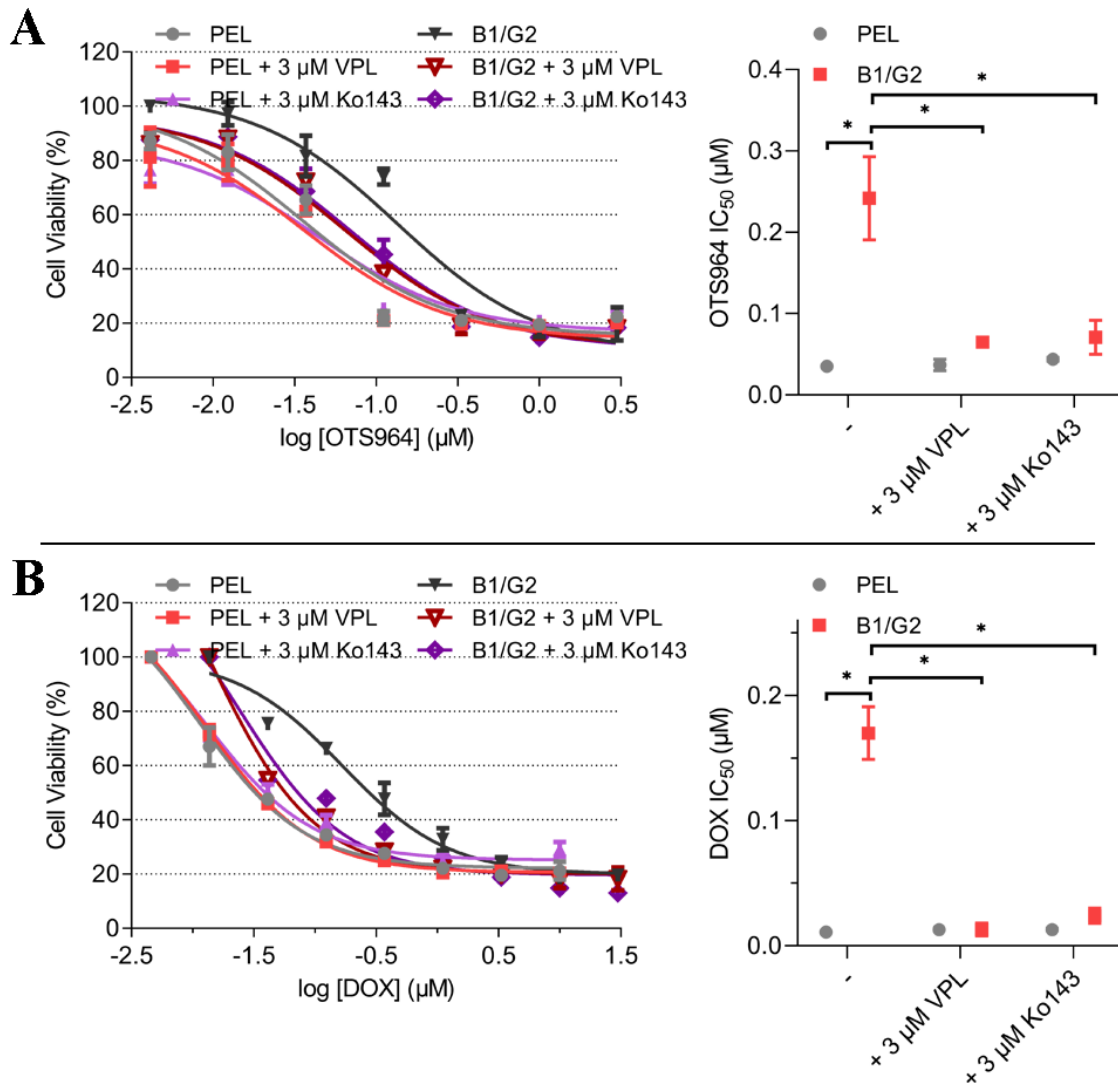
Figure 15. Cytotoxic activity of OTS964 or DOX in cells transfected with both ABCB1 and ABCG2 transporters and its corresponding parental cells.

The concentration-response curves and IC_{50} values for **A)** OTS964 and **B)** DOX with or without a verified ABCB1 or ABCG2 inhibitor in cells transfected with both transporters

(B1/G2 cells) and its corresponding parental cells (PEL cells). The GraphPad software [log(inhibitor) vs. response] was used to fit nonlinear regression and to calculate IC_{50} values. Each dot is expressed as mean ± SD from a representative of three independent experiments. *$p < 0.05$ versus the respective control group.

Table 4. The anticancer effectiveness of OTS964 or DOX in drug-sensitive and ABCB1-overexpressing cell lines.

Treatment	$IC_{50}^{a} \pm SD$ (µM) (RF^{b})	
	KB-3-1	KB-C2
OTS964	0.002 ± 0.002 (1.000)	0.216 ± 0.073 (137.805) *
+ VPL 3 µM	0.002 ± 0.002 (1.481)	0.039 ± 0.004 (24.899)
DOX	0.276 ± 0.012 (1.000)	11.053 ± 2.386 (40.053) *
+ VPL 3 µM	0.227 ± 0.115 (0.822)	0.410 ± 0.203 (1.484)
	HEK293/pcDNA3.1	HEK293/ABCB1
OTS964	0.009 ± 0.004 (1.000)	0.102 ± 0.016 (11.309) *
+ VPL 3 µM	0.008 ± 0.001 (0.907)	0.010 ± 0.003 (1.063)
DOX	0.048 ± 0.008 (1.000)	2.949 ± 0.296 (61.620) *
+ VPL 3 µM	0.035 ± 0.007 (0.740)	0.199 ± 0.028 (4.154)

[a] IC_{50} values are expressed as mean ± SD from a representative of three independent experiments.

[b] Resistance fold (RF) was calculated by dividing the IC_{50} values of verified substrate-drugs with or without modulator in drug-sensitive or drug-resistant cells by the IC_{50} values of verified substrate-drugs without modulator in drug-sensitive cells.

*$p < 0.05$ versus the respective control group without modulator.

Table 5. The anticancer effectiveness of OTS964 or DOX in ABCB1-overexpressing and ABCB1-knockout cell lines.

Treatment	$IC_{50}^{a} \pm SD$ (μM) (RF^{b})	
	SW620	SW620/Ad300
OTS964	0.001 ± 0.001 (1.000)	0.160 ± 0.009 (179.820) [*]
+ VPL 3 μM	0.001 ± 0.002 (1.312)	0.006 ± 0.005 (6.931)
DOX	0.163 ± 0.002 (1.000)	10.845 ± 0.445 (66.452) [*]
+ VPL 3 μM	0.150 ± 0.013 (0.919)	0.684 ± 0.029 (4.191)
	SW620-ABCB1ko	SW620/Ad300-ABCB1ko
OTS964	0.044 ± 0.011 (1.000)	0.047 ± 0.005 (1.056)
+ VPL 3 μM	0.058 ± 0.019 (1.300)	0.039 ± 0.011 (0.891)
DOX	0.268 ± 0.022 (1.000)	0.285 ± 0.099 (1.063)
+ VPL 3 μM	0.280 ± 0.190 (1.045)	0.226 ± 0.036 (0.843)

[a] IC_{50} values are expressed as mean ± SD from a representative of three independent experiments.

[b] Resistance fold (RF) was calculated by dividing the IC_{50} values of verified substrate-drugs with or without modulator in drug-sensitive or drug-resistant cells by the IC_{50} values of verified substrate-drugs without modulator in drug-sensitive cells.

[*] $p < 0.05$ versus the respective control group without modulator.

Table 6. The anticancer effectiveness of OTS964 or DOX with or without modulator in cell line co-expressed with ABCB1 and ABCG2.

Treatment	$IC_{50}^{a} \pm SD$ (μM) (RF^{b})

	PEL	B1/G2
OTS964	0.035 ± 0.006 (1.000)	0.242 ± 0.051 (6.886) [*]
+ VPL 3 μM	0.037 ± 0.007 (1.044)	0.065 ± 0.001 (1.847)
+ Ko143 3 μM	0.044 ± 0.002 (1.247)	0.071 ± 0.021 (2.028)
DOX	0.011 ± 0.003 (1.000)	0.170 ± 0.021 (15.147) [*]
+ VPL 3 μM	0.013 ± 0.001 (1.155)	0.013 ± 0.005 (1.141)
+ Ko143 3 μM	0.013 ± 0.001 (1.151)	0.024 ± 0.006 (2.162)

[a] IC_{50} values are expressed as mean $\pm$ SD from a representative of three independent experiments.

[b] Resistance fold (RF) was calculated by dividing the IC_{50} values of verified substrate-drugs with or without modulator in drug-sensitive or drug-resistant cells by the IC_{50} values of verified substrate-drugs without modulator in drug-sensitive cells.

[*] $p < 0.05$ versus the respective control group without modulator.

3.2.2 OTS964, at a high-concentration and with short-exposure times, increases the intracellular accumulation of [³H]-PTX in cells overexpressed ABCB1.

A [³H]-PTX accumulation assay was conducted to investigate the interaction between OTS964 and ABCB1 transporter. Of note, 4 h short treatment time protected cells from influencing cell viability and other cellular functions, although the concentrations of OTS964 used in this assay was much higher than those for IC_{50} values in respective cell lines. As presented in Fig. 16, 3 μM of OTS964 significantly restored the intracellular [³H]-PTX accumulation from 29% to 82% in KB-C2 cells and from 9% to 35% in HEK293/ABCB1 cells relative to their respective parental cells. Meanwhile, VPL at 3 μM effectively inhibited the efflux activity mediated by ABCB1 transporter,

resulting in an increased amount of PTX accumulating in ABCB1-overexpressing cells. In contrast, treatment with either OTS964 or VPL did not significantly affect the intracellular accumulation level of [^{3}H]-PTX in KB-3-1 and HEK293/pcDNA3.1 cells. Together, these results indicated that OTS964 at high-concentration inhibits the transport function mediated by ABCB1 transporter, which may result from its competition with PTX being pumped out from ABCB1-overespressing cells.
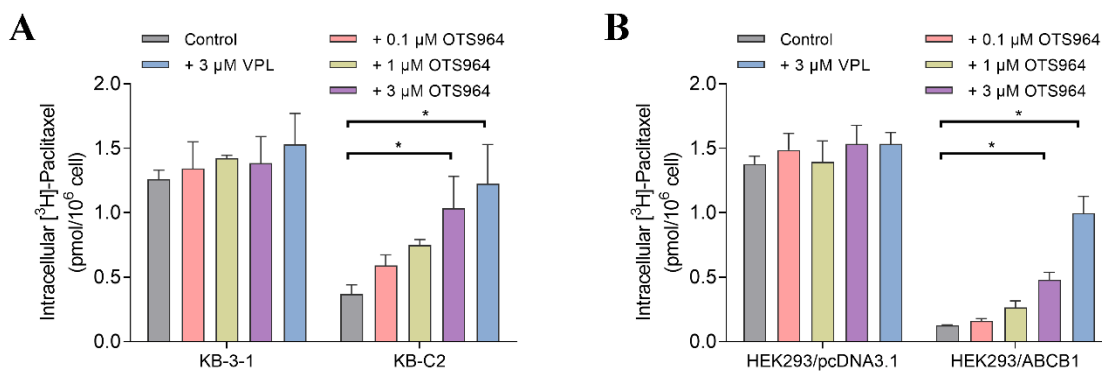
Figure 16. Effects of OTS964 on transport function mediated by ABCB1.

The intracellular accumulation of [^{3}H]-PTX in **A)** KB-C2 and KB-3-1 and **B)** HEK293/ABCB1 and HEK293/pcDNA3.1 cells after 2 h of pretreatment with vehicle, OTS964, or VPL. Data are expressed as mean ± SD from a representative of three independent experiments. *$p < 0.05$ versus the respective control group.

3.2.3 OTS964 stimulated ATPase activity of ABCB1.

Given that ABC transporters utilize energy from ATP hydrolysis to pump out substrate-drugs, an ATPase assay was performed to further explore the possible interaction between OTS964 and ABCB1. As indicated by Fig. 17, OTS964 within 40 µM exhibited stimulating effect on ABCB1 ATPase activity. The ATPase activity reached

a peak of 164.3% of basal activity and achieved 50% of maximum (EC_{50}) at 12.7 µM. It has reported that tepotinib is an inhibitor for ABCB1 ATPase activity [72]. When incubating with 1 µM of tepotinib, the stimulatory effect of OTS964 on ABCB1 ATPase was antagonized and no significant stimulation was observed. Above results demonstrated that OTS964 can bind to the drug-binding pocket of ABCB1, and thereby may be a potential substrate for ABCB1 transporter.
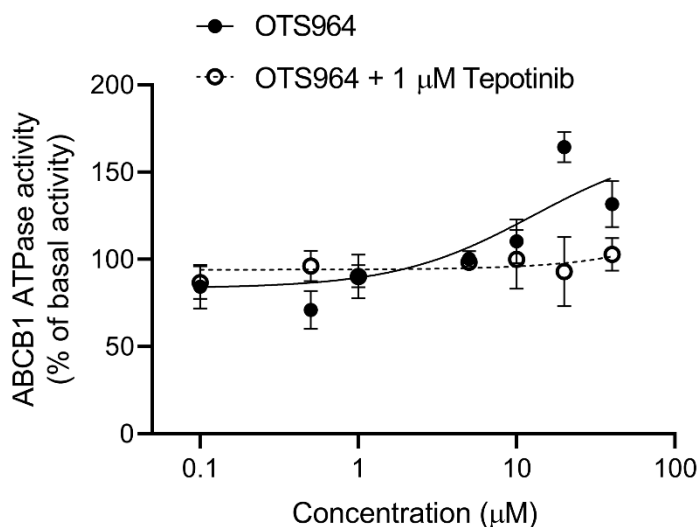
Figure 17. Effects of OTS964 on ATPase activity mediated by ABCB1.

Effects of 0-40 µM OTS964 with or without 1 µM tepotinib on ATPase activity of ABCB1. Concentration of OTS964 was plotted against basal level (without OTS964) of ABCB1 ATPase activity. Data are expressed as mean ± SD from a representative of three independent experiments.

3.2.4 OTS964 docks into the substrate-binding site of human ABCB1 protein.

From ATPase results above, OTS964 exhibited a stimulatory effect due to its interaction at the drug-binding pocket. To evaluate this, docking simulation in the ATPase-stimulator (PTX) binding site of ABCB1 protein (6QEX) was applied. The docking simulation indicated that OTS964 can dock into the ABCB1 substrate-binding

site with an affinity score of -7.2 kcal/mol. Detailed ligand-receptor interaction of

OTS964 and ABCB1 was presented in Fig. 18. The optimal scoring pose of OTS964

coincided with the ligand-binding cavity formed by Leu65, Met68, Met69, Phe72,

Phe336, Tyr953, Phe983, Met986, and Ala987 in the transmembrane region. OTS964 was

positioned and stabilized by a *pi-pi* stacking interaction composed of residue Phe983.

Also, the ionized amine group under pH 7.4 of OTS964 was stabilized by a cation-*pi*

interaction formed with Phe72 and a hydrogen bond formed with Tyr953. To further

assess the possibility that OTS964 may be a substrate for ABCB1, a verified ABCB1

substrate PTX was analyzed under the same parameters. Fig. 19 depicted the detailed

interaction of PTX and ABCB1. The poses of docked OTS964 and PTX (docking score: -

9.8 kcal/mol) overlapped, suggesting that OTS964 possibly shares a similar binding site

with ABCB1 substrates, and thereby has substrate-like behaviors.
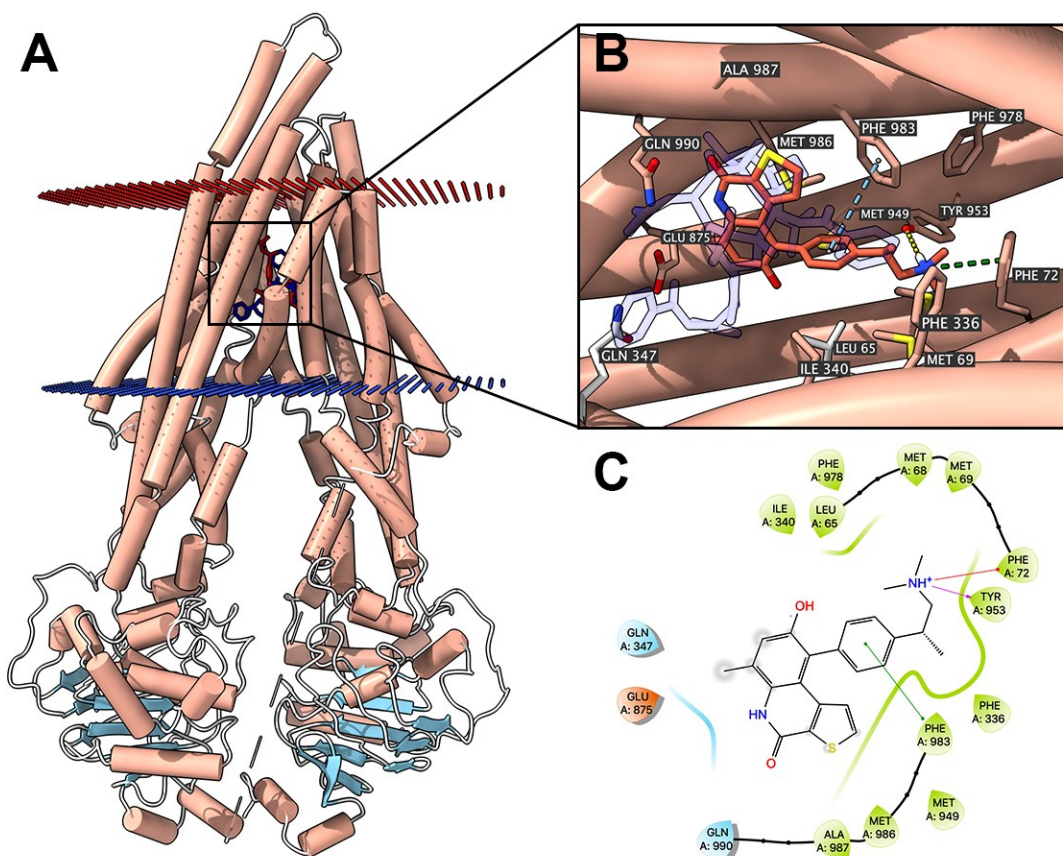
Figure 18. Highest-scoring docked pose of OTS964 within human ABCB1 at substrate-binding site.

A) Overview of PTX and the best-scoring pose of OTS964 in the drug-binding pocket of ABCB1 protein. PTX and OTS964 are displayed as colored sticks, blue: PTX; red: OTS964. **B)** Details of interactions between OTS964 and ABCB1 binding pocket. Predicted bonds are displayed as colored dash lines: hydrogen bond: yellow; *pi-pi* stacking: blue; cation-*pi* interaction: green. **C)** 2D OTS964-ABCB1 interaction. Important amino acids are displayed as colored bubbles (green: hydrophobic; blue: polar; red: positively charged). Predicted bonds are displayed as colored lines: green line: *pi-pi* stacking; purple line with arrow: hydrogen bond; red line: cation-*pi* interaction.
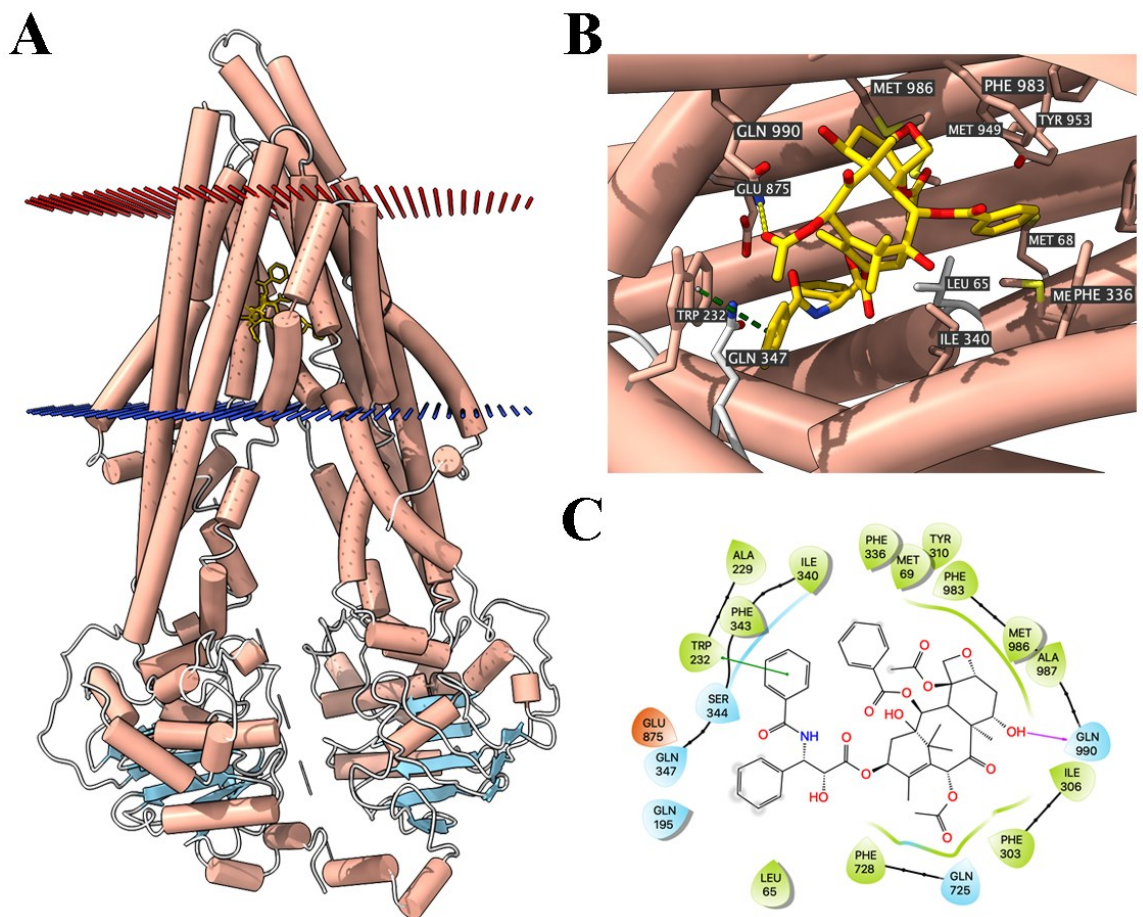
Figure 19. Highest-scoring docked pose of PTX within human ABCB1 at substrate-binding site.

A) Overview of the best-scoring pose of PTX in the drug-binding pocket of ABCB1 protein. **B)** Details of interactions between PTX and ABCB1 binding pocket. Predicted bonds were displayed as colored dash lines: hydrogen bond: yellow; *pi-pi* interaction: green. **C)** 2D PTX-ABCB1 interaction. Important amino acids were displayed as colored bubbles (green: hydrophobic; blue: polar; red: positively charged). Predicted bonds were displayed as colored lines: green line: *pi-pi* stacking; purple line with arrow: hydrogen bond.

3.2.5 OTS964, at a low-concentration and with long-exposure times, decreases the anticancer efficacy of substrate-drugs in cells overexpressed ABCB1.

It has reported that some repurposed compounds can work as chemosensitizers or substrate-drugs based on different cellular situations induced by MDR-associated ABC transporters [70, 71]. Above [^{3}H]-PTX accumulation results suggested that OTS964, at high-concentration and with short-time treatments, behaves like a chemosensitizer to antagonize MDR by competing with PTX for drug efflux. Thus, it is possible that OTS964 works as a modulator to restore efficacy of other ABCB1 substrate-drugs. To this end, an MTT assay was performed. Similarly, to circumvent additive toxic effect from OTS964 and other substrate-drugs, low concentrations (5 nM and 10 nM) of OTS964 were selected for the MTT assay to determine its reversal effect. The concentration-response curves and IC$_{50}$ values for chemotherapeutic drugs with or without OTS964 or modulator in ABCB1-overexpressing cells were presented in Fig. 20 and Fig. 21. Surprisingly, after 72 h of treatment, instead of reversing MDR, OTS964 induced the drug resistance to substrate-drugs of ABCB1 in resistant cells, as indicated by significantly increased IC$_{50}$ and RF values of other substrate-drugs after combined with OTS964, and these effects were not found in their respective parental cells (Fig. 20-21). In detail, as indicated by Table 7, the RF values for PTX, DOX, and VCR increased from 347-fold to 458-fold, from 40-fold to 49-fold, and from 202-fold to 316-fold, respectively, in KB-C2 cells co-treated with 10 nM of OTS964. Similar effects were also observed in ABCB1-transfected HEK293 cells (Fig. 21 and Table 7). Moreover, 3 μM of VPL was used as a positive ABCB1 inhibitor and significantly reversed the substrate resistance in KB-C2 and HEK293/ABCB1 cells (Fig. 20-21). Neither OTS964 nor VPL

affected the cell viability of non-substrate drug CDDP (Fig. 20D and Fig. 21D). Together,

above results demonstrated that rather than restoring the cytotoxic effect of other ABCB1

substrate-drugs, OTS964 may promote the drug resistance mediated by ABCB1.
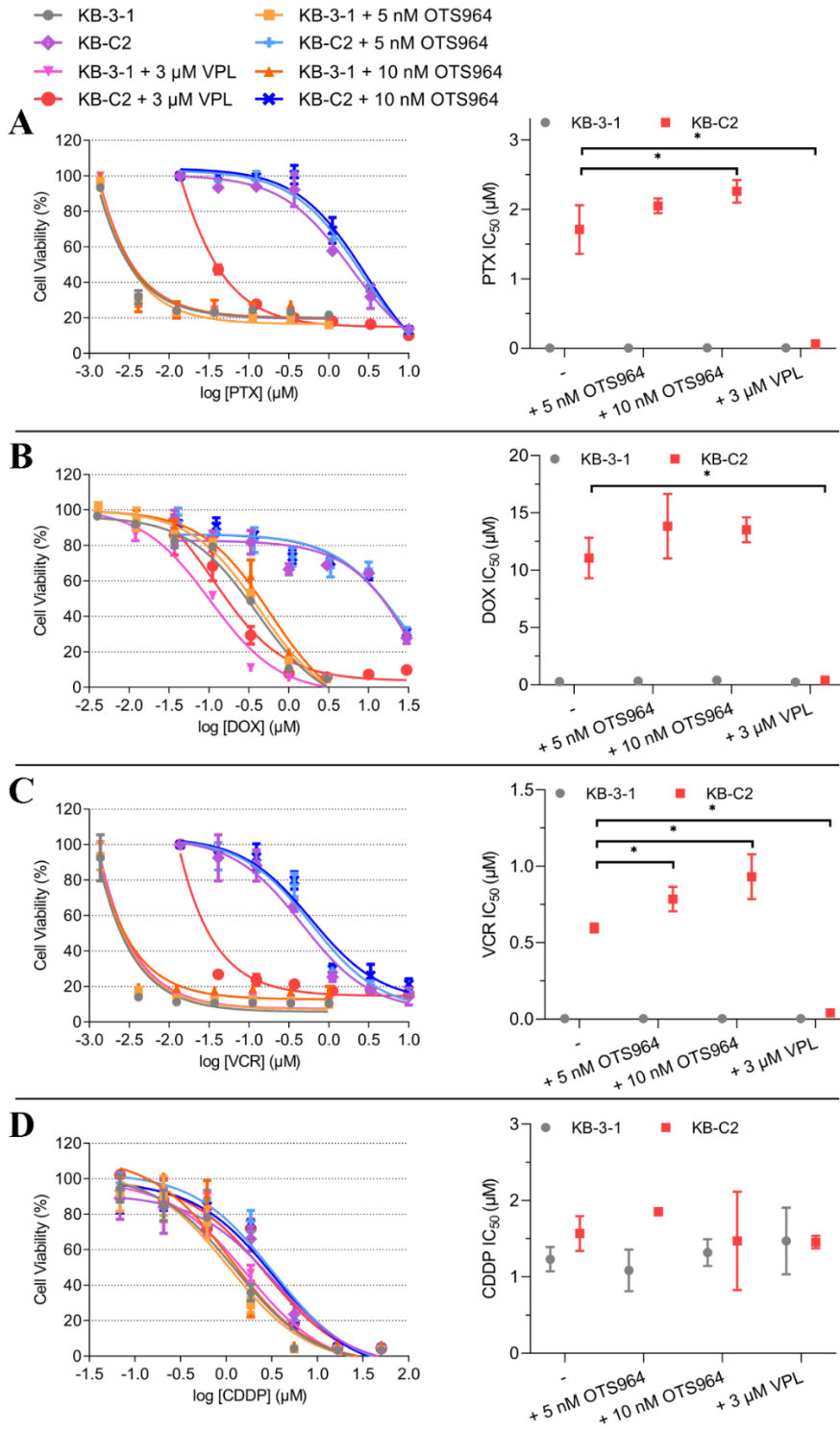
Figure 20. Effects of OTS964 on the cytotoxicity of chemotherapeutic drugs in drug-selected cells overexpressed ABCB1.

The effect of OTS964 on the cytotoxicity of **A)** PTX, **B)** DOX, **C)** VCR, and **D)** CDDP in

KB-C2 and KB-3-1 cells. The GraphPad software [log(inhibitor) vs. response] was used to fit nonlinear regression and to calculate IC_{50} values. Each dot is expressed as mean $\pm$ SD from a representative of three independent experiments. *$p < 0.05$ versus the respective control group.
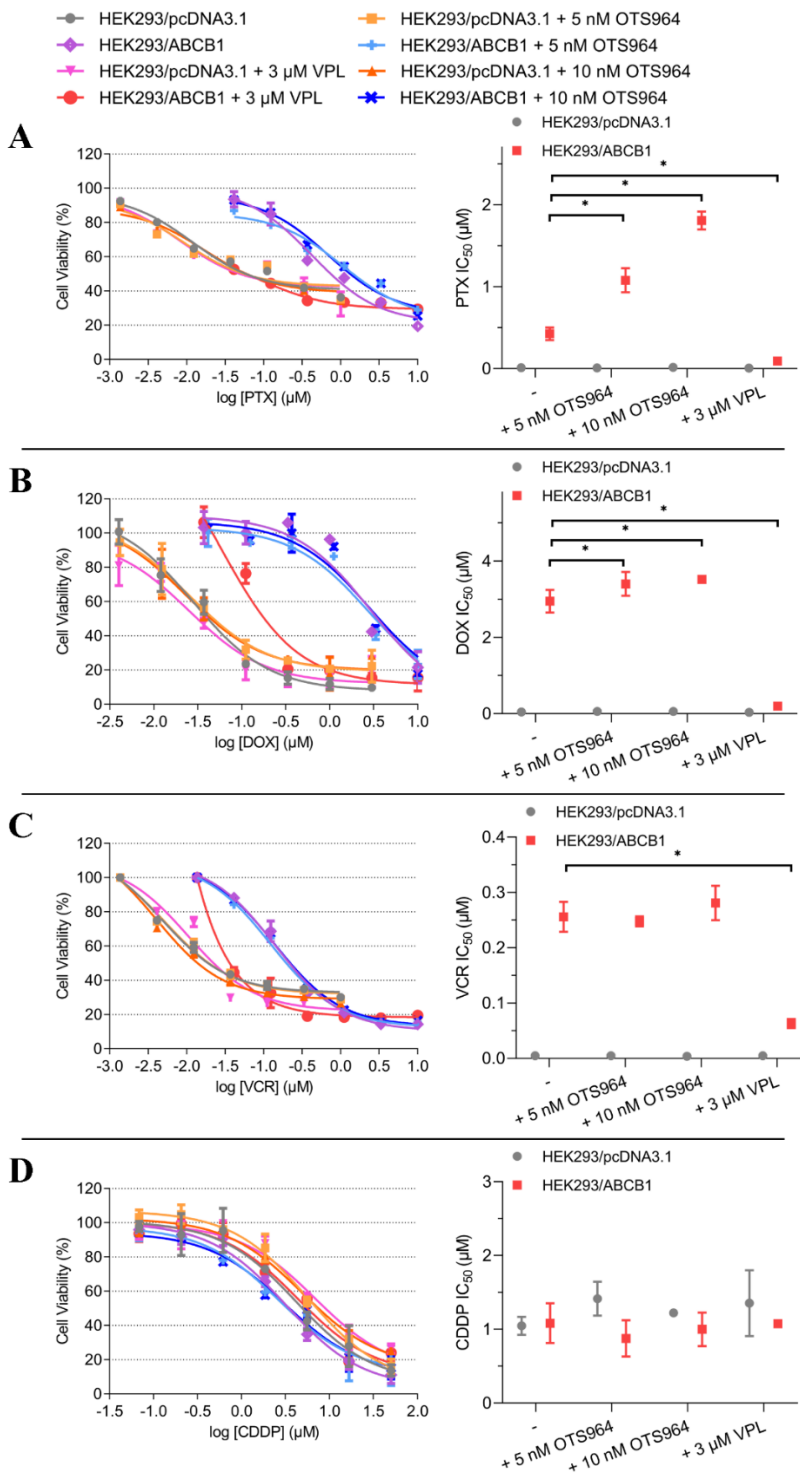
Figure 21. Effects of OTS964 on the cytotoxicity of chemotherapeutic drugs in gene-transfected cells overexpressed ABCB1.

The effect of OTS964 on the cytotoxicity of **A)** PTX, **B)** DOX, **C)** VCR, and **D)** CDDP in

HEK293/ABCB1 and HEK293/pcDNA3.1 cells. The GraphPad software [log(inhibitor) vs. response] was used to fit nonlinear regression and to calculate IC_{50} values. Each dot is expressed as mean $\pm$ SD from a representative of three independent experiments. *$p <$ 0.05 versus the respective control group.

Table 7. The anticancer effectiveness of chemotherapeutic drugs with or without modulator in ABCB1-overexpressing cell lines.

Treatment	$IC_{50}{}^a \pm$ SD (μM) (RF[b])	
	KB-3-1	KB-C2
PTX	0.005 $\pm$ 0.001 (1.000)	1.711 $\pm$ 0.351 (346.672) *
+ OTS964 5 nM	0.005 $\pm$ 0.001 (0.966)	2.051 $\pm$ 0.105 (415.459) *
+ OTS964 10 nM	0.006 $\pm$ 0.001 (1.163)	2.261 $\pm$ 0.164 (458.110) *
+ VPL 3 μM	0.006 $\pm$ 0.001 (1.236)	0.064 $\pm$ 0.001 (12.900)
DOX	0.276 $\pm$ 0.012 (1.000)	11.053 $\pm$ 1.766 (40.053) *
+ OTS964 5 nM	0.331 $\pm$ 0.009 (1.198)	13.835 $\pm$ 2.815 (50.136) *
+ OTS964 10 nM	0.405 $\pm$ 0.053 (1.467)	13.525 $\pm$ 1.082 (49.013) *
+ VPL 3 μM	0.227 $\pm$ 0.115 (0.822)	0.410 $\pm$ 0.203 (1.484)
VCR	0.003 $\pm$ 0.001 (1.000)	0.597 $\pm$ 0.029 (202.238) *
+ OTS964 5 nM	0.003 $\pm$ 0.001 (0.945)	0.785 $\pm$ 0.080 (266.113) *
+ OTS964 10 nM	0.003 $\pm$ 0.001 (0.951)	0.932 $\pm$ 0.146 (315.850) *
+ VPL 3 μM	0.003 $\pm$ 0.001 (1.068)	0.040 $\pm$ 0.011 (13.607)
CDDP	1.232 $\pm$ 0.158 (1.000)	1.568 $\pm$ 0.229 (1.273)
+ OTS964 5 nM	1.085 $\pm$ 0.271 (0.881)	1.853 $\pm$ 0.044 (1.504)
+ OTS964 10 nM	1.319 $\pm$ 0.175 (1.070)	1.472 $\pm$ 0.643 (1.194)

	HEK293/pcDNA3.1	HEK293/ABCB1
+ VPL 3 μM	1.470 ± 0.436 (1.193)	1.456 ± 0.083 (1.181)
	HEK293/pcDNA3.1	HEK293/ABCB1
PTX	0.012 ± 0.001 (1.000)	0.427 ± 0.077 (35.590) [*]
+ OTS964 5 nM	0.010 ± 0.002 (0.795)	1.079 ± 0.146 (90.017) [*]
+ OTS964 10 nM	0.017 ± 0.001 (1.439)	1.808 ± 0.108 (150.814) [*]
+ VPL 3 μM	0.009 ± 0.003 (0.761)	0.093 ± 0.019 (7.730)
DOX	0.048 ± 0.008 (1.000)	2.949 ± 0.296 (61.620) [*]
+ OTS964 5 nM	0.062 ± 0.020 (1.294)	3.402 ± 0.310 (71.087) [*]
+ OTS964 10 nM	0.058 ± 0.008 (1.205)	3.520 ± 0.085 (73.563) [*]
+ VPL 3 μM	0.035 ± 0.007 (0.740)	0.199 ± 0.028 (4.154)
VCR	0.005 ± 0.001 (1.000)	0.256 ± 0.027 (52.010) [*]
+ OTS964 5 nM	0.005 ± 0.001 (1.115)	0.248 ± 0.009 (50.305) [*]
+ OTS964 10 nM	0.004 ± 0.001 (0.829)	0.281 ± 0.031 (56.953) [*]
+ VPL 3 μM	0.005 ± 0.001 (0.964)	0.063 ± 0.008 (12.700) [*]
CDDP	1.048 ± 0.122 (1.000)	1.084 ± 0.270 (1.035)
+ OTS964 5 nM	1.416 ± 0.229 (1.352)	0.877 ± 0.247 (0.837)
+ OTS964 10 nM	1.223 ± 0.035 (1.167)	1.000 ± 0.227 (0.954)
+ VPL 3 μM	1.355 ± 0.447 (1.293)	1.077 ± 0.012 (1.028)

[a] IC_{50} values are expressed as mean ± SD from a representative of three independent experiments.

[b] Resistance fold (RF) was calculated by dividing the IC_{50} values of verified substrate-drugs with or without modulator in drug-sensitive or drug-resistant cells by the IC_{50} values of verified substrate-drugs without modulator in drug-sensitive cells.

3.2.6 OTS964 stimulates ABCB1 expression at protein and mRNA level.

To explore the possible reason for enhanced drug resistance in OTS964-treated cells, a Western blot was performed to determine the effect of OTS964 on ABCB1 protein expression. Herein, to simulate conditions more similar to clinical settings and to reduce its off-target effects, a low-concentration (5 nM) of OTS964 with up to 72 h of treatment and a high-concentration (10-40 nM) of OTS964 with 24 h of treatment were selected for the Western blot analysis. Our results showed that OTS964 at 40 nM significantly promoted ABCB1 protein expression in both resistant KB-C2 cells and HEK293/ABCB1 cells after 24 h of treatment (see Fig. 22A and 22B). Subsequently, a qRT-PCR assay was carried out to evaluate the effect of OTS964 on the mRNA level of ABCB1 expression. As shown in Fig. 22C and 22D, in both drug-selected cancer cells and gene-transfected cells, remarkably increased ABCB1 mRNA expression level was observed after incubation with 5 nM of OTS964 for 72 h and with 20 or 40 nM of OTS964 for 24 h. Above results indicated that OTS964 enables upregulated ABCB1 expression at protein and mRNA levels. Overall, these results, at least in part, may explain the attenuated anticancer efficacy of OTS964 and the induced resistance to ABCB1 substrate-drugs.
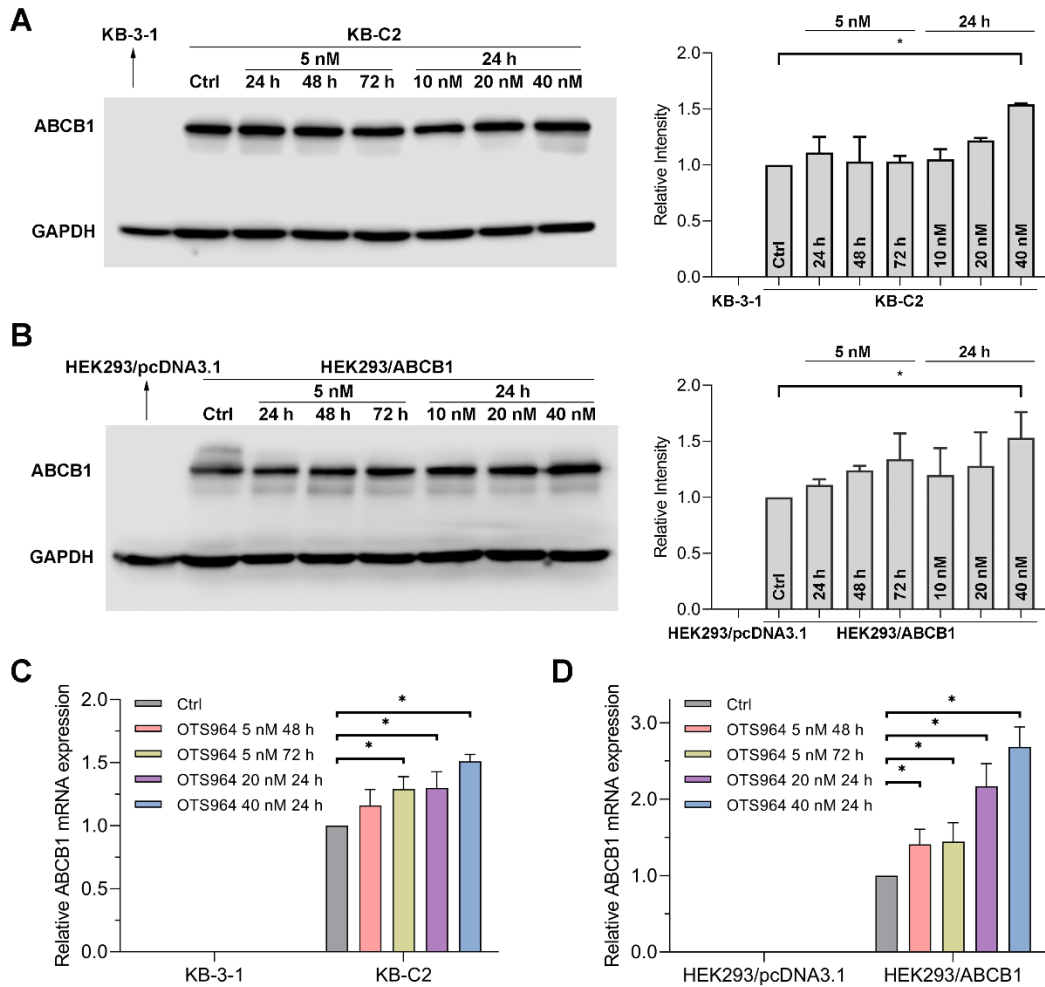
Figure 22. Effects of OTS964 on expression levels of ABCB1 protein and mRNA.
The effect of OTS964 on ABCB1 protein expression in **A)** KB-C2 and **B)**
HEK293/ABCB1 cells. The effect of OTS964 on ABCB1 mRNA expression in **C)** KB-C2 and **D)** HEK293/ABCB1 cells. In the Western blot analysis, the relative density of each protein band was analyzed by Fiji software, and ABCB1 protein expression levels were normalized to GAPDH before comparison. In the qRT-PCR analysis, data were calculated based on the comparative $\Delta\Delta C_T$ method and expressed as the relative fold changes. Data are expressed as mean ± SD from a representative of three independent experiments. *$p < 0.05$ versus the respective control group.

3.2.7 OTS964, at a low-concentration and with 72 h of treatment, decreases the intracellular accumulation and increases the extracellular amount of [^{3}H]-PTX in cells overexpressed ABCB1.

Above results from reversal study and qRT-PCR demonstrated that OTS964 can increase the IC$_{50}$ values for ABCB1 substrate-drugs and upregulate ABCB1 expression level after drug-resistant cells incubated with a low-concentration of OTS964 after 72 h of treatment. To investigate whether more substrate-drug (PTX) would be pumped out to the extracellular space in OTS964-treated cells, a [^{3}H]-PTX accumulation assay with long-exposure time, using the same concentrations (5 nM and 10 nM) as in reversal study, was conducted here. After 72 h of incubation period, both cell pellets and remaining medium were collected to measure the radioactivity. As shown in Fig. 23A, in OTS964 treatment group, a significantly decreased intracellular amount of radiolabeled PTX was observed in resistant KB-C2 cells relative to those in parental KB-3-1 cells. In contrast, ABCB1 inhibitor VPL at 3 μM increased the intracellular PTX accumulation in drug-resistant cells to the similar level of those in parental cells. The amount of PTX in extracellular space was also assessed. As presented in Fig. 23B, compared with the control group of KB-C2 cells, the extracellular amount of PTX in OTS964-treated KB-C2 cells did not significantly altered or had a slight increase, while VPL treatment group had a significant reduction in the amount of extracellular PTX. Similar data was found in ABCB1-transfected HEK293 cells (see Fig. 23C and 23D). Neither OTS964 nor VPL treatment affected the intracellular or extracellular amount of PTX in parental KB-3-1 and HEK293/pcDNA3.1 cells. Overall, these results confirmed that OTS964 can induce a greater amount of ABCB1 substrate-drug being pumped out from resistant cells

overexpressed ABCB1, leading to a less amount of substrate-drug accumulating in cancer cells.
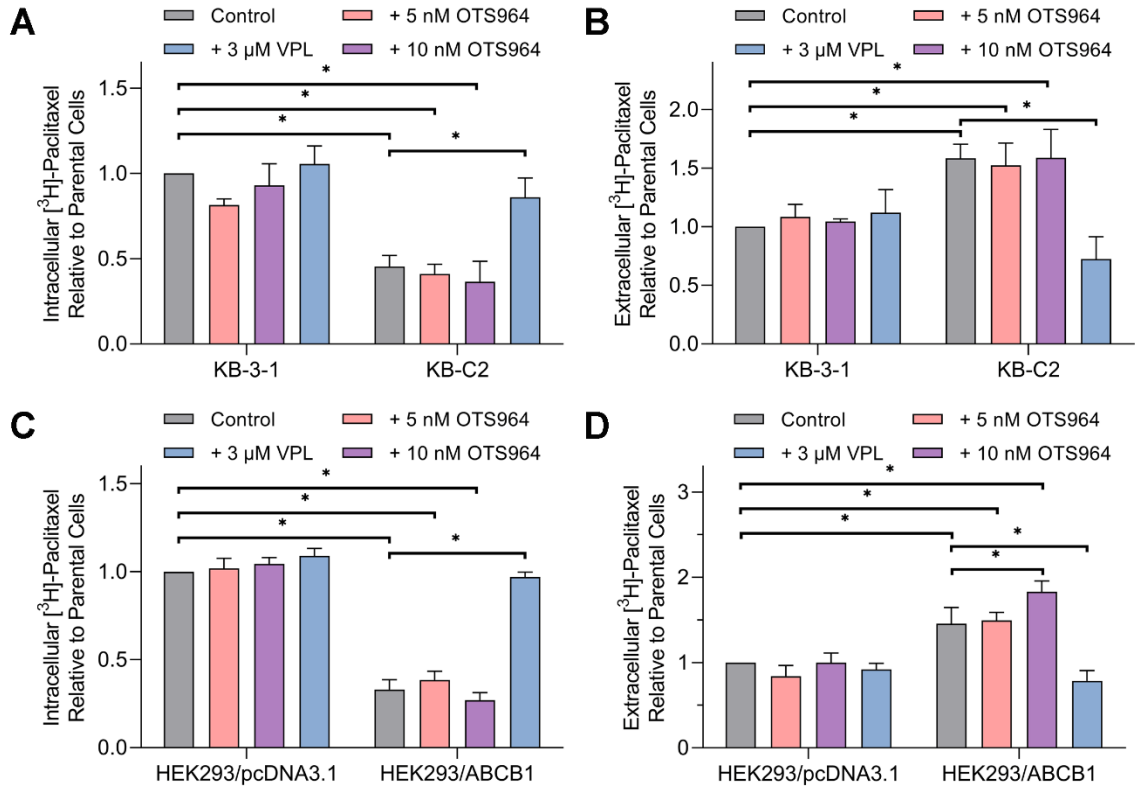
Figure 23. Effects of OTS964 on the intracellular and extracellular amount of [^{3}H]-PTX in ABCB1-overexpressing cells after 72 h of treatment.

The relative ratio of [^{3}H]-PTX for KB-C2 and KB-3-1 cells in **A)** cell pellets or **B)** remaining medium after 72 h of treatment. The relative ratio of [^{3}H]-PTX for HEK293/ABCB1 and HEK293/pcDNA3.1 cells in **C)** cell pellets or **D)** remaining medium after 72 h of treatment. The relative ratio was calculated as the treatment group divided by the parental control group. Data are expressed as mean ± SD from a representative of three independent experiments. *$p < 0.05$ versus the respective control group.

3.2.8 OTS964 is susceptible to ABCB1-overexpressing tumor xenograft model, and these effects can be antagonized by VPL.

An *in vivo* xenograft model was subsequently established to verify the aforementioned *in vitro* findings. Fig. 24A and Fig. 24B depict the excised tumor tissues. In SW620 xenograft model, both OTS964 alone and OTS964 combined with VPL significantly reduced the tumor volume (Fig. 24C) and tumor weight (Fig. 24E) relative to those in control group. By contrast, in SW620/Ad300 tumor-bearing mice model, neither tumor volume (Fig. 24D) nor tumor weight (Fig. 24F) had significant decrease in OTS964-treated mice compared to those in control group. Furthermore, OTS964 combined with VPL significantly inhibited the tumor growth in SW620/Ad300 xenograft model (Fig. 24D and Fig. 24F), suggesting that VLP could restore the efficacy of OTS964 in ABCB1-overexpressing tumor xenograft model. No significant differences in body weight were observed in tumor-bearing mice, indicating that OTS964, either applied alone or used in combination with VPL, is well-tolerated without causing weight loss (Fig. 25A). Considering the toxicity profile, the number of WBCs and platelets were assessed. As shown in Fig. 25B and Fig. 25C, even though the number of platelets had a reduction trend, the number of WBCs and platelets, within normal range for nude mice, did not significantly altered in all treatment group relative to counterparts in control group. Together, above results indicated that efficacy of OTS964 is limited in ABCB1-overexpressing tumor xenograft model, and OTS964-resistant can be re-sensitized by ABCB1 inhibitor VPL.
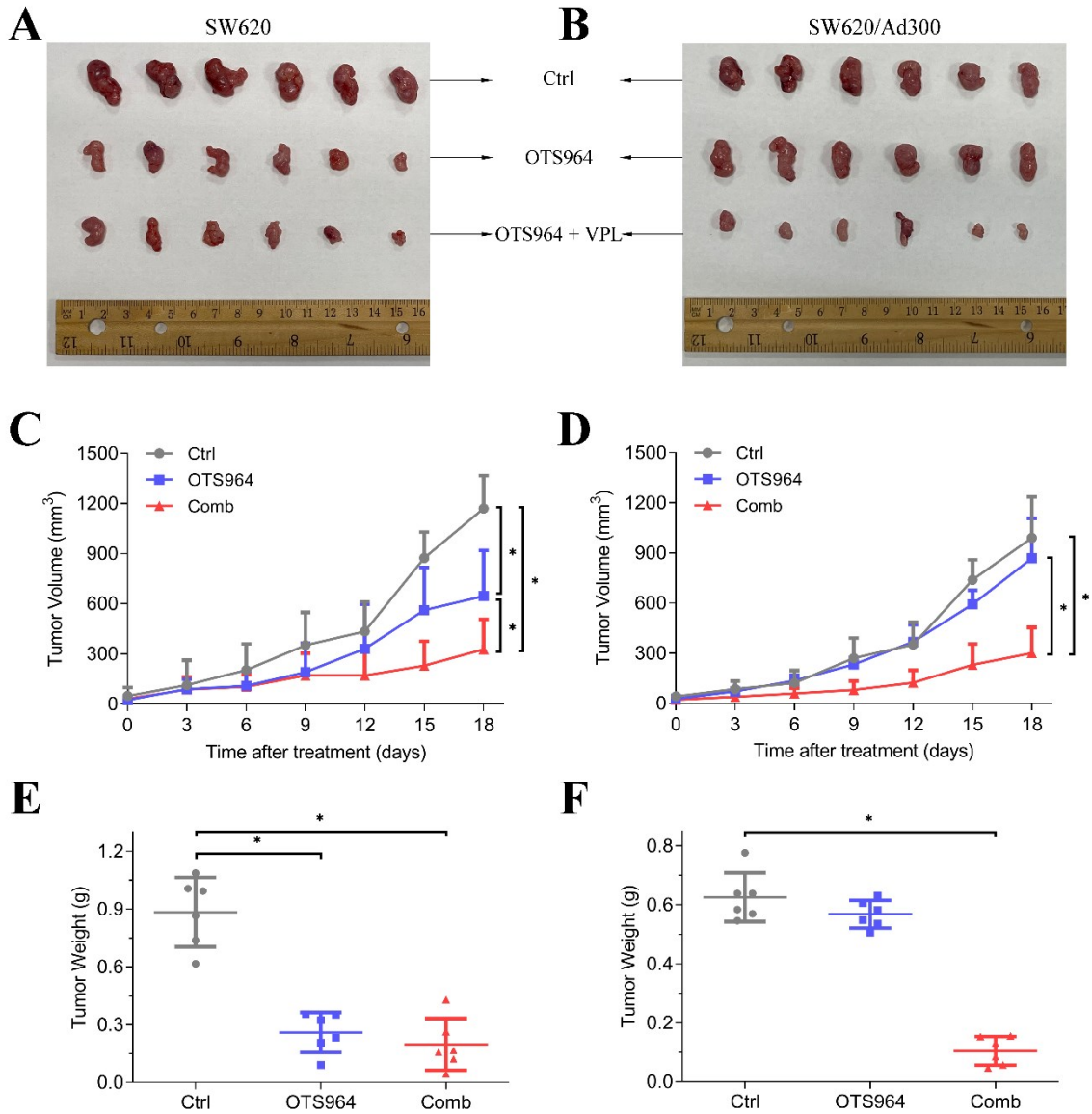
Figure 24. Antitumor activity of OTS964 in SW620 and SW620/Ad300 tumor xenograft models.

Images of excised **A)** SW620 and **B)** SW620/Ad300 tumor tissues from nude athymic mice at the end of treatment period. The changes of tumor volume in **C)** SW620 and **D)** SW620/Ad300 tumor xenograft model over time following the implantation. The weight of excised **E)** SW620 and **F)** SW620/Ad300 tumor tissues from nude athymic mice at the end of treatment period. Data are expressed as mean ± SD. *$p < 0.05$ versus the

respective control group.
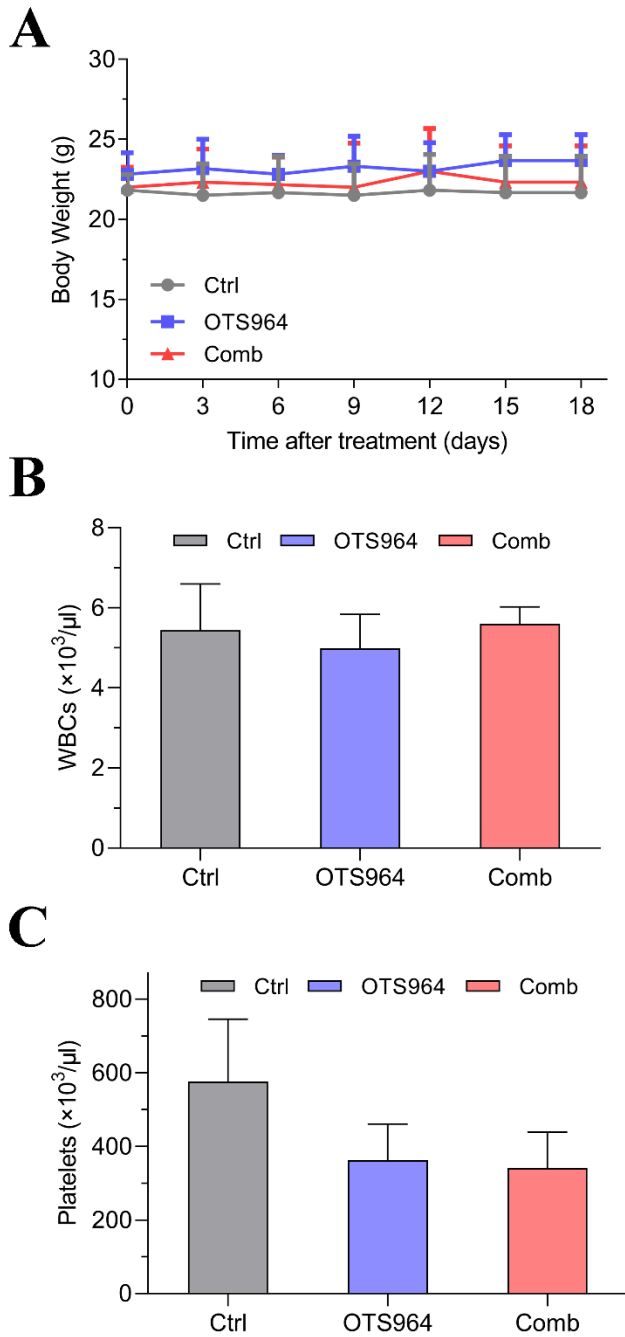
Figure 25. Toxicity profile of OTS964 in SW620 and SW620/Ad300 tumor xenograft models.

A) The changes of body weight during the treatment period. **B)** The WBC counts for

nude athymic mice at the end of treatment period. **C)** The platelet counts for nude

athymic mice at the end of treatment period. Data are expressed as mean $\pm$ SD. $*p < 0.05$

versus the respective control group.

CHAPTER 4

DISCUSSION

MDR in cancer cells is a phenotype whereby cells have attenuated sensitivity to drugs with distinct structures and mechanisms. ABCG2 and ABCB1 are members of the ABC transporter family and involved in MDR. Overexpression of ABCG2 and ABCB1 has been reported in both leukemia and solid tumors, facilitating drug efflux to reduce the intracellular level of chemotherapeutic drugs from accumulating in cancer cells [60, 73]. Thus, identifying drugs that are substrates for ABCG2 and/or ABCB1 can provide directions for treatment strategies in clinical settings and improve the quality of cancer patients' life.

PBK/TOPK has been characterized recently as a potential cancer-specific biomarker and a druggable therapeutic target [23, 29]. OTS964, as a PBK/TOPK inhibitor, suppresses cell proliferation with nanomolar inhibitory potency [39], which is consistent with our results. As mentioned in the section 1.5, evidence from many previous studies has suggested that PBK/TOPK is either directly or indirectly associated with regulation of ABCG2 and ABCB1. Thus, it is reasonable to propose that PBK/TOPK has high possibility to interact with ABC transporters, especially ABCG2 and ABCB1. In this study, we investigated that whether overexpression of ABCG2 and ABCB1 restricts the antitumor effectiveness of PBK/TOPK inhibitor OTS964. In particular, the antitumor efficacy of OTS964 was evaluated in the presence of ABCG2 and ABCB1 in cancer cells.

Our experiments started from an MTT-based cell viability assay. By means of MTT assay, it was found that the effectiveness of OTS964 is limited in cancer cells overexpressed ABCG2, and an ABCG2 inhibitor Ko143 at 3 μM can re-sensitize the

acquired resistance to OTS964 without affecting OTS964 sensitivity in respective parental cells. Subsequently, *ABCG2* gene-knockout sublines were used to corroboration. Upon *ABCG2* gene-knockout, NCI-H460/MX20 ABCG2 KO cells that do not overexpress ABCG2 transporter became more sensitive to OTS964. As NCI-H460 is a lung cancer cell line, and S1 is a colon cancer cell line, it might, to some extent, develop other mechanisms of drug resistance apart from overexpressing ABCG2. Therefore, ABCG2-transfected HEK293 cells were used, in which ABCG2 was a solo contributor to MDR. Additionally, it has documented that switching arginine to glycine (R > G) or threonine (R > T) at amino acid 482 in *ABCG2* gene may occur due to drug induced mutation or genetic polymorphisms, which is possible to cause substrate specificity and different resistance levels to substrate-drugs [54, 74, 75]. For example, MX is found to be a substrate-drug of all ABCG2 variations; however, rhodamine 123, DOX, and daunorubicin are transported by only mutant R482G or R482T but not by the wild-type R482 ABCG2 [52, 54]. Moreover, compared with wild-type ABCG2, an R482G mutant ABCG2 confers relatively less resistance to TPT and SN-38 [52]. Hence, cells transfected with wild-type (R482) or mutant (R482G or R482T) ABCG2 were used here. OTS964-resistant was observed in ABCG2-transfected HEK293 cell lines. The RF values for OTS964 were higher in cells expressing R482G- and R482T-mutant ABCG2 relative to those in cells expressing wild-type ABCG2. Thus, mutant ABCG2 (R482G or R482T) may confer higher level of resistance to OTS964 among all ABCG2 protein variations. Overall, above results indicated that ABCG2 overexpression is possible to confer drug resistance to OTS964, and more importantly, ABCG2 variation at position 482 may have some effect on OTS964-resistant.

Similarly, the effectiveness of OTS964 was also restricted in both drug-selected and gene-transfected cells, which overexpress ABCB1, compared to those of the corresponding parental cells. As expected, an ABCB1 inhibitor VPL at 3 μM can re-sensitize the acquired resistance to OTS964 and restore the efficacy of OTS964 to the similar level as drug-sensitive cells do. Also, *ABCB1* gene-knockout cells were used to confirm ABCB1-conferred drug resistance to OTS964. Upon *ABCB1* gene knockout, the cell viability curves of drug-resistant cells were overlapping with those of the parental cells, and SW620/Ad300 cells became more sensitive to OTS964 after *ABCB1* knockout. In addition, as we demonstrated that OTS964 can be characterized as a substrate-drug for ABCG2, cells transfected with both transporters (B1/G2 cells) were used to verify. The cytotoxic activity of OTS964 was limited in B1/G2 cells relative to that in parental PEL cells, and that this effect can be partially re-sensitized by a known inhibitor of ABCB1 or ABCG2.

Altogether, we hypothesized that overexpression of ABCG2 and ABCB1 is the mechanism to OTS964-resistant. Several mechanistic studies were subsequently carried out to explore its possible underlying mechanism.

To evaluate ABCG2- and ABCB1-mediated transport function, $[^3H]$-MX and $[^3H]$-PTX accumulation assay were carried out. As the cells were incubated with OTS964 for a short time, we supposed that OTS964 is unlikely to affect cell viability or other cellular functions, even though high concentrations were used. The results showed that, after co-treatment of MX with high concentration (3 μM) of OTS964, an increased amount of MX was detected in drug resistance cells but not in their corresponding parental cells. Similar results were found in ABCB1-overexpressing cells. This effect

may be the results of a high concentration of OTS964 competing with another substrate-drug (e.g., MX or PTX) for transport function mediated by ABCG2 or ABCB1, and thus leading to an enhanced intracellular accumulation of other substrate-drugs (e.g., MX or PTX). This assumption is further elucidated in our *in silico* molecular docking analysis.

As ABC transporters are ATP-dependent, stimulated ATP hydrolysis is generally coupled to substrate transportation mediated by ABC transporters [76, 77]. To this end, an ATPase assay was performed to determine whether OTS964 can stimulate ABCG2 and ABCB1 ATPase activity. We found that OTS964 within 40 µM concentration-dependently stimulates the vanadate-sensitive ATPase activity of ABCG2 and ABCB1. The maximum stimulation manner induced by OTS964 is approximately 1.7- and 1.6-fold of basal level for ABCG2 and ABCB1, respectively, which is comparable to other reported substate-drugs, such as WYE-354 (1.4-fold) [78], GSK-1070916 (1.4-fold) [79], and tivantinib (1.7-fold) [60]. In addition, 1 µM of CYB-2, as an inhibitor of ABCG2 ATPase activity, can antagonize the stimulated ATPase activity and restore the ATPase activity of ABCG2 to basal level. After OTS964 combined with 1 µM of tepotinib, as an inhibitor to ATPase activity of ABCB1, a similar trend was found for stimulated ABCB1 ATPase activity. These results demonstrated that OTS964 may interact with the drug-binding domain of ABCG2 and ABCB1 proteins, and behaves as a substrate-drug for ABCG2 and ABCB1 transporters.

The *in silico* molecular docking analysis is widely applied in the field of structural molecular biology as an efficient tool to predict ligand-protein interactions [80, 81]. It has become a reliable methodology in virtual screening substrates and modulators of ABC transporters, although this computational analysis does not reveal the actual binding

interaction [61, 82]. In accordance with stimulatory results from ATPase assay, the docking simulation was conducted in the substrate-binding pocket of ABCG2 (6VXI) and ABCB1 (6QEX). OTS964 docked into the ABCG2 substrate-binding site with a docking score of -8.4 kcal/mol, which is comparable to other reported ABCG2 substrates or inhibitors, MLN7243 (-9.6 kcal/mol) [83], PD153035 (-7.0 kcal/mol) [66], etc. Similarly, OTS964 docked into the ABCB1 substrate-binding site and received a docking score of -7.2 kcal/mol, which is comparable to other reported ABCB1 substrates or inhibitors, such as GSK-1070916 (-8.0 kcal/mol), VPL (-7.4 kcal/mol), and zosuquidar (-8.6 kcal/mol) [7, 79]. These results demonstrated that OTS964 has potent binding affinity with the drug-binding cavity of ABCG2 and ABCB1 protein. Additionally, our results showed that OTS964 is positioned in transmembrane region via hydrophobic interaction with amino acid residues in ABCG2 and ABCB1 models, and stabilized by *pi-pi* stacking interaction, cation-*pi* interaction, as well as hydrogen bond formed with amino acid residues. Among important amino acids in ABCG2 binding pocket, Phe439 and Asn436 have been identified as critical determinants of ligand binding and substrate specificity for ABCG2 transporter, suggesting their central role in the formation of the recognition site for OTS964 as an ABCG2 substrate [63]. In the ABCB1 protein model, Phe72 has been found to be highly conserved among mammalian species [84]. In binding pocket of ABCB1, Phe72, Phe983, and Tyr953 have been identified as common interacting amino acid residues to form hydrophobic interactions with ABCB1 modulators [85, 86], and moreover, it was found that Leu65 is essential in the function and substrate specificity of ABCB1 transporter, suggesting its central role in the formation of the recognition site for OTS964 as an ABCB1 substrate [87]. To further validate the possibility that OTS964 may

be a substrate-drug for human ABCG2 and ABCB1, verified ABCG2 substrate MX and ABCB1 substrate PTX were analyzed under the same parameters. MX and PTX received docking score of -9.2 kcal/mol and -9.8 kcal/mol, respectively, and share similar docking positions with OTS964. Above results combined with ATPase data thereby demonstrated that OTS964 interacts with ligand-binding cavity of ABCG2 and ABCB1 protein and behaves as a substrate for ABCG2 and ABCB1 transporters. Furthermore, the overlapping binding sites, at least in part, can corroborate that OTS964 competes with other substrate-drugs (e.g., MX or PTX) at drug-binding cavity of ABCG2 and ABCB1 transporters, but the binding affinity is not as strong as the verified substrate-drugs for ABCG2 and ABCB1, as indicated by higher absolute value of docking score for MX and PTX.

It is known that some substate-drugs, imatinib, VPL, etc., have the ability to sensitize drug resistant cells overexpressed MDR-associated ABC transporters to chemotherapeutic agents [88, 89]. Mechanistic studies indicated that these inhibitors interact with the substrate-binding site of the transporter and compete with anticancer drugs for transportation, and thereby these modulators are themselves transported [4]. This enables a substrate-drug transported by ABCG2 and ABCB1 can reposition as a competitive inhibitor to antagonize ABCG2- and ABCB1-mediated drug resistance. To this end, a reversal study was conducted to evaluate whether OTS964 can be repurposed as a modulator to ABCG2 and ABCB1. Low concentrations (5 nM and 10 nM), assuming non-toxic concentrations, of OTS964 were selected to rule out the possibility of additive toxicity. The results showed that OTS964 at low concentrations failed to restore drug sensitivity to ABCG2 and ABCB1 substrate-drugs in drug-selected and gene-transfected

cells that overexpress ABCG2 or ABCB1. In contrast, non-toxic OTS964 treatment promoted MX resistance in resistant S1-M1-80 cells and PTX resistance in resistant KB-C2 cells without affecting the drug sensitivity in their respective parental cells. Consistently, a similar trend was observed in OTS964-treated gene-transfected HEK293 cells. Moreover, it was found that the efficacy of non-substrate drug CDDP was not significantly affected in cells treated with OTS964, indicating that this effect may be specific to ABCG2 and ABCB1. It is worthwhile to mention that the exact nature of interaction between OTS964 and the transporter, namely, whether OTS964 acts as a transported substrate or a competitive inhibitor, is dependent on the concentration used, the assay being used, and the varying activities of the transporters in each cell type. Therefore, our results do not warrant further testing of OTS964 as a chemosensitizer.

Since amplifying the ABCG2 and ABCB1 drug efflux pump could be a possible mechanism for acquired drug resistance, a Western blot analysis was conducted to further determine the mechanism of action. Attempts to simulate the clinical settings and circumvent the off-target toxicity, we selected low concentration, assuming negligible cytotoxicity, for up to 72 h of exposure and high concentration, approached IC_{50} value, for 24 h of exposure. The results showed that, within 72 h, a low concentration (5 nM) of OTS964 did not significantly change the ABCG2 or ABCB1 protein level in drug-resistant cells overexpressed ABCG2 or ABCB1. After 40 nM of OTS964 incubated for 24 h, significantly stimulated ABCG2 and ABCB1 protein expression was found in ABCG2- and ABCB1-overexpressing cells, respectively. Given that protein upregulation could be in consequence of gene amplification, we postulated that mRNA level of ABCG2 and ABCB1 could be increased by OTS964. A qRT-PCR analysis was

subsequently carried out. Followed by 24 h of treatment, 40 nM of OTS964 significantly upregulated ABCG2 mRNA level in HEK293 cells transfected with mutant ABCG2 (R482G and R482T). Remarkably upregulated ABCB1 mRNA level was observed in resistant cells treated with OTS964 at low concentration (5 nM) with 72 h of incubation and at high concentrations (20 nM or 40 nM) with 24 h of incubation. Altogether, OTS964 enables upregulation of ABCG2 and ABCB1 expression. Notably, there is a discrepancy between ABCB1 mRNA abundances and ABCB1 protein abundances especially for cells with 5 nM OTS964 treatment. Indeed, it has been shown that mRNA transcript abundances only partially, but not strongly, correlate with protein abundances, and the squared Pearson correlation coefficient is approximately 0.40 [90]. This inconsistency might be the result of post-translational regulation and/or transcriptional and post-transcriptional regulation. For post-translational regulation, protein abundances are dependent on many determinants, for example: (1) MAPK signaling pathway positively modulates ABCB1 protein expression [46]; (2) ubiquitination-proteasome system plays a role in ABCB1 protein turnover, and the enhanced ubiquitination-mediated proteasomal degradation results in a reduction of the function of ABCB1 transporter [91]; (3) endosomal trafficking and recycling pathway control ABCB1 protein degradation and homeostasis [46]; and (4) ABCB1 protein level is associated with ABCB1 protein stability [92], for example, Pim-1 kinase phosphorylates ABCB1 protein, and thereby protects ABCB1 protein from degradation and allows its glycosylation and cell surface expression [93]. For transcriptional and post-transcriptional regulation, mRNA abundances are dependent on many determinants, for example: (1) transcription factors, such as AP-1 and NF-κB, directly bind to the promoter region of *ABCB1* gene,

and thus induce or suppress transcription activities of ABCB1 promoter [46]; (2) pathways, such as PI3K-Akt signaling and Wnt/β-catenin signaling, are involved in *ABCB1* gene transcription [46]; and (3) non-coding RNAs (ncRNAs) promotes *ABCB1* expression [94], such as circRNA MTHFD2 by sponging miR-124 [95] and lncRNA KCNQ1OT1 by sponging miR-138-5p [96]. Additionally, a temporal relationship between producing and degrading should be considered [97]. On average, a cell produces two copies of a given mRNA per hour, whereas it produces dozens of copies of the corresponding protein per mRNA per hour; hence, proteins are produced at a more rapid rate than mRNAs are [90]. Also, mRNAs are less stable than proteins; on average, ABCB1 mRNA has a half-life of 2-6 h [98-100], whereas ABCB1 protein has a half-life of 15-72 h [99, 101, 102]. As above discrepant results are thought to be determined by cofactors, a detailed mechanism of this discrepancy and upregulation remains to be investigated further. Overall, enhanced ABCG2 and ABCB1 expression at protein and mRNA levels is an underlying reason for drug resistance induced by OTS964. Besides stimulated protein and mRNA expression, a comprehensive mechanism for OTS964-induced drug resistance should be determined in the further. For example, the membrane properties, such as an increase in membrane fluidity and membrane potential, are causally related to ABCB1 expression and drug resistance [99].

Combined the results from Western blot and qRT-PCR, we postulated that stimulated ABCB1 protein and mRNA allow a more functionable ABCB1 transporter to pump out its substrates, resulting in a decreased sensitivity to drugs transported by ABCB1. To further examine this assumption, a 72-h accumulation assay was conducted using the same concentrations as in reversal study, and the amounts of [^{3}H]-PTX in both

intracellular and extracellular space were quantified. Consistent with the cytotoxicity results, OTS964 at low concentration induced a reduction of PTX intracellular accumulation and an enhanced level of extracellular PTX in drug-resistant cells. Moreover, this effect was not observed in corresponding drug-sensitive cells. As ABCB1 protein expression is not significantly changed within 72-h exposure of OTS964 at low concentration, we postulated that OTS964 at negligible toxic concentrations may affect the transport function without altering the protein expression level. This hypothesis should be further verified. However, we noticed that, combined the results from 4-h accumulation assay and Western blot analysis, OTS964 at high concentration competitively inhibits PTX efflux leading to more PTX accumulating in drug-resistant cells, but paradoxically promotes ABCB1 expression at both transcriptional and translational level. Therefore, we postulated that OTS964 at approached IC_{50} concentrations may have off-target activities in addition to its interaction with ABCB1 transporter, which needs to be collaborated further. It is also possible that OTS964 may induce a conformational change upon binding with ABCB1 protein, consequently preventing PTX binding and thus resulting in a competitive inhibitory of PTX efflux after short time exposure to OTS964. By contrast, after 72 h of OTS964 treatment, the stimulated ATPase activity, which would supply energy for efflux function, enables more PTX being pumped out from drug-resistant cells. This hypothesis remains to be further validated in the future.

Subsequently, to further translate our *in vitro* findings into *in vivo* evaluation, athymic nude mice were implanted with SW620 and its ABCB1-overexpressing SW620/Ad300 cells to establish tumor xenograft model in this study. As a result, the

tumor growth was significantly suppressed in OTS964-treated mice bearing SW620 tumors compared to the control group. By contrast, in SW620/Ad300 tumor-bearing mice, OTS964 alone treatment did not induce significant reduction in tumor volume or tumor weight relative to those in the control group. These results suggested that the efficacy of OTS964 is restricted by ABCB1-mediated drug resistance. Interestingly, the combination of OTS964 and VPL significantly inhibited the tumor growth in SW620/Ad300 xenograft model compared to the control group, which, at least in part, verified that the limited efficacy of OTS964 is induced by ABCB1 overexpression. Given that toxicity is a major concern for any chemotherapeutic agent, the body weight of mice was used as an indicator of tolerability throughout the course of this study. Our results showed that no remarkable weight loss was caused by OTS964 either administrated alone or used in combination with VPL.

It has reported that PBK/TOPK inhibitors (OTS514 and OTS964) cause dysfunction in the differentiation process of hematopoietic stem cells (HSCs) to WBCs and platelets (reduction of WBCs with an increase in platelets) in a dose-dependent manner [34]. According to the results from Matsuo et al. [34], this unfavorable hematopoietic abnormality is observed in nude mice treated with intravenous administration of OTS964, but this is a transient effect in nude mice treated with oral administration of OTS964, as indicated by the spontaneous recovery from leukocytopenia within 2 weeks after treatment stopped. Hence, it is reasonable that oral administration was chosen here, even though hematopoietic toxicity is still a concern and higher dosage should be given by oral gavage. Herein, WBCs and platelets were also counted to evaluate the toxicity profile of OTS964 after the final administration. Based on the

information from vender (Taconic Farms) and reference [103], the number of WBCs and platelets in all groups was within the normal range in nude mice. Also, our results showed that no marked change in WBC or platelet counts was found in nude mice with OTS964 either administered orally alone or combined with VPL. Notably, Matsuo et al. [34] have revealed that both intravenous and oral administration of liposome-coated OTS964 could circumvent above unexpected hematological abnormalities with complete regression of transplanted tumors. This is a promising step towards clinical use of OTS964.

Of note, in addition to putatively targeting to PBK/TOPK, Lin et al. [39] have found that OTS964 specifically inhibits the cyclin-dependent kinase CDK11, which function is required for mitotic progression, RNA transcription and splicing, autophagy, and apoptosis [104]. This also provides us with a clue that OTS964 may have misidentified targets. Many pan-CDK inhibitors cause myelosuppression leading to decreased production of blood cells (anemia, leukocytopenia, and thrombocytopenia) [104, 105]. Based on our results from blood cell counting, we postulated that the lack of leukocytopenia and thrombocytopenia in OTS964-treated mice may be beneficial from its CDK11-selective inhibition. However, this hypothesis needs corroboration in the future. Additionally, Herbert et al. [106] have reported that PBK/TOPK directly interacts with checkpoint kinase CHK1 and its downstream effector Cdc25C during cell cycle progression. To our knowledge, MDR-associated ABC transporters, especially ABCG2 and ABCB1, are not linked with PBK/TOPK, CDK11, or CHK1. Hence, OTS964 may induce or inhibit mischaracterized proteins that are not closely correlated with its reportedly putative targets. OTS964 has misidentification on reportedly target-specific inhibition, although, PBK/TOPK is still a promising druggable target with minimum

toxicity to extend disease-free survival, since PBK/TOPK is limitedly expressed in

normal tissues. Collectively, the risk of dose-limiting toxicity profile is still a concern and

has been a major challenge to overcome for potent PBK/TOPK inhibitor.

CHAPTER 5

SUMMARY

This study presents evidence that OTS964 is susceptible to ABCG2- and ABCB1-mediated drug resistance, and that this effect can be antagonized by known inhibitors. Consistently, a similar trend was observed in tumor-bearing mice.

Mechanistic studies suggested that acquired resistance to OTS964 could be in consequence of stimulated ATPase activity and upregulated expression of ABCG2 and ABCB1, which allows a more functionable transporter to pump out its substrates. This results in decreased sensitivity to drugs transported by ABCG2 or ABCB1, and promotes ABCG2- or ABCB1-mediated MDR rather than antagonizing drug resistance.

Identifying OTS964 that behaves as a substrate-drug for ABCG2 and ABCB1 can provide directions for follow-up clinical use of OTS964, and thereby, improve the quality of cancer patients' life. Our findings strongly support the importance of monitoring the ABCG2 and ABCB1 levels in cancer patients under OTS964 treatment.

REFERENCES

1. Siegel RL, Miller KD, Jemal A: **Cancer statistics, 2020.** *CA Cancer J Clin* 2020, **70:**7-30.

2. Keefe DM, Bateman EH: **Tumor control versus adverse events with targeted anticancer therapies.** *Nat Rev Clin Oncol* 2011, **9:**98-109.

3. Mohammad IS, He W, Yin L: **Understanding of human ATP binding cassette superfamily and novel multidrug resistance modulators to overcome MDR.** *Biomed Pharmacother* 2018, **100:**335-348.

4. Eckford PD, Sharom FJ: **ABC efflux pump-based resistance to chemotherapy drugs.** *Chem Rev* 2009, **109:**2989-3011.

5. Zhang YK, Wang YJ, Gupta P, Chen ZS: **Multidrug Resistance Proteins (MRPs) and Cancer Therapy.** *Aaps j* 2015, **17:**802-812.

6. Rees DC, Johnson E, Lewinson O: **ABC transporters: the power to change.** *Nat Rev Mol Cell Biol* 2009, **10:**218-227.

7. Yang Y, Ji N, Cai CY, Wang JQ, Lei ZN, Teng QX, Wu ZX, Cui Q, Pan Y, Chen ZS: **Modulating the function of ABCB1: in vitro and in vivo characterization of sitravatinib, a tyrosine kinase inhibitor.** *Cancer Commun (Lond)* 2020, **40:**285-300.

8. Glavinas H, Méhn D, Jani M, Oosterhuis B, Herédi-Szabó K, Krajcsi P: **Utilization of membrane vesicle preparations to study drug-ABC transporter interactions.** *Expert Opin Drug Metab Toxicol* 2008, **4:**721-732.

9. Szöllősi D, Szakács G, Chiba P, Stockner T: **Dissecting the Forces that Dominate Dimerization of the Nucleotide Binding Domains of ABCB1.**

Biophys J 2018, **114:**331-342.

10. Szöllősi D, Chiba P, Szakacs G, Stockner T: **Conversion of chemical to mechanical energy by the nucleotide binding domains of ABCB1.** *Sci Rep* 2020, **10:**2589.

11. Mansoori B, Mohammadi A, Davudian S, Shirjang S, Baradaran B: **The Different Mechanisms of Cancer Drug Resistance: A Brief Review.** *Adv Pharm Bull* 2017, **7:**339-348.

12. Sarkadi B, Homolya L, Szakács G, Váradi A: **Human multidrug resistance ABCB and ABCG transporters: participation in a chemoimmunity defense system.** *Physiol Rev* 2006, **86:**1179-1236.

13. Knutsen T, Rao VK, Ried T, Mickley L, Schneider E, Miyake K, Ghadimi BM, Padilla-Nash H, Pack S, Greenberger L, et al: **Amplification of 4q21-q22 and the MXR gene in independently derived mitoxantrone-resistant cell lines.** *Genes Chromosomes Cancer* 2000, **27:**110-116.

14. Toyoda Y, Takada T, Suzuki H: **Inhibitors of Human ABCG2: From Technical Background to Recent Updates With Clinical Implications.** *Front Pharmacol* 2019, **10:**208.

15. Mo W, Zhang JT: **Human ABCG2: structure, function, and its role in multidrug resistance.** *Int J Biochem Mol Biol* 2012, **3:**1-27.

16. Szakács G, Váradi A, Ozvegy-Laczka C, Sarkadi B: **The role of ABC transporters in drug absorption, distribution, metabolism, excretion and toxicity (ADME-Tox).** *Drug Discov Today* 2008, **13:**379-393.

17. Ni Z, Bikadi Z, Rosenberg MF, Mao Q: **Structure and function of the human**

breast cancer resistance protein (BCRP/ABCG2). *Curr Drug Metab* 2010, **11:**603-617.

18. Manolaridis I, Jackson SM, Taylor NMI, Kowal J, Stahlberg H, Locher KP: **Cryo-EM structures of a human ABCG2 mutant trapped in ATP-bound and substrate-bound states.** *Nature* 2018, **563:**426-430.

19. Levran O, O'Hara K, Peles E, Li D, Barral S, Ray B, Borg L, Ott J, Adelson M, Kreek MJ: **ABCB1 (MDR1) genetic variants are associated with methadone doses required for effective treatment of heroin dependence.** *Hum Mol Genet* 2008, **17:**2219-2227.

20. Dietrich CG, Geier A, Oude Elferink RP: **ABC of oral bioavailability: transporters as gatekeepers in the gut.** *Gut* 2003, **52:**1788-1795.

21. Kalabis GM, Kostaki A, Andrews MH, Petropoulos S, Gibb W, Matthews SG: **Multidrug resistance phosphoglycoprotein (ABCB1) in the mouse placenta: fetal protection.** *Biol Reprod* 2005, **73:**591-597.

22. Germann UA: **P-glycoprotein--a mediator of multidrug resistance in tumour cells.** *Eur J Cancer* 1996, **32a:**927-944.

23. Huang H, Lee MH, Liu K, Dong Z, Ryoo Z, Kim MO: **PBK/TOPK: An Effective Drug Target with Diverse Therapeutic Potential.** *Cancers (Basel)* 2021, **13**.

24. Ikeda Y, Park JH, Miyamoto T, Takamatsu N, Kato T, Iwasa A, Okabe S, Imai Y, Fujiwara K, Nakamura Y, Hasegawa K: **T-LAK Cell-Originated Protein Kinase (TOPK) as a Prognostic Factor and a Potential Therapeutic Target in Ovarian Cancer.** *Clin Cancer Res* 2016, **22:**6110-6117.

25.   Shih MC, Chen JY, Wu YC, Jan YH, Yang BM, Lu PJ, Cheng HC, Huang MS, Yang CJ, Hsiao M, Lai JM: **TOPK/PBK promotes cell migration via modulation of the PI3K/PTEN/AKT pathway and is associated with poor prognosis in lung cancer.** *Oncogene* 2012, **31:**2389-2400.

26.   Thanindratarn P, Dean DC, Nelson SD, Hornicek FJ, Duan Z: **T-LAK cell-originated protein kinase (TOPK) is a Novel Prognostic and Therapeutic Target in Chordoma.** *Cell Prolif* 2020, **53:**e12901.

27.   Ohashi T, Komatsu S, Ichikawa D, Miyamae M, Okajima W, Imamura T, Kiuchi J, Kosuga T, Konishi H, Shiozaki A, et al: **Overexpression of PBK/TOPK relates to tumour malignant potential and poor outcome of gastric carcinoma.** *Br J Cancer* 2017, **116:**218-226.

28.   Joel M, Mughal AA, Grieg Z, Murrell W, Palmero S, Mikkelsen B, Fjerdingstad HB, Sandberg CJ, Behnan J, Glover JC, et al: **Targeting PBK/TOPK decreases growth and survival of glioma initiating cells in vitro and attenuates tumor growth in vivo.** *Mol Cancer* 2015, **14:**121.

29.   Herbert KJ, Ashton TM, Prevo R, Pirovano G, Higgins GS: **T-LAK cell-originated protein kinase (TOPK): an emerging target for cancer-specific therapeutics.** *Cell Death Dis* 2018, **9:**1089.

30.   Hu QF, Gao TT, Shi YJ, Lei Q, Liu ZH, Feng Q, Chen ZJ, Yu LT: **Design, synthesis and biological evaluation of novel 1-phenyl phenanthridin-6(5H)-one derivatives as anti-tumor agents targeting TOPK.** *Eur J Med Chem* 2019, **162:**407-422.

31.   Pirovano G, Roberts S, Reiner T: **TOPKi-NBD: a fluorescent small molecule**

for tumor imaging. *Eur J Nucl Med Mol Imaging* 2020, **47:**1003-1010.

32. Pirovano G, Roberts S, Brand C, Donabedian PL, Mason C, de Souza PD, Higgins GS, Reiner T: **[(18)F]FE-OTS964: a Small Molecule Targeting TOPK for In Vivo PET Imaging in a Glioblastoma Xenograft Model.** *Mol Imaging Biol* 2019, **21:**705-712.

33. Kim DJ, Li Y, Reddy K, Lee MH, Kim MO, Cho YY, Lee SY, Kim JE, Bode AM, Dong Z: **Novel TOPK inhibitor HI-TOPK-032 effectively suppresses colon cancer growth.** *Cancer Res* 2012, **72:**3060-3068.

34. Matsuo Y, Park JH, Miyamoto T, Yamamoto S, Hisada S, Alachkar H, Nakamura Y: **TOPK inhibitor induces complete tumor regression in xenograft models of human cancer through inhibition of cytokinesis.** *Sci Transl Med* 2014, **6:**259ra145.

35. Gao G, Zhang T, Wang Q, Reddy K, Chen H, Yao K, Wang K, Roh E, Zykova T, Ma W, et al: **ADA-07 Suppresses Solar Ultraviolet-Induced Skin Carcinogenesis by Directly Inhibiting TOPK.** *Mol Cancer Ther* 2017, **16:**1843-1854.

36. Gao T, Hu Q, Hu X, Lei Q, Feng Z, Yu X, Peng C, Song X, He H, Xu Y, et al: **Novel selective TOPK inhibitor SKLB-C05 inhibits colorectal carcinoma growth and metastasis.** *Cancer Lett* 2019, **445:**11-23.

37. Lu S, Ye L, Yin S, Zhao C, Yan M, Liu X, Cui J, Hu H: **Glycyrol exerts potent therapeutic effect on lung cancer via directly inactivating T-LAK cell-originated protein kinase.** *Pharmacol Res* 2019, **147:**104366.

38. Zou L, Gao Z, Zeng F, Xiao J, Chen J, Feng X, Chen D, Fang Y, Cui J, Liu Y, et

al: **Sulfasalazine suppresses thyroid cancer cell proliferation and metastasis through T-cell originated protein kinase.** *Oncol Lett* 2019, **18:**3517-3526.

39.   Lin A, Giuliano CJ, Palladino A, John KM, Abramowicz C, Yuan ML, Sausville EL, Lukow DA, Liu L, Chait AR, et al: **Off-target toxicity is a common mechanism of action of cancer drugs undergoing clinical trials.** *Sci Transl Med* 2019, **11**.

40.   Han Z, Li L, Huang Y, Zhao H, Luo Y: **PBK/TOPK: A Therapeutic Target Worthy of Attention.** *Cells* 2021, **10**.

41.   Wang L, Lin N, Li Y: **The PI3K/AKT signaling pathway regulates ABCG2 expression and confers resistance to chemotherapy in human multiple myeloma.** *Oncol Rep* 2019, **41:**1678-1690.

42.   Hu CF, Huang YY, Wang YJ, Gao FG: **Upregulation of ABCG2 via the PI3K-Akt pathway contributes to acidic microenvironment-induced cisplatin resistance in A549 and LTEP-a-2 lung cancer cells.** *Oncol Rep* 2016, **36:**455-461.

43.   Xie J, Jin B, Li DW, Shen B, Cong N, Zhang TZ, Dong P: **ABCG2 regulated by MAPK pathways is associated with cancer progression in laryngeal squamous cell carcinoma.** *Am J Cancer Res* 2014, **4:**698-709.

44.   Tomiyasu H, Watanabe M, Sugita K, Goto-Koshino Y, Fujino Y, Ohno K, Sugano S, Tsujimoto H: **Regulations of ABCB1 and ABCG2 expression through MAPK pathways in acute lymphoblastic leukemia cell lines.** *Anticancer Res* 2013, **33:**5317-5323.

45.   To KK, Tomlinson B: **Targeting the ABCG2-overexpressing multidrug**

resistant (MDR) cancer cells by PPARγ agonists.** *Br J Pharmacol* 2013, **170:**1137-1151.

46. Katayama K, Noguchi K, Sugimoto YJNJoS: **Regulations of P-glycoprotein/ABCB1/MDR1 in human cancer cells.** 2014, **2014**.

47. Stefka AT, Johnson D, Rosebeck S, Park JH, Nakamura Y, Jakubowiak AJ: **Potent anti-myeloma activity of the TOPK inhibitor OTS514 in pre-clinical models.** *Cancer Med* 2020, **9:**324-334.

48. Yang Y, Wu ZX, Wang JQ, Teng QX, Lei ZN, Lusvarghi S, Ambudkar SV, Chen ZS, Yang DH: **OTS964, a TOPK Inhibitor, Is Susceptible to ABCG2-Mediated Drug Resistance.** *Front Pharmacol* 2021, **12:**620874.

49. Henrich CJ, Bokesch HR, Dean M, Bates SE, Robey RW, Goncharova EI, Wilson JA, McMahon JB: **A high-throughput cell-based assay for inhibitors of ABCG2 activity.** *J Biomol Screen* 2006, **11:**176-183.

50. Robey RW, Honjo Y, van de Laar A, Miyake K, Regis JT, Litman T, Bates SE: **A functional assay for detection of the mitoxantrone resistance protein, MXR (ABCG2).** *Biochim Biophys Acta* 2001, **1512:**171-182.

51. Miyake K, Mickley L, Litman T, Zhan Z, Robey R, Cristensen B, Brangi M, Greenberger L, Dean M, Fojo T, Bates SE: **Molecular cloning of cDNAs which are highly overexpressed in mitoxantrone-resistant cells: demonstration of homology to ABC transport genes.** *Cancer Res* 1999, **59:**8-13.

52. Honjo Y, Hrycyna CA, Yan QW, Medina-Pérez WY, Robey RW, van de Laar A, Litman T, Dean M, Bates SE: **Acquired mutations in the MXR/BCRP/ABCP gene alter substrate specificity in MXR/BCRP/ABCP-overexpressing cells.**

Cancer Res 2001, **61:**6635-6639.

53. Lei ZN, Teng QX, Zhang W, Fan YF, Wang JQ, Cai CY, Lu KW, Yang DH, Wurpel JND, Chen ZS: **Establishment and Characterization of a Topotecan Resistant Non-small Cell Lung Cancer NCI-H460/TPT10 Cell Line.** *Front Cell Dev Biol* 2020, **8:**607275.

54. Robey RW, Honjo Y, Morisaki K, Nadjem TA, Runge S, Risbood M, Poruchynsky MS, Bates SE: **Mutations at amino-acid 482 in the ABCG2 gene affect substrate and antagonist specificity.** *Br J Cancer* 2003, **89:**1971-1978.

55. Yoshimura A, Kuwazuru Y, Sumizawa T, Ikeda S, Ichikawa M, Usagawa T, Akiyama S: **Biosynthesis, processing and half-life of P-glycoprotein in a human multidrug-resistant KB cell.** *Biochim Biophys Acta* 1989, **992:**307-314.

56. Lai GM, Chen YN, Mickley LA, Fojo AT, Bates SE: **P-glycoprotein expression and schedule dependence of adriamycin cytotoxicity in human colon carcinoma cell lines.** *Int J Cancer* 1991, **49:**696-703.

57. Lei ZN, Teng QX, Wu ZX, Ping FF, Song P, Wurpel JND, Chen ZS: **Overcoming multidrug resistance by knockout of ABCB1 gene using CRISPR/Cas9 system in SW620/Ad300 colorectal cancer cells.** *MedComm (2020)* 2021, **2:**765-777.

58. Ji N, Yang Y, Cai CY, Lei ZN, Wang JQ, Gupta P, Shukla S, Ambudkar SV, Kong D, Chen ZS: **Selonsertib (GS-4997), an ASK1 inhibitor, antagonizes multidrug resistance in ABCB1- and ABCG2-overexpressing cancer cells.** *Cancer Lett* 2019, **440-441:**82-93.

59. Robinson AN, Tebase BG, Francone SC, Huff LM, Kozlowski H, Cossari D, Lee

JM, Esposito D, Robey RW, Gottesman MM: **Coexpression of ABCB1 and ABCG2 in a Cell Line Model Reveals Both Independent and Additive Transporter Function.** *Drug Metab Dispos* 2019, **47:**715-723.

60. Wu ZX, Yang Y, Teng QX, Wang JQ, Lei ZN, Wang JQ, Lusvarghi S, Ambudkar SV, Yang DH, Chen ZS: **Tivantinib, A c-Met Inhibitor in Clinical Trials, Is Susceptible to ABCG2-Mediated Drug Resistance.** *Cancers (Basel)* 2020, **12**.

61. Yang Y, Ji N, Teng QX, Cai CY, Wang JQ, Wu ZX, Lei ZN, Lusvarghi S, Ambudkar SV, Chen ZS: **Sitravatinib, a Tyrosine Kinase Inhibitor, Inhibits the Transport Function of ABCG2 and Restores Sensitivity to Chemotherapy-Resistant Cancer Cells in vitro.** *Front Oncol* 2020, **10:**700.

62. Wu ZX, Yang Y, Wang G, Wang JQ, Teng QX, Sun L, Lei ZN, Lin L, Chen ZS, Zou C: **Dual TTK/CLK2 inhibitor, CC-671, selectively antagonizes ABCG2-mediated multidrug resistance in lung cancer cells.** *Cancer Sci* 2020, **111:**2872-2882.

63. Orlando BJ, Liao M: **ABCG2 transports anticancer drugs via a closed-to-open switch.** *Nat Commun* 2020, **11:**2264.

64. Alam A, Kowal J, Broude E, Roninson I, Locher KP: **Structural insight into substrate and inhibitor discrimination by human P-glycoprotein.** *Science* 2019, **363:**753-756.

65. Trott O, Olson AJ: **AutoDock Vina: improving the speed and accuracy of docking with a new scoring function, efficient optimization, and multithreading.** *J Comput Chem* 2010, **31:**455-461.

66. Zhang GN, Zhang YK, Wang YJ, Gupta P, Ashby CR, Jr., Alqahtani S, Deng T,

Bates SE, Kaddoumi A, Wurpel JND, et al: **Epidermal growth factor receptor (EGFR) inhibitor PD153035 reverses ABCG2-mediated multidrug resistance in non-small cell lung cancer: In vitro and in vivo.** *Cancer Lett* 2018, **424:**19-29.

67.   Wang YJ, Zhang YK, Zhang GN, Al Rihani SB, Wei MN, Gupta P, Zhang XY, Shukla S, Ambudkar SV, Kaddoumi A, et al: **Regorafenib overcomes chemotherapeutic multidrug resistance mediated by ABCB1 transporter in colorectal cancer: In vitro and in vivo study.** *Cancer Lett* 2017, **396:**145-154.

68.   Shen F, Chu S, Bence AK, Bailey B, Xue X, Erickson PA, Montrose MH, Beck WT, Erickson LC: **Quantitation of doxorubicin uptake, efflux, and modulation of multidrug resistance (MDR) in MDR human cancer cells.** *J Pharmacol Exp Ther* 2008, **324:**95-102.

69.   Cai CY, Zhang W, Wang JQ, Lei ZN, Zhang YK, Wang YJ, Gupta P, Tan CP, Wang B, Chen ZS: **Biological evaluation of non-basic chalcone CYB-2 as a dual ABCG2/ABCB1 inhibitor.** *Biochem Pharmacol* 2020, **175:**113848.

70.   Brózik A, Hegedüs C, Erdei Z, Hegedus T, Özvegy-Laczka C, Szakács G, Sarkadi B: **Tyrosine kinase inhibitors as modulators of ATP binding cassette multidrug transporters: substrates, chemosensitizers or inducers of acquired multidrug resistance?** *Expert Opin Drug Metab Toxicol* 2011, **7:**623-642.

71.   Beretta GL, Cassinelli G, Pennati M, Zuco V, Gatti L: **Overcoming ABC transporter-mediated multidrug resistance: The dual role of tyrosine kinase inhibitors as multitargeting agents.** *Eur J Med Chem* 2017, **142:**271-289.

72.   Wu ZX, Teng QX, Cai CY, Wang JQ, Lei ZN, Yang Y, Fan YF, Zhang JY, Li J,

Chen ZS: **Tepotinib reverses ABCB1-mediated multidrug resistance in cancer cells.** *Biochem Pharmacol* 2019, **166:**120-127.

73. Boyer T, Gonzales F, Barthélémy A, Marceau-Renaut A, Peyrouze P, Guihard S, Lepelley P, Plesa A, Nibourel O, Delattre C, et al: **Clinical Significance of ABCB1 in Acute Myeloid Leukemia: A Comprehensive Study.** *Cancers (Basel)* 2019, **11**.

74. Alqawi O, Bates S, Georges E: **Arginine482 to threonine mutation in the breast cancer resistance protein ABCG2 inhibits rhodamine 123 transport while increasing binding.** *Biochem J* 2004, **382:**711-716.

75. Ejendal KF, Diop NK, Schweiger LC, Hrycyna CA: **The nature of amino acid 482 of human ABCG2 affects substrate transport and ATP hydrolysis but not substrate binding.** *Protein Sci* 2006, **15:**1597-1607.

76. Ambudkar SV, Dey S, Hrycyna CA, Ramachandra M, Pastan I, Gottesman MM: **Biochemical, cellular, and pharmacological aspects of the multidrug transporter.** *Annu Rev Pharmacol Toxicol* 1999, **39:**361-398.

77. Ambudkar SV, Kimchi-Sarfaty C, Sauna ZE, Gottesman MM: **P-glycoprotein: from genomics to mechanism.** *Oncogene* 2003, **22:**7468-7485.

78. Wang J, Yang DH, Yang Y, Wang JQ, Cai CY, Lei ZN, Teng QX, Wu ZX, Zhao L, Chen ZS: **Overexpression of ABCB1 Transporter Confers Resistance to mTOR Inhibitor WYE-354 in Cancer Cells.** *Int J Mol Sci* 2020, **21**.

79. Wu ZX, Yang Y, Wang JQ, Zhou WM, Chen J, Fu YG, Patel K, Chen ZS, Zhang JY: **Elevated ABCB1 Expression Confers Acquired Resistance to Aurora Kinase Inhibitor GSK-1070916 in Cancer Cells.** *Front Pharmacol* 2020,

11:615824.

80.   Ferreira RJ, Bonito CA, Cordeiro M, Ferreira MU, Dos Santos D: **Structure-function relationships in ABCG2: insights from molecular dynamics simulations and molecular docking studies.** *Sci Rep* 2017, **7:**15534.

81.   Morris GM, Lim-Wilby M: **Molecular docking.** *Methods Mol Biol* 2008, **443:**365-382.

82.   Lionta E, Spyrou G, Vassilatis DK, Cournia Z: **Structure-based virtual screening for drug discovery: principles, applications and recent advances.** *Curr Top Med Chem* 2014, **14:**1923-1938.

83.   Wu ZX, Yang Y, Wang JQ, Narayanan S, Lei ZN, Teng QX, Zeng L, Chen ZS: **Overexpression of ABCG2 Confers Resistance to MLN7243, a Ubiquitin-Activating Enzyme (UAE) Inhibitor.** *Front Cell Dev Biol* 2021, **9:**697927.

84.   Sajid A, Lusvarghi S, Chufan EE, Ambudkar SV: **Evidence for the critical role of transmembrane helices 1 and 7 in substrate transport by human P-glycoprotein (ABCB1).** *PLoS One* 2018, **13:**e0204693.

85.   Tinoush B, Shirdel I, Wink M: **Phytochemicals: Potential Lead Molecules for MDR Reversal.** *Front Pharmacol* 2020, **11:**832.

86.   Wu X, Yin C, Ma J, Chai S, Zhang C, Yao S, Kadioglu O, Efferth T, Ye Y, To KK, Lin G: **Polyoxypregnanes as safe, potent, and specific ABCB1-inhibitory pro-drugs to overcome multidrug resistance in cancer chemotherapy in vitro and in vivo.** *Acta Pharm Sin B* 2021, **11:**1885-1902.

87.   Taguchi Y, Morishima M, Komano T, Ueda K: **Amino acid substitutions in the first transmembrane domain (TM1) of P-glycoprotein that alter substrate**

specificity. *FEBS Lett* 1997, **413:**142-146.

88. Eadie LN, Hughes TP, White DL: **Interaction of the efflux transporters ABCB1 and ABCG2 with imatinib, nilotinib, and dasatinib.** *Clin Pharmacol Ther* 2014, **95:**294-306.

89. Nanayakkara AK, Follit CA, Chen G, Williams NS, Vogel PD, Wise JG: **Targeted inhibitors of P-glycoprotein increase chemotherapeutic-induced mortality of multidrug resistant tumor cells.**

90. Vogel C, Marcotte EM: **Insights into the regulation of protein abundance from proteomic and transcriptomic analyses.** *Nat Rev Genet* 2012, **13:**227-232.

91. Zhang Z, Wu JY, Hait WN, Yang JM: **Regulation of the stability of P-glycoprotein by ubiquitination.** *Mol Pharmacol* 2004, **66:**395-403.

92. Yan YY, Wang F, Zhao XQ, Wang XK, Chen YF, Liu H, Xie Y, Fu LW: **Degradation of P-glycoprotein by pristimerin contributes to overcoming ABCB1-mediated chemotherapeutic drug resistance in vitro.** *Oncol Rep* 2017, **37:**31-40.

93. Xie Y, Burcu M, Linn DE, Qiu Y, Baer MR: **Pim-1 kinase protects P-glycoprotein from degradation and enables its glycosylation and cell surface expression.** *Mol Pharmacol* 2010, **78:**310-318.

94. Wang Y, Wang Y, Qin Z, Cai S, Yu L, Hu H, Zeng S: **The role of non-coding RNAs in ABC transporters regulation and their clinical implications of multidrug resistance in cancer.** *Expert Opin Drug Metab Toxicol* 2021, **17:**291-306.

95. Xu QY, Xie MJ, Huang J, Wang ZW: **Effect of circ MTHFD2 on resistance to**

pemetrexed in gastric cancer through regulating expression of miR-124. *Eur Rev Med Pharmacol Sci* 2019, **23:**10290-10299.

96.   Xie Y, Wang M, Shao Y, Deng X, Chen Y: **Long Non-coding RNA KCNQ1OT1 Contributes to Antiepileptic Drug Resistance Through the miR-138-5p/ABCB1 Axis in vitro.** *Front Neurosci* 2019, **13:**1358.

97.   Reed K, Hembruff SL, Sprowl JA, Parissenti AM: **The temporal relationship between ABCB1 promoter hypomethylation, ABCB1 expression and acquisition of drug resistance.** *Pharmacogenomics J* 2010, **10:**489-504.

98.   Gómez-Martínez A, García-Morales P, Carrato A, Castro-Galache MD, Soto JL, Carrasco-García E, García-Bautista M, Guaraz P, Ferragut JA, Saceda M: **Post-transcriptional regulation of P-glycoprotein expression in cancer cell lines.** *Mol Cancer Res* 2007, **5:**641-653.

99.   Alemán C, Annereau JP, Liang XJ, Cardarelli CO, Taylor B, Yin JJ, Aszalos A, Gottesman MM: **P-glycoprotein, expressed in multidrug resistant cells, is not responsible for alterations in membrane fluidity or membrane potential.** *Cancer Res* 2003, **63:**3084-3091.

100.   Baker EK, Johnstone RW, Zalcberg JR, El-Osta A: **Epigenetic changes to the MDR1 locus in response to chemotherapeutic drugs.** *Oncogene* 2005, **24:**8061-8075.

101.   Mickley LA, Bates SE, Richert ND, Currier S, Tanaka S, Foss F, Rosen N, Fojo AT: **Modulation of the expression of a multidrug resistance gene (mdr-1/P-glycoprotein) by differentiating agents.** *J Biol Chem* 1989, **264:**18031-18040.

102.   Richert ND, Aldwin L, Nitecki D, Gottesman MM, Pastan I: **Stability and**

covalent modification of P-glycoprotein in multidrug-resistant KB cells. *Biochemistry* 1988, **27:**7607-7613.

103.   Nemzek JA, Bolgos GL, Williams BA, Remick DG: **Differences in normal values for murine white blood cell counts and other hematological parameters based on sampling site.** *Inflamm Res* 2001, **50:**523-527.

104.   Ding L, Cao J, Lin W, Chen H, Xiong X, Ao H, Yu M, Lin J, Cui Q: **The Roles of Cyclin-Dependent Kinases in Cell-Cycle Progression and Therapeutic Strategies in Human Breast Cancer.** *Int J Mol Sci* 2020, **21**.

105.   Asghar U, Witkiewicz AK, Turner NC, Knudsen ES: **The history and future of targeting cyclin-dependent kinases in cancer therapy.** *Nat Rev Drug Discov* 2015, **14:**130-146.

106.   Herbert KJ, Puliyadi R, Prevo R, Rodriguez-Berriguete G, Ryan A, Ramadan K, Higgins GS: **Targeting TOPK sensitises tumour cells to radiation-induced damage by enhancing replication stress.** *Cell Death Differ* 2021, **28:**1333-1346.

VITA

Name: Yuqi Yang

Baccalaureate Degree: Bachelor of Science,

                                                            Tianjin Medical University,

                                                            Tianjin, China

                                                            Major: Pharmacy

Date Graduated: June, 2017